NEUSE RIVER ESTUARY MODELING AND MONITORING PROJECT STAGE 1: PREDICTIONS AND UNCERTAINTY ANALYSIS OF RESPONSE TO NUTRIENT LOADING USING A MECHANISTIC EUTROPHICATION MODEL

James D. Bowen and Jeffrey Hieronymus

Department of Civil Engineering
William States Lee College of Engineering
University of North Carolina at Charlotte
Charlotte, NC 28223

WRRI Project No. 50222
September 2000

ACKNOWLEDGMENTS

The authors wish to thank all those who assisted in the preparation of the data files needed to run the Neuse Estuary Eutrophication Model and to compare its predictions to observed data. The input data files were assembled initially by Juan Mangles of the North Carolina Division of Water Quality (DWQ) and Jerad Bales of the US Geological Survey (USGS). Hans Paerl, Jay Pinckney, Rick Luettich, Jessie McNinch, Crystal Fulcher, Ben Peierls, and Tammi Richardson of the UNC Institute of Marine Sciences provided bathymetric, hydrographic, water quality, and phytoplankton pigment measurements. Doug Walters of the USGS provided data on river flows, water elevation and velocity, and assorted water quality information. Chris Roessler of the DWQ helped assemble information on point source discharges to the Neuse Estuary. Craig Stow of Duke University's Nicholas School of the Environment provided water quality observations in the estuary and nutrient concentrations in the riverine sections of the Neuse River. Additional assistance was provided by various personnel from the DWQ, the USGS, and the National Weather Service. The authors would also like to acknowledge the excellent work of three undergraduate research assistants at UNC Charlotte, Jason Smith, Stephen Carter, and John Vandergrift, who helped gather the data, create input files, and execute model runs. Funding for the project was provided by the Water Resources Research Institute of the University of North Carolina and the North Carolina Division of Water Quality.

ABSTRACT

Eutrophication modeling of the Neuse River Estuary was conducted using a modified version of an existing two-dimensional, laterally averaged model (CE-QUAL-W2). The calibrated model was used to predict the water quality improvement in the estuary associated with a 30% reduction in riverine loading of inorganic nutrients. Three cases were examined: 1) reduced inorganic nitrogen, 2) reduced inorganic phosphorus, and 3) reduced inorganic nitrogen and phosphorus. Water quality improvement was quantified by comparing the predicted chlorophyll-a and dissolved oxygen concentrations for the nutrient reduction scenarios to a case without nutrient reduction. An uncertainty analysis was also performed to investigate the feasibility of the method and to quantify the uncertainty of model predictions. The uncertainty analysis examined only model specification error, using a regional sensitivity method, for a small subset of the model parameters that were considered to be important to quantifying phytoplankton growth.

Based upon comparison of the three inorganic nutrient reduction scenarios, nitrogen reduction was found to be more effective than phosphorus reduction in producing water quality improvements. For each nutrient reduction scenario, the largest reduction in phytoplankton biomass was predicted to occur in the lower estuary. In this area, a 30 percent reduction in riverine inorganic nitrogen loading decreased median chlorophyll concentrations by 2 - 20%. For the entire estuary, nutrient reduction was predicted to reduce median chlorophyll concentrations by 7 - 11%. The model predicted that dissolved oxygen concentrations would increase only very slightly in response to nutrient reduction, which was considered to be indicative of the important role that sediment processes play in determining water column dissolved oxygen concentrations. The regional sensitivity analysis approach was found to be a computationally time consuming method for assessing model specification error, necessitating an initial parameter filtering procedure. The uncertainty analysis also indicated that predictions of changes in median chlorophyll concentration were significantly more certain than predictions of changes in the frequency and intensity of phytoplankton blooms. (Keywords: eutrophication modeling, water quality, Neuse River Estuary, nutrients, phytoplankton abundance)

TABLE OF CONTENTS

ACKNOWLEDGMENTS ii

ABSTRACT iii

TABLE OF CONTENTS iv

LIST OF FIGURES vi

LIST OF TABLES x

SUMMARY AND CONCLUSIONS xi

RECOMMENDATIONS xiii

1. INTRODUCTION 1

1.1 Need for Research 1

1.2 Study Objectives 1

2. BACKGROUND 4

2.1 Study Area Description 4

2.2 Previous Studies 5

2.3 Description of Hydrologic Conditions 6

2.3.1 March – September 1991 6
2.3.2 June 1997 – December 1998 8

3. METHODS 11

3.1 Model Description 11

3.2 Model Input Data 13

3.2.1 Model Grid and Bathymetry 14
3.2.2 Branch and Tributary Boundary Conditions 18
3.2.3 Downstream Boundary Conditions 21
3.2.4 Meteorological and Atmospheric Deposition Data 22

3.3 Model Development/Calibration/Verification 23

3.4 Nutrient Reduction Scenarios 24

3.5 Uncertainty Analysis 25

4. RESULTS 28

4.1 Predictions Using the 1997-1998 Data Set 28

4.1.1 Hydrodynamic Model Calibration 28
4.1.2 Water Quality Model Calibration 33
4.1.3 Water Quality Predictions 38

4.2 Predictions of Water Quality Improvement 53

4.3 Model Verification Attempt 56

4.4 Uncertainty Analysis 61

4.4.1 Feasible Parameter Vectors 61
4.4.2 Variability of Predicted Water Quality Conditions 64
4.4.3 Variability in Predictions of Water Quality Improvement 64

5. DISCUSSION AND CONCLUSIONS 69

5.1 Predicted Water Quality Improvement 69

5.2 Prediction Uncertainty 70

5.3 Limitations of the Analysis 71

5.4 Need for Additional Research 74

6. REFERENCES 76

Appendix A. Model Parameter Specification 79

LIST OF FIGURES

Figure 1. Neuse River Estuary, NC. 2
Figure 2. Loadings of freshwater and inorganic nutrients to the Neuse River Estuary at Streets Ferry, NC during 1991, 1997, and 1998. 7
Figure 3. Inorganic nitrogen to phosphorus molar ratio of the inflowing water to the Neuse River Estuary at Streets Ferry, NC during 1991, 1997 and 1998. 9
Figure 4. Comparison of Neuse River inflows to the estuary for the three years simulated using the Neuse Estuary Eutrophication Model. 10
Figure 5. Neuse Estuary Eutrophication Model segmentation and MODMON monitoring stations. 16
Figure 6. Neuse Estuary Eutrophication Model segment dimensions for the Neuse River (segments 2-60) and the Trent River (segments 63-65). Segments 61 and 62 are dummy segments that separate model branches 1 and 2, thus their dimensions are not defined. . 17
Figure 7. Model predicted and observed water surface elevations in the Neuse River Estuary near New Bern, NC during 1997 and 1998. The model's output frequency is 1 day; the observed data frequency is 1 hour. 29
Figure 8. Model predicted and observed water levels in the Neuse River Estuary at New Bern, NC during July 1998. 29
Figure 9. Relative amplitudes (m) of water surface elevation fluctuations based on model predictions and observations in the Neuse River Estuary near New Bern, NC during June through October 1997 31
Figure 10. Model predicted (solid lines) and observed (symbols) salinities (g/l or PSU) for near-surface and near-bottom mid-channel waters in the Neuse River Estuary near New Bern, NC during 1997 and 1998. 32
Figure 11. Model predicted (solid lines) and observed (symbols) salinities (g/l or PSU) for near-surface and near-bottom mid-channel waters in the Neuse River Estuary near Cherry Point, NC during 1997 and 1998. 32
Figure 12. Model predicted (solid lines) and observed (symbols) temperatures (°C) for near-surface and near-bottom mid-channel waters in the Neuse River Estuary near New Bern, NC during 1997 and 1998. 34
Figure 13. Model predicted (solid lines) and observed (symbols) temperatures (°C) for near-surface and near-bottom mid-channel waters in the Neuse River Estuary near Cherry Point, NC during 1997 and 1998. 34
Figure 14. Cumulative frequency distributions for predicted and observed salinities in the mid-channel waters of the Neuse River Estuary during 1997 and 1998. 35
Figure 15. Wind speeds (top panel, mi/hr.), observed top and bottom salinities (middle panel, PSU), and predicted top and bottom salinities (bottom panel, g/l) in the mid-channel waters of the Neuse River Estuary near Cherry Point, NC during July, 1998 (Julian Day 546 = July 1, 1998). 36
Figure 16. Wind speeds (top panel, mi/hr.), observed near-surface currents (middle panel, cm/s), and model predicted near-surface currents (bottom panel, m/s) in the mid-channel waters of the Neuse River Estuary near Cherry Point, NC during July, 1998 (Julian Day 546 = July 1, 1998). 37

Figure 17. Observed particulate organic carbon (µg/l) vs. particulate organic nitrogen (µg N/l) in the mid-channel waters of Neuse River Estuary during 1997 and 1998. 39
Figure 18. Observed particulate organic carbon concentrations (µg/l) vs. observed chlorophyll-a concentrations (µg/l) in mid-channel waters of the Neuse River Estuary during 1997 and 1998. 40
Figure 19. Calibrated growth rates (day^{-1}) vs. temperature for the three phytoplankton groups used to model the phytoplankton community in the Neuse Estuary Eutrophication Model. 41
Figure 20. Model predicted longitudinal and vertical variations in salinity (g/l) in the Neuse River Estuary on July 20, 1998. . . . . after 41
Figure 21. Model predicted longitudinal and vertical variations in nitrate + nitrite concentrations (mg N/l) in the Neuse River Estuary on July 20, 1998. . . . . after 41
Figure 22. Model predicted longitudinal and vertical variations in chlorophyll-a concentrations (µg/l) in the Neuse River Estuary on July 20, 1998. . . . . after 41
Figure 23. Model predicted longitudinal and vertical variations in dissolved oxygen concentrations (mg/l) in the Neuse River Estuary on July 20, 1998. . . . . after 41
Figure 24. Model predicted (solid lines) and observed (symbols) nitrate + nitrite concentrations (mg N/l) for near-surface and near-bottom waters in the Neuse River Estuary near New Bern, NC during 1997 and 1998. 43
Figure 25. Model predicted (solid lines) and observed (symbols) nitrate + nitrite concentrations (mg N/l) for near-surface and near-bottom waters in the Neuse River Estuary near Cherry Point, NC during 1997 and 1998. 43
Figure 26. Model predicted (solid lines) and observed (symbols) ammonia concentrations (mg N/l) for near-surface and near-bottom waters in the Neuse River Estuary near New Bern, NC during 1997 and 1998. 44
Figure 27. Model predicted (solid lines) and observed (symbols) ammonia concentrations (mg N/l) for near-surface and near-bottom waters in the Neuse River Estuary near Cherry Point, NC during 1997 and 1998. 44
Figure 28. Model predicted (solid lines) and observed (symbols) orthophosphate concentrations (mg P/l) for near-surface and near-bottom waters in the Neuse River Estuary near New Bern, NC during 1997 and 1998. 45
Figure 29. Model predicted (solid lines) and observed (symbols) orthophosphate concentrations (mg P/l) for near-surface and near-bottom waters in the Neuse River Estuary near Cherry Point, NC during 1997 and 1998. 45
Figure 30. Model predicted (solid lines) and observed (symbols) chlorophyll-a concentrations (µg/l) for near-surface and near-bottom waters in the Neuse River Estuary near New Bern, NC during 1997 and 1998. 46
Figure 31. Model predicted (solid lines) and observed (symbols) chlorophyll-a concentrations (µg/l) for near-surface and near-bottom waters in the Neuse River Estuary near Cherry Point, NC during 1997 and 1998. 46
Figure 32. Model Predicted (solid lines) and observed (symbols) dissolved oxygen concentrations (mg/l) for near-surface and near-bottom waters in the Neuse River Estuary near New Bern, NC during 1997 and 1998. 47

Figure 33. Model predicted (solid lines) and observed (symbols) dissolved oxygen concentrations (mg/l) for near-surface and near-bottom waters in the Neuse River Estuary near Cherry Point, NC during 1997 and 1998. 47
Figure 34. Predicted nitrate + nitrite concentrations (mg N/l) in the mid-channel surface waters of the Neuse River Estuary during 1997 and 1998. . . . . after 47
Figure 35. Observed nitrate + nitrite concentrations (mg/l) in the mid-channel surface waters of the Neuse River Estuary during 1997 and 1998. . . . . after 47
Figure 36. Predicted chlorophyll-a concentrations (µg/l) in the mid-channel surface waters of the Neuse River Estuary during 1997 and 1998. . . . . after 47
Figure 37. Observed chlorophyll-a concentrations (µg/l) in the mid-channel surface waters of the Neuse River Estuary during 1997 and 1998. . . . . after 47
Figure 38. Predicted dissolved oxygen concentrations (mg/l) in the mid-channel surface waters of the Neuse River Estuary during 1997 and 1998. . . . . after 48
Figure 39. Observed dissolved oxygen concentrations (mg/l) in the mid-channel surface waters of the Neuse River Estuary during 1997 and 1998. . . . . after 48
Figure 40. Predicted sediment oxygen demand ($g/m^2/d$) in the mid-channel bottom sediments of the Neuse River Estuary during 1997 and 1998. . . . . after 48
Figure 41. Cumulative frequency distribution of predicted and observed orthophosphate concentrations (mg P/l) in the mid-channel waters of the Neuse River Estuary during 1997 and 1998. 49
Figure 42. Cumulative frequency distribution of predicted and observed ammonia concentrations (mg N/l) in the mid-channel waters of the Neuse River Estuary during 1997 and 1998. . 50
Figure 43. Cumulative frequency distribution of predicted and observed nitrate + nitrite concentrations (mg N/l) in the mid-channel waters of the Neuse River Estuary during 1997 and 1998. 51
Figure 44. Cumulative frequency distribution of predicted and observed chlorophyll-a concentrations (µg/l) in the mid-channel waters of the Neuse River Estuary during 1997 and 1998. 52
Figure 45. Cumulative frequency distribution of predicted and observed dissolved oxygen concentrations (mg/l) in the mid-channel waters of the Neuse River Estuary during 1997 and 1998. 54
Figure 46. Comparison of 1997-1998 model predicted cumulative frequency distributions of chlorophyll-a concentrations in the Neuse River Estuary for a base case (100% loadings) and for three nutrient loading reduction scenarios. 55
Figure 47. Comparison of 1997-1998 model predicted cumulative frequency distributions of chlorophyll-a concentrations in the Neuse River Estuary near Cherry Point, NC for a base case (100% loadings) and for three nutrient loading reduction scenarios. 57
Figure 48. Comparison of 1997-1998 model predicted cumulative frequency distributions of chlorophyll-a concentrations in the Neuse River Estuary near New Bern, NC for a base case (100% loadings) and for three nutrient loading reduction scenarios. 58
Figure 49. Comparison of 1997-1998 model predicted cumulative frequency distributions of dissolved oxygen concentrations in the Neuse River Estuary for a base case (100% loadings) and for three nutrient loading reduction scenarios. 59

Figure 50. Comparison of 1997-1998 model predicted cumulative frequency distributions of dissolved oxygen concentrations in the Neuse River Estuary near New Bern, NC for a base case (100% loadings) and for three nutrient loading reduction scenarios. 59
Figure 51. Comparison of 1997-1998 model predicted cumulative frequency distributions of dissolved oxygen concentrations in the Neuse River Estuary near New Bern, NC for a base case (100% loadings) and for a case with reduced nutrient load and reduced sediment organic carbon. 60
Figure 52. Model computed and observed water levels in the Neuse River Estuary at New Bern, NC during July 1991. 62
Figure 53. Model computed and observed salinities in the Neuse River Estuary at Cherry Point, NC during July 1991. 62
Figure 54. Distribution of parameter levels (see Table 7 for values) of the seven variable parameters for the 220 feasible parameter vectors. The base case had all seven variable parameters at level 1. 63
Figure 55. Distribution of median and maximum model predicted chlorophyll-a concentrations and the percentage above 25 µg/l in the Neuse River Estuary for 220 model runs using feasible parameter vectors with either 100% or 70% nutrient loading. 65
Figure 56. Distribution of median and maximum model predicted chlorophyll-a concentrations and the percentage above 25 µg/l in the Neuse River Estuary near Cherry Point, NC for 220 model runs using feasible parameter vectors with either 100% or 70% nutrient loading. 65
Figure 57. Distribution of median predicted dissolved oxygen concentrations and the percentage of concentrations below 2.0 mg/l in the Neuse River Estuary for 220 model runs using feasible parameter vectors with either 100% or 70% nutrient loading. 66
Figure 58. Distribution of median predicted dissolved oxygen concentrations and the percentage of concentrations below 2.0 mg/l in the Neuse River Estuary near Cherry Point, NC for 220 model runs using feasible parameter vectors with either 100% or 70% nutrient loading. 66
Figure 59. Distribution of predicted percent reduction in median. maximum, and fraction above 25 µg/l for mid-channel chlorophyll-a concentrations in the Neuse River Estuary using 220 model runs with feasible parameter vectors and a 30% nutrient load (N+P) reduction. 67
Figure 60. Distribution of predicted percent change in median and fraction below 2.0 mg/l for mid-channel dissolved oxygen concentrations in the Neuse River Estuary using 220 model runs with feasible parameter vectors and a 30% nutrient load (N+P) reduction. 68
Figure 61. Inflows from the Neuse River to the estuary at Streets Ferry, NC during 1991, 1997, 1998, and 1999. 75

LIST OF TABLES

Table 1. Drainage Areas of Watersheds Within the Neuse River Basin. 5

Table 2. Neuse Estuary Eutrophication Model Constituents. 12

Table 3. Branch Inflow Boundary Condition Data Description. 19

Table 4. Tributary Boundary Condition Data Description. 20

Table 5. Downstream Head Boundary Condition Data Description. 22

Table 6. Meteorological Data Description. 22

Table 7. Variable Parameters for Uncertainty Analysis. 26

Table 8. Comparisons of Model Predictions to Observed Data. 53

Table 9. Parameter Levels for the 220 Feasible Parameter Vectors. 71

SUMMARY AND CONCLUSIONS

In response to major fish kills in the Neuse River Estuary in 1995 and 1996, designation of the Neuse River as nutrient-sensitive, and the widespread perception that water quality in the estuary has been degraded by excessive nutrient loading, the State has drafted regulations aimed at reducing nitrogen loading to the estuary by 30 percent. In deciding upon this initial target for nutrient reduction, it was recognized that the level of nutrient reduction necessary to achieve desired water quality improvements was, and is a critical research need.

In this study a water quality model of the Neuse River Estuary was used to examine the interaction between nutrient loading, algal blooms, and estuarine water quality. An extensively modified version of an existing two-dimensional, laterally averaged model (CE-QUAL-W2) was applied to predict water quality conditions in the lower 80-km of the estuary, between Streets Ferry and Oriental, NC. The calibrated model was used to predict the water quality improvement associated with a 30% reduction in riverine inorganic nutrient loading to the estuary. Input data sets were developed using observed data gathered from the United States Geological Survey, the North Carolina Division of Water Quality, Weyerhaeuser, the National Weather Service, and the University of North Carolina Institute of Marine Science. Two periods were found to have sufficient data to create the necessary model data sets (March – September 1991, June 1997 – December 1998), although the 1991 time period was found to have very limited water quality data.

The 1997-1998 data set was used for model calibration, for predicting water quality improvement, and for an uncertainty analysis. Nutrient reduction scenarios examined only riverine loadings of inorganic nutrients. Three cases were examined: 1) reduced inorganic nitrogen, 2) reduced inorganic phosphorus, and 3) reduced inorganic nitrogen and phosphorus. Water quality improvement was quantified by comparing the predicted concentrations of chlorophyll-a and dissolved oxygen for the various nutrient reduction scenarios as compared to a case without nutrient reduction. The uncertainty analysis was performed as an assessment of methods to quantify the uncertainty of model predictions. The analysis examined only model specification error, using a regional sensitivity method, for a small subset of the model parameters that were considered to be important to quantifying phytoplankton growth. The 1991 data set, which had limited water quality information and spanned a relatively brief time period, was used for hydrodynamic model verification only.

The degree to which the calibrated model fit the observed data varied widely between the model constituents. Correlation coefficients (r^2) between model predictions and observations were .89 for salinity, .76 for nitrite+nitrate, .52 for dissolved oxygen, and .18 for chlorophyll-a. This level of calibration was comparable to that achieved in other eutrophication model studies of eastern U.S. estuaries. Based upon comparison of the three inorganic nutrient reduction scenarios, nitrogen reduction was found to be more effective than phosphorus reduction in producing water quality improvements. In each scenario, the largest reduction in phytoplankton biomass was predicted to occur in the lower estuary. In this area, a 30 percent reduction in riverine inorganic nitrogen loading decreased median chlorophyll by 2 – 20%. For the entire estuary, nutrient

reduction was predicted to reduce median chlorophyll concentration by 7 - 11%. The oligohaline portion of the estuary was predicted to be less affected by nutrient reduction. This was consistent with the higher nutrient concentrations typically observed in this area. The model predicted that dissolved oxygen concentrations would increase only very slightly in response to nutrient reduction, which was considered to be indicative of the important role that sediment processes play in determining water column dissolved oxygen concentrations. The regional sensitivity analysis approach was found to be a computationally time consuming method for assessing model specification error. Results of the uncertainty analysis also indicated that predictions of changes in median chlorophyll concentration were significantly more certain than predictions of changes in water quality measures based on extreme values such as the frequency of bloom conditions. In addition, prediction of changes in spatially averaged conditions were more certain than prediction of changes in any one particular area.

RECOMMENDATIONS

Based on the results of the study, it can be concluded that a mechanistic eutrophication model is capable of simulating chlorophyll-a, nutrient, and dissolved oxygen dynamics in the Neuse River Estuary. The two years used to predict water quality improvement (1997-1998) were found to be rather benign with respect to water quality. No serious algal blooms occurred during these two years. It is not known at this time the degree to which model predictions of water quality improvement are affected by the relatively short data set. Further research should be conducted to collect the data needed to simulate a wider range of hydrologic and estuarine water quality conditions. Prediction capability of the existing model was found to be limited by its relatively simple sediment diagenesis model. Future research should focus on improving the sediment prediction capabilities. This research also demonstrated the utility of an uncertainty analysis in quantifying the reliability of model predictions, but the effort was limited in its examinations of error sources. The computational burden of the regional sensitivity approach makes it impossible to fully consider every possible parameter in quantifying model specification error. In this study a literature review was used to select a relatively small number of parameters for inclusion in the uncertainty analysis. Future research should develop the uncertainty analysis method so that a subset of variable parameters can be determined based on model predictions rather than a literature review. In addition, future research should be conducted to determine the feasibility of including other potential error sources into the uncertainty analysis.

1. INTRODUCTION

1.1 Need for Research

Concern about the water quality of the Neuse River Estuary is not strictly a recent phenomenon. Blooms of the blue-green algae *Microcystis aeruginosa* were a frequent nuisance in the oligohaline portion of the estuary during the 1970's and 1980's. These blooms, which generally occurred in the summer and early fall, were considered to be the result of a combination of relatively high nutrient loads and lengthened water residence times (Hobbie 1975, Paerl 1987). Research at the time using nutrient bioassays suggested that nutrient loading reductions of at least 30% might be effective in reducing the magnitude and frequency of the blooms (Paerl 1987).

Massive fish kills in 1995 and 1996 re-energized the public's interest in the water quality of the Neuse River Estuary. The State of North Carolina has designated the Neuse as a "nutrient sensitive water," and has drafted a management strategy aimed at reducing nitrogen loading to the estuary by 30% from a baseline value equal to the yearly average loading for the period from 1991 - 1995. Although the management strategy is designed to reduce estuarine nutrient loading by a particular amount, the magnitude of the reduction needed to achieve water quality objectives continues to be a critical, unanswered research question.

Since our interest in predicting the relationship between nutrient loading reduction and water quality improvement is important to water quality management issues, we should therefore endeavor to produce results that are useful in this context. Both the magnitude of the system's response to reduced nutrient loading, and the relative certainty of this prediction are important considerations to water quality managers and stakeholders. Estimates of an estuary's response to changing nutrient loading have often been, and are in this study, accomplished with a "conservation based" simulation model of the physical simulation. These models have as their basis conservation equations for fluid momentum and mass, and constituent mass. This type of model is usually referred to as a "mechanistic" model since each term in the conservation equations relate to specific mechanisms of momentum or mass fate and transport. Development of methods to quantify prediction uncertainty of mechanistic eutrophication models is an ongoing research area (e.g. Adams 1998), and is a second research objective of this study.

1.2 Study Objectives

In this study we utilize a mechanistic eutrophication model to study the linkages between physical transport and mixing, nutrient inputs, phytoplankton growth, sediment diagenesis, and dissolved oxygen dynamics. The physical system to be modeled is the Neuse River Estuary between Streets Ferry and Oriental (Figure 1). The study has the following objectives:

- develop and calibrate a two-dimensional, vertically averaged model of the Neuse River Estuary for the period from June 1, 1997 through December 31, 1998 using bathymetric,

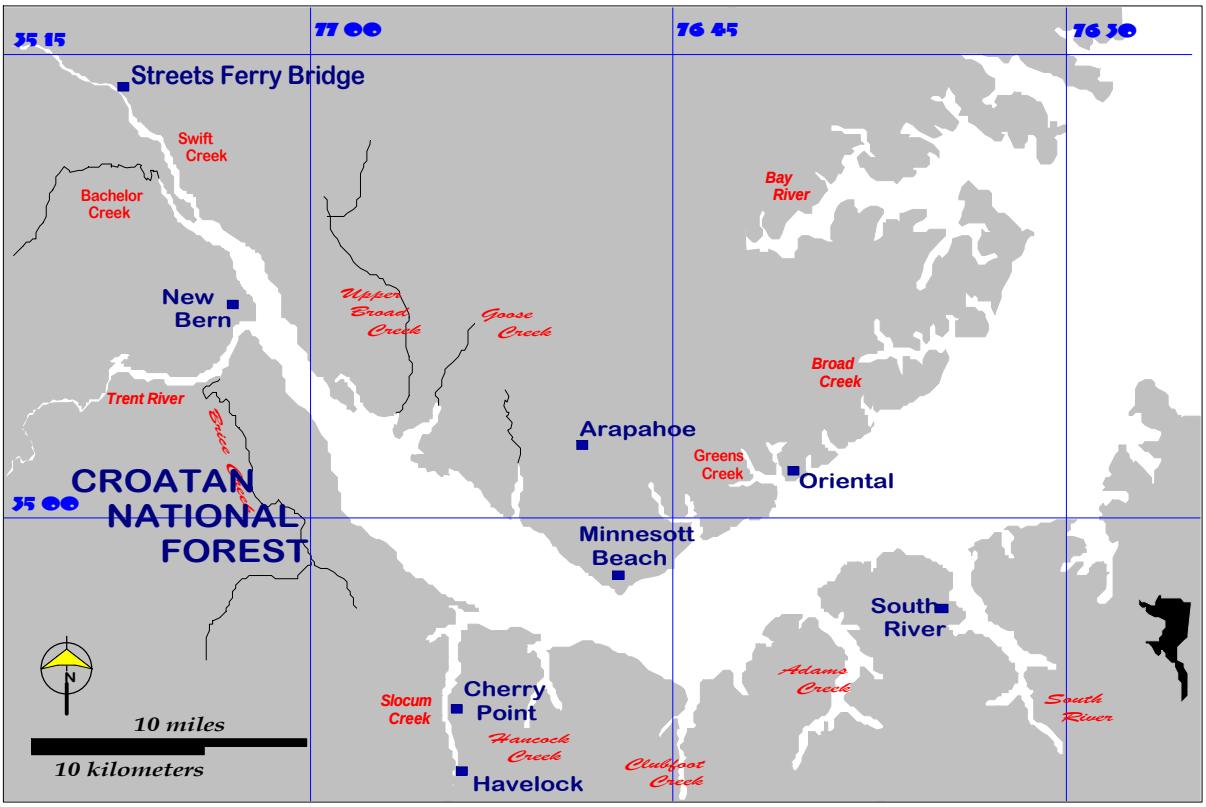

Figure 1. Neuse River Estuary, NC.

hydrodynamic, and water quality data collected from the Neuse River MODeling and MONitoring (MODMON) project (Luettich et al. 2000) and other sources,

- complete the assembly of a model input data set for the period from March 1, 1991 through September 30, 1991 begun through the joint efforts of the United States Geological Survey (USGS) and the NC Division of Water Quality (DWQ) (Bales and Robbins 1999) and use this data set to perform a model verification exercise,

- apply the calibrated model, using the 1997-1998 data, to predict the water quality impact of a 30% reduction in riverine loading of inorganic nutrients (nitrogen and/or phosphorus) to the estuary,

- use the to model to determine which gaps in scientific knowledge are most important to future predictions of system response, and

- develop and test the feasibility of implementing an analysis to estimate the uncertainty of the water quality improvement predictions.

2. BACKGROUND

2.1 Study Area Description

North Carolina's Neuse River drains approximately 16,000 km^2, and empties into the southwestern corner of the Pamlico Sound. The Raleigh-Durham metropolitan area is within the basin, near the river's headwaters. Nearly 1.5 million people live in the river basin. The basin is also used intensively for agricultural and livestock production. The estuary occupies the lower 80 km of the river. It is broad and shallow, with average depths ranging from approximately 4 m near New Bern to 6 m at the mouth.

Surface water loadings to the estuary come from two rivers and nine creeks, as well as from direct runoff (Figure 1). Three of these water bodies (Neuse River, Trent River, Swift Creek) account for more than 90% of the total watershed area (Table 1). None of the remaining creeks has a watershed area more than 1.1% of the total. Direct runoff to the estuary accounts for 3.9% of the watershed area (Table 1).

For the purposes of this study, the Neuse River Estuary between Streets Ferry and Oriental can be divided into three sections, as was done in studies of benthic nutrient and dissolved fluxes (NC DWQ 1998). The upper estuary, from Streets Ferry to just upstream of Upper Broad Creek, is oligohaline. Velocities and salinities in this section are strongly affected by riverine flushing (Giese et al 1985). The upper estuary is considered eutrophic and has experienced numerous blooms of blue-green algae (Hobbie and Smith 1975, Paerl 1987).

The middle estuary is much wider and generally shallower than the upper estuary. It runs southwesterly to Cherry Point, where the estuary makes a perpendicular bend to the northeast. Cherry Point is considered the downstream extent of the middle estuary. The lower estuary is generally wider and deeper than the other sections. The middle and lower estuary reaches are considered to be mesohaline and mesotrophic. Recently dinoflagellate blooms have plagued these sections of the estuary (Rudek et al. 1991, Mallin and Paerl 1994).

Unfortunately, serious water quality problems have existed in three of the last four years, and have been observed in all three sections of the estuary. Periods with low dissolved oxygen (DO) concentrations and fish kills have occurred in the past, but were widespread and serious in both 1995 and 1996. In 1995, heavy summer rains followed by a prolonged period of density stratification lead to summer algal blooms, widespread anoxia (defined here as DO concentration < 2 mg/l), and massive fish kills (Paerl and Pinckney 1996). An outbreak of the toxic algae *Pfiesteria piscicida* (Burkholder et al 1995) also occurred, and may have been the cause of many of the fish deaths. A similar scenario occurred in 1996 after the passage of Hurricane Fran. Anoxia and fish kills occurred along the entire estuary. A smaller, although significant fish kill occurred in the middle estuary in late July 1998. While problems associated with excessive nutrient loading such as algal blooms, anoxia, macrophyte mortality, and fish kills have occurred occasionally in the Neuse Estuary in the past, all of these water quality problems appear presently to be at all time highs.

Table 1. Drainage Areas of Watersheds Within the Neuse River Basin (from Bales and Robbins 1999)

Location	Drainage Area (km^2)	Percentage of Total
Neuse River at Streets Ferry	10,497	74.7
Trent River at mouth	1,350	9.6
Swift Creek at mouth	869	6.2
Bachelor Creek at mouth	166	1.1
Upper Broad Creek at mouth	143	1.0
Goose Creek at SR1100	65	0.5
Slocum Creek at mouth	135	1.0
Hancock Creek at mouth	84	0.6
Clubfoot Creek at mouth	60	0.4
Adams Creek at mouth	107	0.8
Greens Creek near Oriental	37	0.3
Direct Runoff to Estuary	542	3.9
Neuse River near Oriental	14,055	100.0

2.2 Previous Studies

Measurement based research on nutrient dynamics in the water column and sediments of the Neuse River Estuary have been ongoing for over twenty years. During the last decade, there have been studies of nutrient distributions within the estuary (Christian et al. 1991 Paerl et al 1995), on the local and ecosystem level factors regulating primary production (Rudek et al.1991, Boyer et al. 1993), on the significance of nutrient and oxygen exchange with the sediments (Rizzo and Christian 1996, NC DWQ 1998), and on zooplankton grazing rates (Mallin and Paerl 1994).

A number of patterns have emerged from the monitoring work. Nutrient concentrations generally decrease downstream, although at different rates, so that the time-averaged N:P ratio decreases downstream (Christian et al. 1991, Paerl et al. 1995). Nitrate concentrations in the upper estuary are generally more than an order of magnitude higher than the lower estuary. Temporal variability in both nutrient concentrations, chlorophyll-a concentrations, and primary productivity are significant, with variations occurring both seasonally and associated with loading events from high river flows (Rudek et al. 1991, Boyer et al. 1993, Mallin et al. 1993, Paerl et al. 1995). The monitoring data suggest that limitation of phytoplankton productivity may result from low temperature, light, or nutrients at certain times and places within the estuary and that accumulation of chlorophyll biomass is also affected greatly by changing water residence times.

Two previous transport model studies have been completed for the Neuse River Estuary. Lung (1988) used WASP to investigate the factors related to blue-algal blooms. Robbins and Bales

(1995) used a two-dimensional, vertically averaged circulation and transport model to predict water motions and salinity distributions within the estuary during 1991. The monitoring effort associated with the transport modeling of Robbins and Bales (1995) was utilized to provide the downstream boundary elevation, water velocity, and salinity data for the March - September 1991 data set. Robbins and Bales (1995) predicted that lateral variations in longitudinal water velocities could be significant during certain forcing conditions within the estuary over relatively short time periods.

2.3 Description of Hydrologic Conditions

2.3.1. March – September 1991

As mentioned earlier, two separate data sets were prepared for this study. The first data set covers the time period March – September 1991. This particular time period was selected because it had sufficient boundary condition data at both the upstream and downstream boundaries of the model region. Initial collection and preparation of the data set was conducted by the USGS and DWQ. Preparation of these data files is described elsewhere (Bales and Robbins 1999).

Nineteen ninety-one was a relatively normal year hydrologically, with Neuse River streamflows that were on average not significantly different from historical averages (Figure 2). Compared to Neuse River flows measured at Kinston (reported in Paerl et al. 1995) from 1987 – 1993, the 1991 monthly and yearly average flows were similar to these other years. The time period under study was distinctive, however, in having several relatively large runoff events during the summer months. In late June and again in early August, high runoff events occurred. The August event was particularly impressive, with streamflows that for an entire week were nearly three times the average for August (Figure 2). Inorganic nitrogen loading during this time also greatly exceeded the longer-term average, so that a significant fraction of the total summer inorganic nitrogen load was associated with three high-flow events in late May, late June, and early August. Overall, the summer of 1991 was relatively dry, with June, July, and September all below average with respect to Neuse River streamflow (Figure 2). Spring flows were also generally below average, although not dramatically so.

The molar ratio of inorganic nitrogen to phosphorus was quite variable in 1991, although the value was generally above the Redfield molar ratio value of 16:1 (Figure 3). The Redfield ratio is that assumed to be representative of phytoplankton biomass (Redfield et al. 1963), thus measured N:P molar ratios above the Redfield value might indicate a relative abundance of nitrogen compared to phosphorus, i.e., phosphorus limitation of phytoplankton growth. Some seasonality in the ratio is apparent, with higher ratios in the summer and fall (> 20:1) than in the spring (< 20:1). The three high-flow events mentioned earlier produce N:P ratios that are somewhat lower than for other times during 1991, although these lower values (17:1 – 22:1) are still well above the Redfield molar N:P ratio (Figure 3).

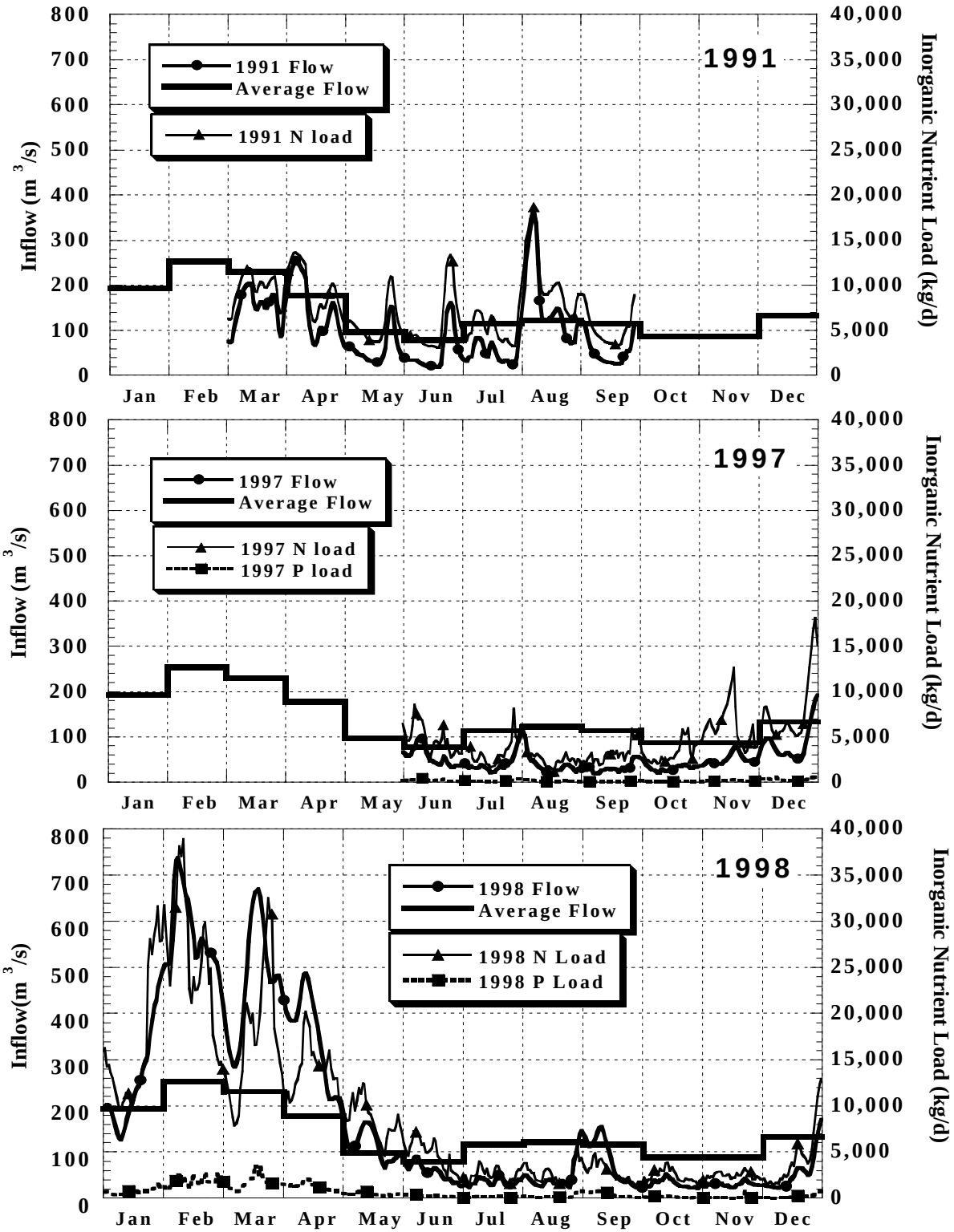

Figure 2. Loadings of freshwater and inorganic nutrients to the Neuse River Estuary at Streets Ferry, NC during 1991, 1997, and 1998.

2.3.2 June 1997 – December 1998

The latter half of 1997 was an uneventful year hydrologically with regard to the Neuse River Basin, and relatively benign compared to previous years. Nineteen ninety-seven followed two years where significant loading events occurred. In 1995, a high-flow event occurred in June, which was followed by a long period of hot dry conditions. This lead eventually to serious water quality problems as mentioned earlier, and discussed elsewhere (Paerl and Pinckney 1996). In September of 1996, an historic event runoff event occurred as Hurricane Fran dumped over 10 inches of rain in two days onto much of the watershed. High river flows and high nutrient and organic matter loading ensued, which was quickly followed by anoxia and a major fish kill. In contrast, 1997 had no high flow events during the period from June to December. All seven months during the period had Neuse River flows below the monthly average (Figure 2). The two relatively high-flow events, which occurred in early June and early August, brought the flow only up to the average monthly values. Throughout 1997, the ratio of inorganic nitrogen to phosphorus was above 20:1, and also above the levels seen in 1991 (Figure 3). The nitrogen to phosphorus ratio was generally lower in the summer than in the fall and early winter.

In contrast to the other two years, 1998 had a very wet spring, with Neuse River inflows above the historical average for January, February, March and April (Figure 2). Over this period, Neuse River inflows were more than twice the historical average for the period (Figure 2). Not surprisingly, nutrient loadings were also relatively high during this period (Figure 2). The nitrogen to phosphorus molar ratio for the period was relatively low (Figure 3). As for 1991, the nitrogen to phosphorus molar ratio was generally above 16:1, indicating the possibility of phosphorus limitation of algal growth (Figure 3). The remainder of 1998 was relatively dry, with every single month from May through December below the historical average. The only significant inflow during the period occurred during late August and early September. During this period, inflows were at or just above the historical monthly averages (Figure 3). As in 1997, N:P ratios are generally higher than in 1991, but are highly variable (Figure 3). As for the other years, the inorganic nitrogen to phosphorus concentration ratios are above the Redfield ratio value of 16:1.

The three years simulated were distinctly different in the timing of high flow events. Only one of the years, 1998, had cumulative inflows above the historical average (Figure 4). The highest flows in this year were in January, February, March and April. In contrast, 1997 had cumulative inflows much below average, and had no significant inflow events (Figure 4). In this year every single monthly average inflow was below average. Only 1991 had significant inflows in the summer months (Figure 4). The cumulative inflow over the seven month simulation period in 1991 was near the historical average value. In summary the three simulation years include a dry (1997), average (1991), and wet (1998) year. High flow events occurred in two of these years; in the summer of 1991 and the winter and early spring of 1998.

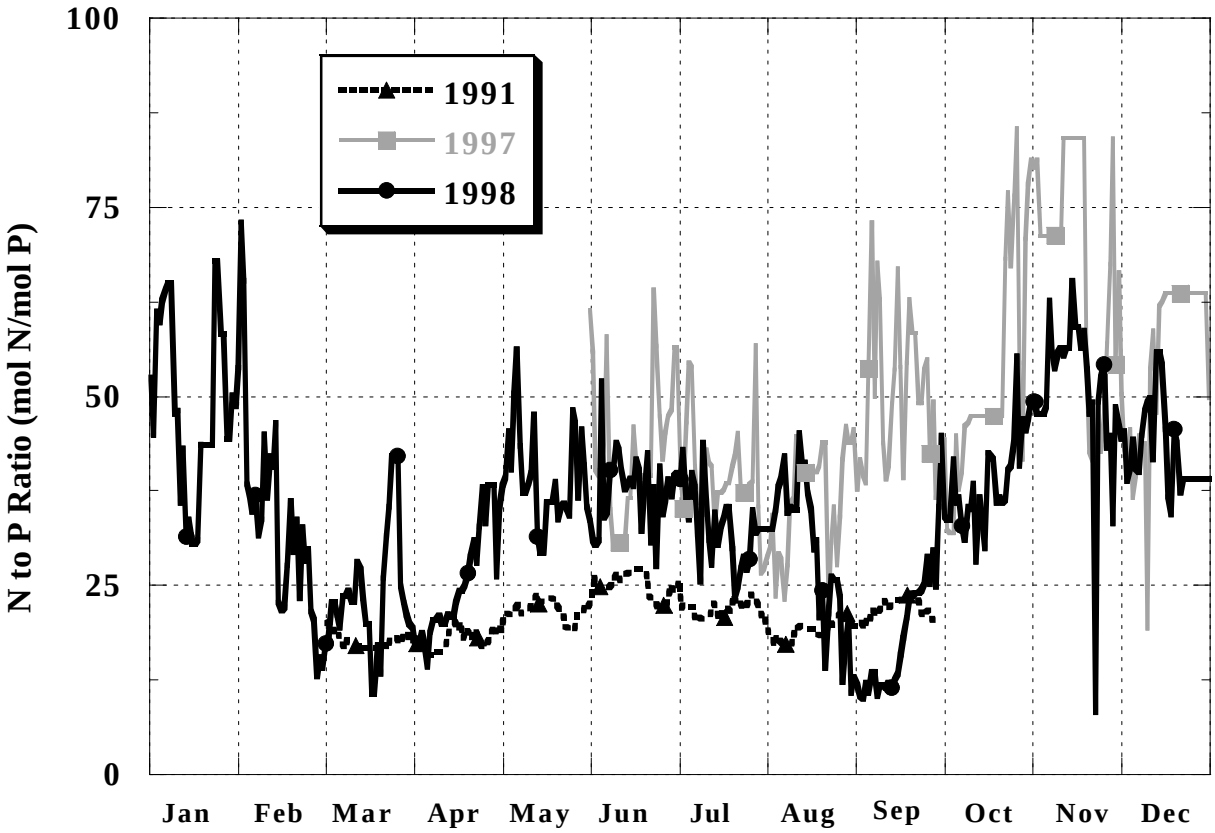

Figure 3. Inorganic nitrogen to phosphorus molar ratio of the inflowing water to the Neuse River Estuary at Streets Ferry, NC during 1991, 1997 and 1998.

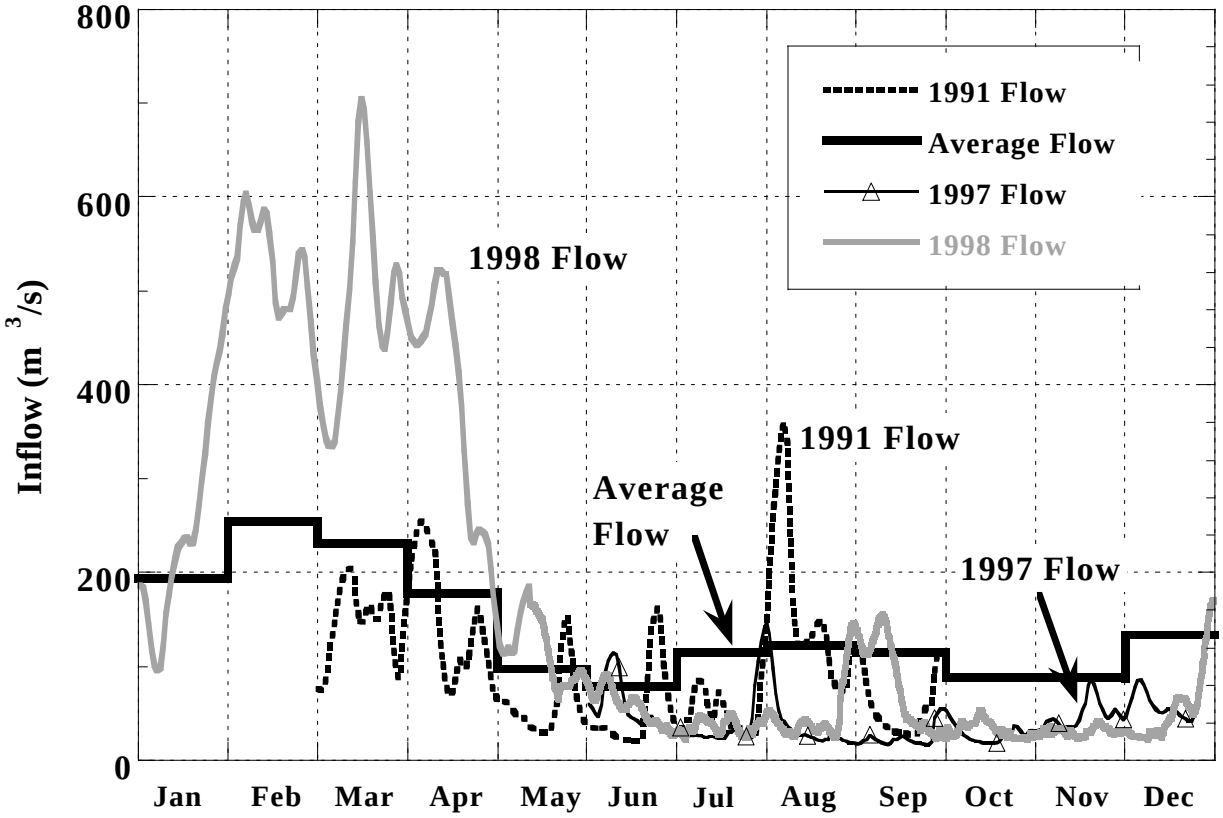

Figure 4. Comparison of Neuse River inflows to the estuary for the three years simulated using the Neuse Estuary Eutrophication Model.

3. METHODS

3.1 Model Description

Development of the Neuse Estuary Eutrophication Model was begun through the joint effort of the USGS and the NC DWQ (Bales and Robbins 1999). In developing a eutrophication model for the Neuse Estuary it was considered critical that vertical and longitudinal variations in water quality be considered. Monitoring had determined that significant longitudinal and vertical variations occur in the estuary in salinity, nutrients, chlorophyll-a, and dissolved oxygen, (e.g. Christian et al. 1991, Paerl et al. 1995). Longitudinal variations in primary productivity and benthic nutrient and dissolved oxygen fluxes (Boyer et al. 1993, Rizzo et al. 1992) were also observed. While lateral variations in circulation patterns were observed in one study (e.g. Robbins and Bales, 1995), it was decided during model selection that these motions act primarily as a source of lateral mixing rather than as an important factor in determining estuarine flushing. In addition, the existing monitoring data showed no evidence of significant lateral differences in seasonally averaged water quality constituents. Considering these factors it was decided to apply a two-dimensional, laterally averaged model. At the same time a monitoring program was initiated that would collect the monitoring data needed to apply the two-dimensional model while further investigating the extent to which water quality conditions varied across the channel (Luettich et al. 2000). CE-QUAL-W2 was chosen for application to the Neuse River Estuary.

CE-QUAL-W2 is a laterally averaged, two-dimensional hydrodynamic and water quality model (Cole and Buchak 1995). Due to the assumption of lateral homogeneity, the model is best suited for long and narrow bodies of water. However, the model can be applied to many types of waterbodies where lateral variations are less significant than variations in the other two directions. The model has been applied to a variety of rivers, lakes, and estuaries, typically by specifying upstream flow and downstream elevation or flow boundary conditions. The model also allows for application to complex waterbodies by incorporating multiple branch algorithms and provisions for multiple inflows from point/nonpoint sources and precipitation. The hydrodynamic capabilities of W2 include prediction of water surface elevation, velocities, and temperatures.

In addition to the hydrodynamic aspects, W2's water quality algorithms incorporate 23 constituents, 18 of which are used in this application (Table 2). These 18 constituents are linked to one another (Table 2) to simulate: 1) phytoplankton uptake and release of nutrients and CO_2 through photosynthesis and respiration; 2) remineralization of carbon and nutrients through phytoplankton mortality, exudation, and water column respiration; 3) consumption and production, and transport of dissolved oxygen (DO) through respiration, reaeration, and photosynthesis; and 4) recycling of nutrients and consumption of DO through sediment diagenesis.

Relative to other eutrophication models currently in use, CE-QUAL-W2 is of intermediate complexity. Its uses an "algebraic" turbulence model whereby vertical eddy viscosities and diffusivities, which determine vertical momentum and mass transport rates, are calculated using Prandtl's "mixing length" concept. Eddy viscosities vary both in time and space according to the

mixing energy available from wind and shear, as well as the turbulence suppressing effects of vertical density stratification. Eddy diffusivities are assumed to be a constant fraction of the calculated eddy viscosities. CE-QUAL-W2's water quality simulation routines use a relatively simple, single-constituent sediment diagenesis model. Other simplifications in the water quality model include a fixed carbon to chlorophyll ratio, fixed phytoplankton cell quotas for nutrients and carbon, and organic matter constituents that are all made up of identical fractions of carbon, nitrogen, and phosphorus (Cole and Buchak 1995). Even with these simplifications CE-QUAL-W2 is significantly more complex in its water quality routines than other commonly used eutrophication models such as WASP5 (Ambrose et al. 1993) or QUAL-2E (Brown and Barnwell 1987).

Table 2. Neuse Estuary Eutrophication Model Constituents

No.	Constituent	Input from Constituents	Output to Constituents	Unit
1	Tracer	None	None	mg/l
2	Salinity	None	none	g/l
3	Orthophosphate	8,9,10,11,13,14,15,18	13,14,15	mg/l
4	Ammonia	8,9,10,11,13,14,15,18	5,13,14,15	mg/l
5	Nitrite-Nitrate	4,18	13,14,15, N_2	mg/l
6	Dissolved Silica	7,8,9,10,11,13,14,15,18	13,14,15	mg/l
7	Particulate Silica	None	6	mg/l
8	Labile Dissolved Organic Matter (DOM)	13,14,15,16	9,3,4,6, CO_2	mg/l
9	Refractory DOM	8,16	3,4,6, CO_2	mg/l
10	Labile Particulate Organic Matter (POM)	13,14,15,16	13,14,15	mg/l
11	Refractory POM	11,16	3,4,6,18, CO_2	mg/l
12	BOD	16	CO_2	mg/l
13	Diatom OM	CO_2, 3,4,5,6,16	3,4,5,6,8,10,16, CO_2	mg/l
14	Green OM	CO_2, 3,4,5,6,16	3,4,5,6,8,10,16, CO_2	mg/l
15	Blue-Green OM	CO_2, 3,4,5,6,16	3,4,5,6,8,10,16, CO_2	mg/l
16	Dissolved Oxygen	13,14,15	5,8,9,10,11,12,13,14,15,18	mg/l
17	Temperature	None	none	deg C
18	Sediment OM	10,11,13,14,15,16	3,4,6, CO_2	mg/l

Note: All organic matter constituents (8-11, 13-15, 18) are assumed to be made up of identical fractions of carbon, nitrogen, and phosphorus.

3.2 Model Input Data

This study utilized the work done previously by Bales and Robbins (1999) to establish an initial model framework for the Neuse River Estuary. Model grid, bathymetry, branch and tributary inflow, downstream elevation, and meteorology data files had been prepared previously, and were used as a starting point for the preparation of the model grid and the 1991 input data set. Water quality information at the downstream boundary had also been assembled previously (Paerl et al. 1995), and was used in this study to create the necessary downstream boundary conditions files for 1991 temperature and water quality constituents. A more extensive water quality data set was available for 1997 and 1998 (Luettich et al. 2000). Both the 1991 and the 1997-1998 input data sets relied on water quality, sediment and water property, and meteorologic information originally collected by the National Weather Service, the NC Division of Water Quality, Weyerhaeuser, and the UNC Institute of Marine Sciences. More specific information on the procedures for creating model inputs from these data is provided in the following sections.

As mentioned earlier, work on the laterally averaged, two-dimensional model framework was begun before this study. An excellent review of the assumptions and capabilities associated with creation of such a framework is provided by Bales and Robbins (1999). The most important of these assumptions and capabilities can be summarized as follows:

- all lateral variations in model state variables are assumed to be less important than variations in the longitudinal and vertical directions, so that the assumption of lateral averaging is appropriate;

- the assumption used in CE-QUAL-W2 that all turbulence model and kinetic rate parameters are spatially and temporally invariant is appropriate;

- the estuary can be adequately represented by a relatively coarse grid having eight branches (Neuse and Trent Rivers, Upper Broad, Goose, Slocum, Hancock, Clubfoot, and Adams Creeks), three point-source discharges (Weyerhaeuser, New Bern, and Cherry Point Wastewater Treatment Plants), and three tributary streams (Swift, Bachelor, and Greens Creeks);

- using interpolation, a 1991 water quality data set can be assembled using available data collected on a biweekly to bimonthly frequency;

- all tributary and branch flow data can be estimated using streamflow yields for the Neuse and Trent Rivers;

- tributary and branch temperature data can be estimated using data collected in the estuary; and

- tributary and branch inflow water quality data can be adequately represented using available data with the assumptions that salinities are zero, that nutrients and

chlorophyll-a concentrations are equal to the method detection limit, and that dissolved oxygen concentrations are equal to 5.0 mg/l.

As will be seen in the following sections, a number of changes were made to the Bales and Robbins framework. A brief description of these changes is as follows.

- Water quality was simulated only for two branches (Neuse River, Trent River). Six other branches in the original model framework (Upper Broad Creek, Goose Creek, Slocum, Hancock Creek, Clubfoot Creek, and Adams Creek) were small in inflow, small in volume relative to the adjoining mainstem segment, and had no monitoring data available for calibration. Given the lateral homogeneity assumption in the model it seemed appropriate to neglect the impact that in-creek processes would have on material loading from these creeks to the Neuse mainstem. Therefore these six creeks were considered to be tributaries instead.

- The horizontal segmentation of the modeled region was developed further to improve numerical accuracy and improve execution time. This development resulted in more segments and less difference between the length of segments.

- A later version of CE-QUAL-W2 was used that allowed for multiple phytoplankton groups. Three groups rather than one were used to represent the phytoplankton population.

- Atmospheric deposition of ammonia, nitrate-nitrite, and phosphate was considered as an input into the estuary.

- A one-component sediment diagenesis model was utilized that allowed for temporal and spatial variations in benthic nutrient and oxygen fluxes.

- The model was developed so that bottom roughness could be spatially variant, and so that parameters in the turbulence model could be adjusted to optimize the model's fit to observed stratification data.

The following sections provide a detailed description of the development of the model and the data files necessary to run it.

3.2.1 Model Grid and Bathymetry

The model uses a computational grid for the discretized representation of the waterbody. The grid geometry is determined by specifying the length of every longitudinal segment, and the width and thickness of every vertical layer. As the number of segments increases, the spatial resolution increases as does the computation time, while numerical errors related to discretization decrease. It is desirable to determine a segmentation that gives good spatial resolution, acceptable levels of discretization error, and acceptable run times (Cole and Buchak 1995).

The study area consists of two rivers, nine creeks, and three wastewater treatment plants. As mentioned earlier, it was decided that the two rivers, Neuse and Trent, would be used as the branches making up the computational grid, and the creeks and wastewater treatment plants would be treated as tributaries, i.e., point source loadings into these two branches. The tributaries enter the system at a user-defined segment of the computational grid. The computational grid received from the USGS had 42 segments for the Neuse and Trent River branches (Bales and Robbins 1999). The Neuse River consisted of segments one through 37 and the Trent River segments 38 through 42.

In the original grid, the 42 segments varied greatly in length. It was a concern that the model would not make accurate predictions as a result, considering the relatively small number of segments, and the relatively large changes in segment length. Convergence testing was performed to determine the effects of changing the number of the segments on computational time and numerical accuracy. The transport and mixing of a hypothetical, conservative tracer was simulated in the convergence testing; the number of segments was varied from 42 to 147. The starting point for convergence testing was the existing 42 segment system. Each of these segments were first split in half to create a new bathymetry file with 80 segments, as each branch boundary has an upstream and downstream 'dummy' segment. The original bathymetry file was next split into thirds to create a 112 segment file and into fourths to create a 147 segment file. Through comparison of these cases it was determined that segment lengths longer than approximately 1.5 km produced unacceptably high amounts of numerical error.

Unfortunately, the preferred bathymetry file developed using the process described above produced very long run times because of very short segments (250 m) in the upper estuary. It was determined through additional testing that these short segments were providing little advantage with respect to numerical accuracy. It was therefore decided to create a new bathymetry file based on the NOAA navigation chart (NOAA Map 11552, Neuse River and Upper Part of Bay River), which allowed for complete control over segment length. The initial bathymetry file created from this map consisted of 50 segments. This new bathymetry file greatly improved execution speed. Based on a second round of numerical testing, it was decided to shorten the segments downstream of New Bern. With this final modification, the bathymetry file consisted of 66 segments (Figure 5).

In the bathymetry input file, the Neuse River includes segments one through 61, while the Trent River includes segments 62 through 66. The segment lengths are fairly uniform (Figure 6), with lengths that produce an acceptably low amount of numerical error. The numerical grid is made up a maximum of eighteen active vertical layers. All but the upper three active layers have thicknesses of 0.5 meters. The active layer third from the top is almost always the surface layer. This layer is one meter thick, and is centered at mean sea level. The grid was set up in this way to minimize layer addition and subtraction, which is computationally time consuming, and can introduce unwanted numerical dispersion. The two active layers above, which are utilized only during flood conditions, are two meters thick. The depth below mean sea level of the bottommost layer varies from segment to segment (Figure 6) and ranges from 4.0 meters (10 active layers) to 7.5 meters (17 active layers). Water depths generally increase downstream with relatively shallow spots near New Bern, Hampton Shoals, and Cherry Point. The top width of the estuary increases

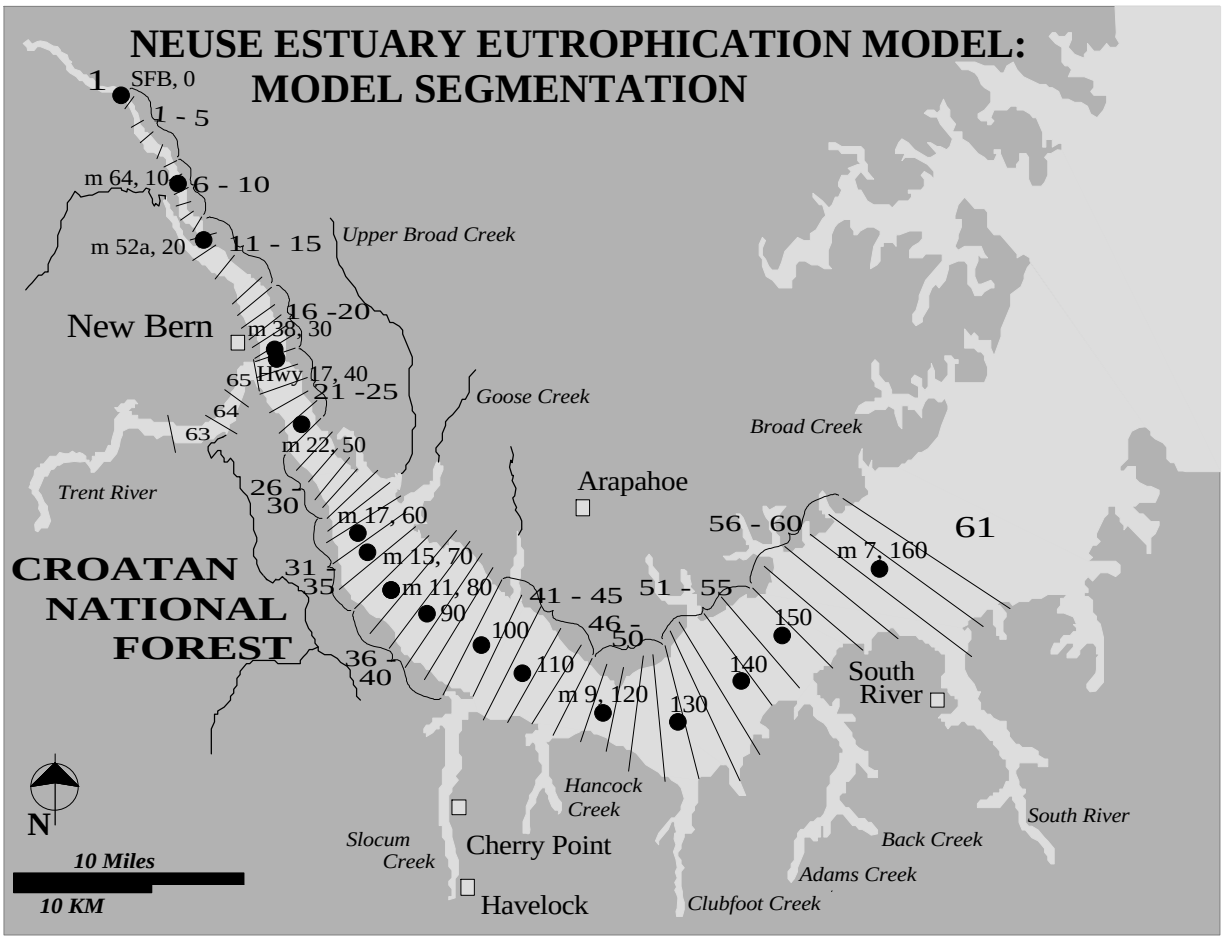

Figure 5. Neuse Estuary Eutrophication Model segmentation and MODMON monitoring stations.

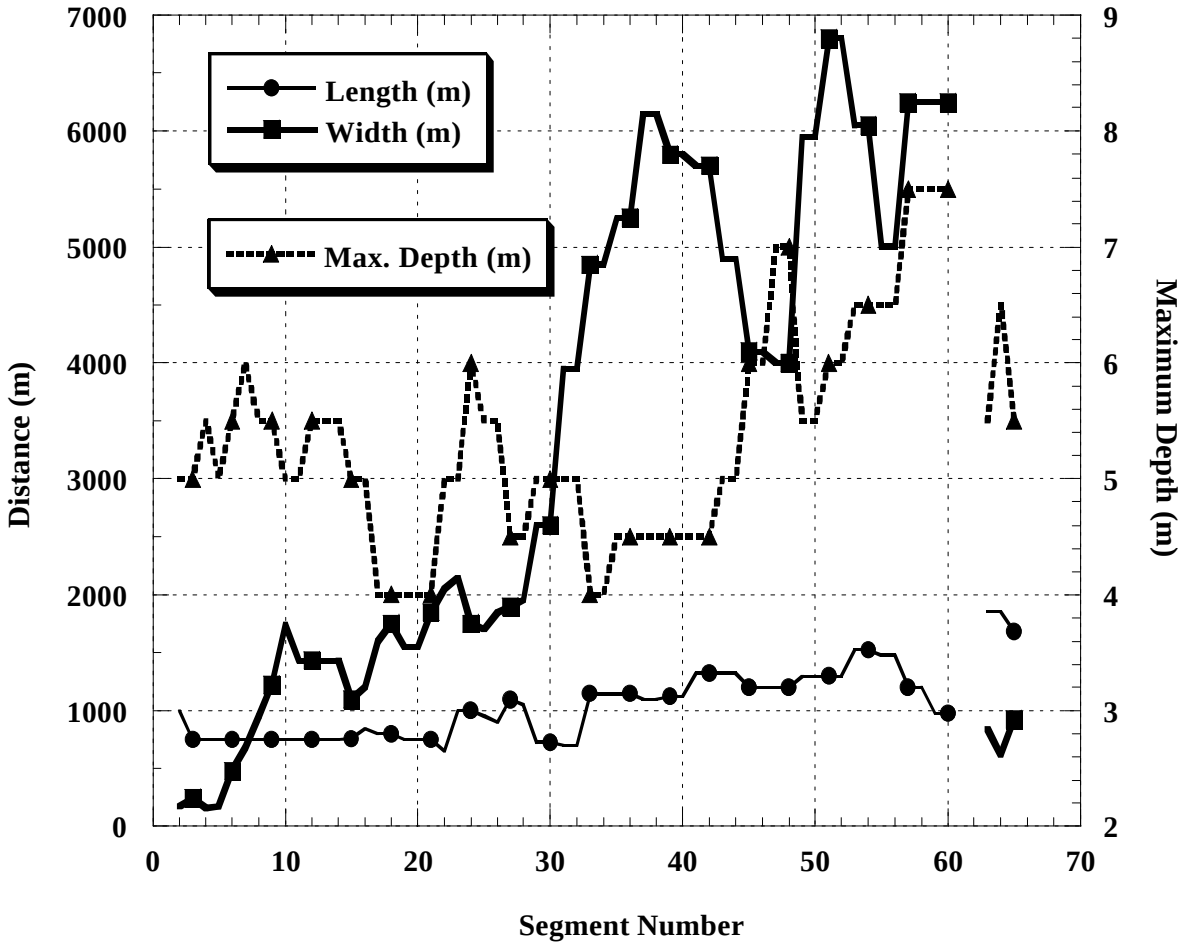

Figure 6. Neuse Estuary Eutrophication Model segment dimensions for the Neuse River (segments 2-60) and the Trent River (segments 63-65). Segments 61 and 62 are dummy segments that separate model branches 1 and 2, thus their dimensions are not defined.

downstream with the exception of the 'elbow' at Cherry Point. The model allows for specification of trapezoidally shaped cross-sections by allowing widths to be specified layer-by-layer, with the restriction that the widths be monotonically decreasing with increasing depth.

3.2.2 Branch and Tributary Boundary Conditions

The model allows the user to select either inflow/outflow or head boundary conditions. The type of boundary condition can be different at the upstream and downstream boundaries, but multiple upstream or downstream boundaries must be of the same type. Inflows were selected as the upstream boundary condition. Three data inflow files were specified for each branch and tributary within the modeled area. These files specify flows, temperatures, and constituent inflow concentrations.

The 1991 boundary data utilized the model framework developed by the USGS and NC DWQ (Bales and Robbins 1999). A variety of data sources were utilized in developing the branch inflow (Table 3) and tributary inflow (Table 4) data files. In some cases it was necessary to assume water quality conditions (Table 3, Table 4). The 1997-1998 data set was more complete as daily inorganic nitrogen concentrations and temperature were available for both branches, and water quality data were also available in the estuary as part of the MODMON monitoring program (Luettich et al. 2000). Data sources for the 1997-1998 branch inflow data were identical to those from 1991.

In 1991, the flows for Swift Creek, Bachelor Creek, Upper Broad Creek, Goose Creek, Slocum Creek, Hancock Creek, Clubfoot Creek, Adams Creek, and Greens Creek were not available. Flows for these watersheds were estimated by assuming that watershed yield (flow/drainage area) for each watershed was the same as for the Neuse River at Kinston. The Kinston flow record could then be used to estimate flows according to the relative drainage areas (Table 1). More information on this procedure is available elsewhere (Bales and Robbins 1999). In 1997 and 1998 a flow record for Swift Creek was available and was used. The other flows were calculated as for 1991. Branch inflow temperature data was unavailable for 1991, and was therefore estimated from water temperature data at USGS stations S2 and S4 and air temperature data at the New Bern Airport and the Cherry Point Naval Air Station (Bales and Robbins 1999). The temperature data used for each inflow boundary corresponds to the nearest data station to the branch or tributary. In 1997 and 1998 daily temperature data were available from the USGS for the Neuse and Trent Rivers and Swift Creek. The remaining creeks were assumed to have the same inflow temperature as the Trent River. Daily temperature records were obtained from the NC Division of Water Quality for the three wastewater treatment plants (Weyerhaeuser, New Bern, Cherry Point).

Inflow concentrations were specified for each branch and tributary for each model constituent. Salinities were assumed to be zero for all branches and tributaries. In 1991 it was necessary to estimate many of the water quality constituent concentrations (Table 3). For 1997 and 1998, most of the constituents concentrations were established using monitoring data collected by the collective efforts of the NC DWQ, Weyerhaeuser, USGS, and the UNC Institute of Marine Sciences (e.g. Luettich et al. 2000). Daily nitrite/nitrate, ammonia, and total phosphorus and

weekly chlorophyll and dissolved oxygen concentrations were obtained from the NC DWQ for the Neuse and Trent Rivers and Swifts Creek. Weekly monitoring data for chlorophyll, particulate organic carbon, orthophosphate, and dissolved oxygen concentrations were available for the upstream boundary of the Neuse River at Streets Ferry from the MODMON monitoring program. These data were used to specify organic matter for all rivers and creeks, as described below.

Even with the comprehensive river and estuary monitoring program, however, some constituent concentrations still needed to be estimated. Concentrations of organic matter, which were assumed to be composed of fixed fractions of carbon, nitrogen, and phosphorus, were estimated from measurements of particulate organic carbon concentration at Streets Ferry (Luettich et al 2000). Particulate organic carbon (POC) was converted to total organic matter by regressing these measurements against corresponding BOD-5 measurements taken at Streets Ferry by NC DWQ, and applying two conversion factors, as follows. The BOD-5 concentrations were first converted to ultimate BOD by multiplying by 1.85, then the ultimate BOD was converted to total organic matter by assuming a stoichiometric ratio of 1.4 grams oxygen utilized per gram of organic matter (Bowie et al.1985). The riverine organic matter was then assumed to be 75% refractory and 25% labile, as was done previously when modeling the Tar-Pamlico Estuary (Hydroqual 1995). Dissolved silica concentrations in the tributaries and branch inflows were assumed to be one milligram per liter. This relatively high value was used to avoid silica limitation of diatom growth, which is not expected to occur in the Neuse (Hans Paerl, UNC Institute of Marine Science, personal communication, May 1998). Also, BOD-5 was added as a tributary inflow when data were available from the wastewater treatment plants. For these tributaries, other organic matter concentrations were assumed to be zero. BOD-5 concentrations

Table 3. 1991 Branch Inflow Boundary Condition Data Description

No.	Branch	Flows			Temps			Constituents		
		Data Location	Collected By	Freq.	Data Location	Collected By	Freq.	Data Location	Collected By	Freq.
1	Neuse River	Kinston	USGS	D	S2 & New Bern Airport	USGS/ NWS	H	Streets Ferry, Salinity assumed = 0	DWQ, IMS & Weyer-hauser	M
2	Trent River	Trenton	USGS	D	S2 & New Bern Airport	USGS/ NWS	H	Salinity assumed = 0; DO assumed = 5; NH_4, NOx, PO_4, algae assumed @ DWQ method detection limit	NA	M

Notes:

Frequency: H = hourly, D = daily, M = monthly

USGS = United States Geological Survey, DWQ = NC Division of Water Quality, NWS = National Weather Service

DO = dissolved oxygen, NOx = Nitrate + Nitrite

S2 = USGS monitoring station (Robbins & Bales 1995)

Table 4. 1991 Tributary Boundary Condition Data Description

No.	Tributary	Flows			Temps			Constituents		
		Data Location	Collected By	Freq.	Data Location	Collected By	Freq.	Data Location	Collected By	Freq.
1	Weyerhaeuser WWTP	@ WWTP	DWQ	Avg. M	@ WWTP	DWQ	Avg. M	@ WWTP	DWQ	Avg. M
2	Swift Ck.	Kinston	USGS	D	S2 & New Bern Airport	USGS/ NWS	H	Swift Ck mouth	DWQ	M
3	Bachelor Ck.	Kinston	USGS	D	S2 & New Bern Airport	USGS/ NWS	H	Salinity assumed = 0; DO @ 5 mg/l; NH_4, NOx, PO_4, algae @ DWQ method detection limit	NA	M
4	New Bern WWTP	@ WWTP	DWQ	Avg. M	@ WWTP	DWQ	Avg. M	@ WWTP	DWQ	Avg. M
5	Upper Broad Ck.	Kinston	USGS	D	S2 & New Bern Airport	USGS/ NWS	H	Same as Bachelor Ck. (see above)	NA	M
6	Goose Ck.	Kinston	USGS	D.	S2 & New Bern Airport	USGS/ NWS	H	Same as Bachelor Ck. (see above)	NA	M
7	Slocum Ck.	Kinston	USGS	D	S4 & Cherry Pt. NAS	USGS/ NWS	H	Same as Bachelor Ck. (see above)	NA	M
8	Cherry Point WWTP	@ WWTP	DWQ	Avg. M	@ WWTP	DWQ	Avg. M	@ WWTP	DWQ	Avg. M
9	Hancock Ck.	Kinston	USGS	D	S4 & Cherry Pt. NAS	USGS/ NWS	H	Same as Bachelor Ck. (see above)	NA	M
10	Clubfoot Ck.	Kinston	USGS	D	S4 & Cherry Pt. NAS	USGS/ NWS	H	same as Bachelor Ck. (see above)		M
11	Adams Ck.	Kinston	USGS	D	S4 & Cherry Pt. NAS	USGS/ NWS	H	same as Bachelor Ck. (see above)	NA	M
12	Greens Ck.	Kinston	USGS	D	S4 & Cherry Pt. NAS	USGS/ NWS	H	same as br 2-8 (see above)	NA	M

Notes:

Frequency: H = hourly, D = daily, M = monthly, Avg. M = average monthly

WWTP = wastewater treatment plant, NAS = Naval Air Station

USGS = United States Geological Survey, DWQ = NC Division of Water Quality, NWS = National Weather Service

DO = dissolved oxygen, NOx = Nitrate + Nitrite

S2, S4 = USGS monitoring station (Robbins & Bales 1995)

were assumed to be zero in all other tributaries. Daily orthophosphate concentrations were estimated from the total phosphorus measurements by regressing the MODMON orthophosphate concentrations at Streets Ferry against corresponding measurements of total phosphorus taken by the NC DWQ. Daily estimates of other parameters were obtained from the weekly measurements by linear interpolation.

3.2.3 Downstream Boundary Conditions

As previously stated, the model allows for inflow/outflow or head boundary conditions. There are two types of head boundary conditions, external and internal. The external specification requires separate files for vertical temperature profiles, vertical profiles for each constituent concentration, and a file containing time-varying elevations. Internal head boundaries are specified at the confluence of one branch with another. In this case temperature, constituent concentration, and water surface elevation are internally calculated by the model. The external head boundary condition is intended for estuarine simulations (Cole and Buchak 1995). External head boundary conditions were used at the downstream boundary of the model region near Oriental. In 1991, the downstream head data were collected from a variety of sources (Table 5). The downstream elevation file contained average hourly water elevation data collected from station WL4 near Oriental by the USGS (Robbins and Bales 1999). Downstream temperatures were assumed to be constant throughout the water column. The temperatures used were hourly averages from station S4 collected by the USGS. Constituent concentration data from Marker 6, collected monthly, were utilized to specify downstream constituent concentrations (Paerl et al. 1995). Constituent concentrations were assumed to vary linearly in time between monitoring events. A complete vertical profile of constituent concentrations was created through interpolation of near-surface and near-bottom data. Ideally an interpolation function could be developed based upon measured vertical profiles of either temperature or salinity. No such information was available for 1991, so a single vertical interpolation function was developed by assuming that the surface layer was always 2.5 m deep and the vertical variation was linear below the surface layer.

Monitoring data collected as part of the MODMON project were utilized for the 1997-1998 downstream boundary conditions (Luettich et al. 2000). Water level elevations were collected by the MODMON program at Light 1AC near Adams Creek (near MODMON station 150, Figure 5) for the last five months (August - December 1998) of the simulation period, which made it necessary to synthesize a downstream boundary elevation data set for the remaining 14 months. To do this, water levels from the Light 1AC location were compared to levels collected from the USGS site near New Bern (Hwy. 17, Figure 5). A phase lag of 0.75 hr. was applied to the Light 1AC data, then linear regression was utilized to determine an elevation offset and amplification factor (Light 1AC = 0.0015 + 0.8306 * New Bern). The full New Bern elevation data record was then modified in this way and used to represent the downstream elevation boundary condition. Biweekly water quality monitoring data were available from the MODMON program from surface and bottom samples taken at a site (Station 160, Figure 5) near the downstream boundary. Interpolation functions were developed using vertical salinity profiles collected at half meter intervals through the water column. Linear temporal interpolation was then used to develop the

Table 5. 1991 Downstream Head Boundary Condition Data Description

Elevations			Temperatures			Constituents		
Locn=	**Agency**	**Fr.**	**Locn=**	**Agency**	**Fr.**	**Locn=**	**Agency**	**Fr.**
WL4 (Oriental)	USGS	Avg. H.	S4 (Light 1AC, Adams Ck.) assumed isothermal	USGS	Avg. H	Marker 6 (Neuse R. mouth)	Paerl	M

Notes:
Avg. H = Average Hourly, M = monthly
USGS = United States Geological Survey, Paerl = Hans Paerl (UNC Institute of Marine Science, unpublished data)
WL4, S4 = USGS monitoring station (Robbins & Bales 1995)

complete time history for the downstream boundary. Particulate and dissolved organic matter concentrations consisting of organic carbon, nitrogen, and phosphorus fractions were estimated as described previously for the inflow concentrations using linear regression between measured BOD-5 and POC concentrations. In this case, however, the matter was assumed to be 50% refractory and 50% labile as was done in the Tar-Pamlico modeling study (Hydroqual, Inc. 1995).

3.2.4 Meteorological and Atmospheric Deposition Data

The meteorological data needed for the 1991 and 1997-1998 simulations (Table 6) were provided by the National Weather Service. The data were collected from the Cherry Point Naval Air Station. Parameters included in this file include air temperature, dew point temperature, wind speed, wind direction, and cloud cover. It was assumed these conditions were uniform throughout the study area. Wet deposition of nitrogen and phosphorus utilized measurements taken at Morehead City (Paerl et al. 1995), which is approximately 30 miles south of the Neuse Estuary. Dry deposition was assumed to be on average equal in magnitude to wet deposition (personal communication, Robin Dennis , Environmental Protection Agency, May 1998). Wet deposition concentrations were therefore multiplied by a factor of 2.0 to account for dry deposition.

Table 6. Meteorological Data Description

Parameter	Location	Agency/Reference	Frequency
Air Temperature	Cherry Pt. NAS	NWS	H
Dewpoint Temperature	Cherry Pt. NAS	NWS	H
Cloud Cover	Cherry Pt. NAS	NWS	H
Wind Direction	Cherry Pt. NAS	NWS	H
Windspeed	Cherry Pt. NAS	NWS	H

3.3 Model Development/Calibration/Verification

Early in the project it was decided that the currently available version of W2 (Version 2) lacked some features that were considered essential. The model developer, Tom Cole of the Waterways Experiment Station, was contacted, and he agreed to make available a pre-release copy of W2 version 3. This later version had the following advantages over version 2:

- capability to model multiple algal groups,
- addition of dissolved and particulate silica as constituents,
- addition of refractory particulate organic matter as a constituent, and
- capability to print out various derived constituents (e.g. phytoplankton community chlorophyll) and fluxes (e.g. sediment/water-column fluxes).

Several other improvements were made to the model during the study to improve the model's prediction capability or to improve the capability to display model output. These improvements included:

- specification of spatially varying bottom roughness,
- creation of additional derived constituents for the hydrodynamic model (e.g. gradient Richardson number),
- creation of an additional model output file tailored for use as input to a data post-processing system

Additional model development was conducted during calibration, as described below.

Model calibration work was conducted using both the 1991 and 1997-1998 data sets. Calibration of the Neuse Estuary Eutrophication model took place in three steps. The first step was water elevation calibration. This process involved comparing predicted elevations to observed elevations provided by the USGS. The data were compared by plotting a time history of model output to a corresponding time history of observed values.

The second step of the process was to calibrate the hydrodynamic model parameters by comparing model predictions and observations of water velocity, temperature, and salinity. Hydrodynamics model calculations are affected by longitudinal eddy viscosity (dispersion of momentum), longitudinal eddy diffusivity (dispersion of heat and constituents), and Chezy coefficients (bottom friction). The maximum eddy viscosity and the Chezy coefficients were the two parameters varied in the hydrodynamic calibration. Model runs were made with maximum eddy viscosities ranging from 10^{-4} to $3x10^{-3}$ m^2/s. Manning's n values, which were used to compute Chezy coefficients, were varied from 0.015 to 0.03. During model calibration it was found that the model as written did not allow for calibration of parameters in the turbulence model. It was found that these parameters needed to be varied to produce higher eddy viscosities in order to achieve acceptable fits to observed salinities. As will be discussed in the results section, the modeled salinities compared well to the observed data using higher maximum eddy viscosities, but a problem arose. The larger the maximum eddy viscosity, the slower the model ran, because of a numerical stability constraint related to the model's explicit numerical scheme

for velocity calculation. Also, it was discovered that the eddy viscosity was reaching the specified maximum value much more frequently than expected. It was decided therefore to rewrite the code so the maximum eddy viscosity could be increased to a point that would prevent the maximum eddy viscosity value from limiting momentum dispersion. The numerical scheme was also rewritten to have an implicit method for velocity calculation, which removed the numerical stability constraint on the execution time step. This model development produced a model that predicted salinities well and ran in a reasonable amount of time

Water quality calibration was conducted after hydrodynamic calibration. Water quality kinetic coefficients were set initially to values used for modeling eutrophication in North Carolina's Tar-Pamlico Estuary (Hydroqual, Inc. 1995). These values were considered to be an appropriate starting point for calibration because of the proximity of the Tar-Pamlico, and because of the similarity in the two model formulations. Kinetic parameters were then adjusted in order to produce an acceptable fit to observed data. Adjustments were made to all of the parameters that quantify phytoplankton growth, including temperature and light optima, nutrient half-saturation constants, sinking speeds, and mortality and respiration rates. Several of these parameters were also varied as part of the uncertainty analyses described in a following section. Many other rates of water column or sediment organic matter degradation or transformation were adjusted during the calibration in order to optimize the model's fit to the observed water quality data.

Additional sediment diagenesis model development was conducted during calibration. To produce an acceptable fit to observed dissolved oxygen data, it was necessary to initialize the sediment organic matter constituent to a non-zero value that varied spatially. A new parameter was added to the model that allowed the initial sediment organic matter to be specified individually for each layer of each segment.

Since both the 1991 and 1997-1998 data sets were used for calibration, it was not possible to perform a typical model verification exercise. Calibration was performed sequentially, first using the 1991 data set, and then using the 1997-1998 data set. It was decided, therefore, to verify the calibrated model using the 1991 model input data set. Unfortunately, because of the relatively scant 1991 water quality monitoring data, much of the 1991 water quality model input data were estimated, thus no conclusive information could be obtained by performing water quality model verification using the 1991 model input data set. Verification of the Neuse Estuary Eutrophication Model was therefore limited to the hydrodynamic and conservative transport routines, using the 1991 data set. The quality of the 1991 hydrodynamic data was considered to be acceptable for this purpose. Verification was accomplished by running the calibrated model with the 1991 data set without adjusting model coefficients. Results of these simulations are presented in the results section.

3.4 Nutrient Reduction Scenarios

One of the main objectives of developing the Neuse Estuary Eutrophication Model was to evaluate the impact of a 30 percent reduction in nutrient loading to the estuary. In this study we focused solely on consideration of reductions in inorganic nitrogen (nitrate/nitrite and ammonia)

and phosphate loadings. Reductions in organic nutrients were not considered. Nutrient loading reductions scenarios were accomplished by reducing the concentration of inorganic nitrogen and/or phosphorus in the freshwater entering the estuary from rivers, creeks, and wastewater treatment plants. No changes were made to precipitation or downstream boundary concentrations. All freshwater flows were held constant at the measured or estimated values. The nutrient concentrations were reduced in the two branch inflow constituent files and the 12 tributary inflow concentration files. The model was first run using two reduction scenarios: (1) reduced nitrate/nitrite inflow concentrations, (2) reduced nitrate/nitrite and orthophosphate concentrations. Based upon the results of these runs it was later decided to add a third scenario that reduced only the orthophosphate inflow concentrations.

3.5 Uncertainty Analysis

The objective of the uncertainty analysis was to estimate the degree to which errors in model formulation, boundary and initial condition specification, and parameter selection can produce uncertainty in model predictions. Development of methods for considering all these error sources was considered to be beyond the scope of this study. In this study we focused on the degree to which uncertainty (i.e. error) in model parameter specification could be propagated to produce uncertainty in endpoint predictions such as water quality improvement. A prediction uncertainty analysis of this sort, using CE-QUAL-W2, has been performed previously for an application in which dissolved oxygen depletion was predicted for an estuary receiving natural and anthropogenic loadings of organic matter (Bowen 1997). In that application the objective was to determine the degree to which dissolved concentrations would increase with reduced anthropogenic BOD loadings. The analysis method described in that study formed the basis for the uncertainty analysis described here. In addition, the results of Adams' (1998) analysis of parameter uncertainty magnitudes for a WASP5 model application to Lake Okeechobee were also utilized for this study.

The following is a brief description of the uncertainty analysis procedure. The method used has been referred to as a "regional sensitivity analysis" (Adams 1998). In this method, many feasible parameter vectors are identified through a trial and error process. Feasible parameter vectors are those that produce model simulations exhibiting a desirable system behavior, such as an acceptable fit to observed data. Candidate parameter vectors are produced by random or systematic sampling of individual parameters, each of which is considered to be variable over a specified range of values. The model is then executed repeatedly using each of the candidate parameter vectors. A quantitative screening procedure is then utilized to cull the feasible parameter vectors from all the candidate vectors. Once the set of feasible parameter vectors is established, then model predictions are determined for each vector, and the variability, or uncertainty of these predictions is determined. While the method examines only parameter specification error, it is useful in that it quantifies one of the sources of model uncertainty.

In this application all 115 kinetic parameters were initially considered as candidates for the uncertainty analysis. The multi-dimensional parameter space was sampled by selecting one of three possible values for each parameter considered to be variable. If all 115 parameters were considered variable, then $3^{115} = 7.4 \times 10^{54}$ parameter vectors would have to be evaluated for

feasibility by making a model run. Clearly, an initial parameter filtering was needed to reduce the number of variables, since each model run took a few minutes to complete. It was decided to focus the analysis on parameters that were most likely to produce variability in predictions of dissolved oxygen and/or chlorophyll. The set of variable parameters was first reduced to 20 by adopting the list of important model parameters identified by Adams (1998). From the list of 20 parameters, seven were identified as most important to predictions of DO and chlorophyll. (Table 7). Three parameter levels were tested for each of the seven variable parameters. The first level was the "base case" determined through calibration. The second and third levels were then determined by increasing or decreasing the base case values by 40%. The range of values for each parameter were then adjusted if necessary after comparing them to the parameter ranges determined by Adams (1998) through literature review. Using three levels for each of the seven variable parameters (Table 7) resulted in an analysis that considered 2187 candidate parameter vectors.

Table 7. Variable Parameters for Uncertainty Analysis

Parameter	No. of Levels*	Values	Units
Carbon to chlorophyll-a ratio	3	74.6, 45.0, 104	g/g
Phytoplankton N fraction	3	.070, .042, .098	(g/g dry
Labile POM decay rate	3	0.06, 0.036, 0.084	1/day
Maximum phytoplankton growth rate	3x3	3.0 2.4 3.8; 1.8 1.4 2.3; 4.2 3.4 5.3	1/day
½ sat'n cst. growth, N	3x3	0.030 0.020 0.300, 0.018 0.012 0.180, 0.042 0.028 0.420	g/m^3
Phytoplankton settling velocity	3x3	0.080 0.100 0.200, 0.048 0.060 0.120, 0.112 0.140 0.280	m/d
½ sat'n cst. growth, P	3x3	0.0040 0.0040 0.0200, 0.0024 0.0024 0.0120, 0.0056 0.0056 0.0280	g/m^3

* Phytoplankton kinetic parameters were specified for each of the three phytoplankton groups at three levels

The model was run with each of the 2187 candidate vectors and the model results compared to a specification of system behavior to determine which candidate vectors were feasible. The 1997-1998 input data set was utilized for the model runs. To minimize computational burden, the analysis was performed in two phases. In the initial phase all candidate vectors were considered, and a quantitative measure of the model's fit to observed data was determined. These 2187 runs simulated Neuse River water quality for a duration of 150 days, from July 20 - December 23, 1997. This time range was considered sufficient for identifying feasible parameter vectors in that it spanned a period from late summer through early winter. Comparisons were made between model predictions and observations of nitrate/nitrite, ammonia, orthophosphate, dissolved oxygen, and chlorophyll-a concentrations collected between August 20 and December 17, 1997. Using the MODMON data set (Luettich et al. 2000), surface and bottom observed data were available biweekly during this time period at approximately ten stations for each of the parameters listed.

Two statistical measures of model fit were calculated for each parameter: the mean of the absolute errors between predictions and observations, and the correlation coefficient between predictions and observations. A candidate parameter vector was considered feasible if the degree of model fit using each of the two measures for the five parameters was at least as good as the base case determined through calibration. Each feasible parameter vector was then used for two additional model runs. The full 578 day 1997-1998 input data set (June 1, 1997 - December 31, 1998) was used for these two runs. In the first of the two runs all nutrient concentrations were left unchanged, while in the second run both the inorganic nitrogen and inorganic phosphorus concentrations were reduced by 30% as described earlier. Dissolved oxygen and chlorophyll-a concentrations were then compared for each set of two runs. Results of the uncertainty analysis are presented in the following section.

4. RESULTS

4.1 Predictions Using the 1997-1998 Data Set

The 1997-1998 data set was used for three purposes: 1) to set model parameters through calibration to observed data, 2) to predict the impact on water quality of a 30% reduction in inorganic nutrient loading (nitrogen and/or phosphorus), and 3) to estimate the uncertainty in the prediction of water quality improvement. Results of the simulations of 1997-1998 hydrodynamic and water quality conditions are presented in the following sections.

4.1.1 Hydrodynamic Model Calibration

Each of these observed data sets was utilized during the hydrodynamic model calibration. Hourly observed water level data were available from the USGS at a station on the Highway 17 bridge in New Bern. Vertical salinity and temperature profiles were collected from 10 to 16 stations (Figure 5) on a weekly basis as part of the MODMON monitoring program. The MODMON program also included continuous monitoring of water velocities from a moored acoustic doppler current profiler near Cherry Point.

Overall, the model calibrated well to the observed water elevation data set. Over the 19 month 1997-1998 simulation period (June 1, 1997 – December 31, 1998) the water surface elevations varied by approximately 1 m around mean sea level at New Bern (Figure 7). For this time period, the mean absolute error between predictions and observations (MAE) was 0.0413 m, and the root mean square error (RMSE) was 0.0527 m. These errors are approximately 1% of the water depth at this location (segment 21, Figure 5, 6). Longer-term variations in the observed elevations were also present in the predicted values. For instance, a gradual decline in water elevations was seen in both the predicted and observed water levels between October 1997 and January 1998 (Figure 7). Beginning in January 1998, however, the Neuse River flows increased dramatically (Figure 4). Predicted and observed water levels show nearly identical increases (Figure 7) for this time period.

Focusing on a shorter period allowed for assessment of the model's ability to simulate higher frequency variations in water surface elevations. During July 1998 measured water surface elevations at New Bern consist of peaks that occur roughly once per day, with longer time scale variations of several days also visible (Figure 8). Differences between predictions and observations are usually less than 10 cm. Statistical measures of model fit for July 1998 (MAE = 0.0461 m, RMSE = 0.0596 m) are similar to those for the full simulation period.

The entire range of frequencies in water surface elevation variation can be examined by performing a spectral decomposition of the elevation time record. The resulting power spectrum for model predictions and observations can then be compared to assess the model's prediction ability over various time scales. The power spectrum of observed water surface elevations indicates the importance of diurnal and semi-diurnal variations, as peaks in the observed water level power spectrum occur near frequencies of one and two per day (Figure 9).

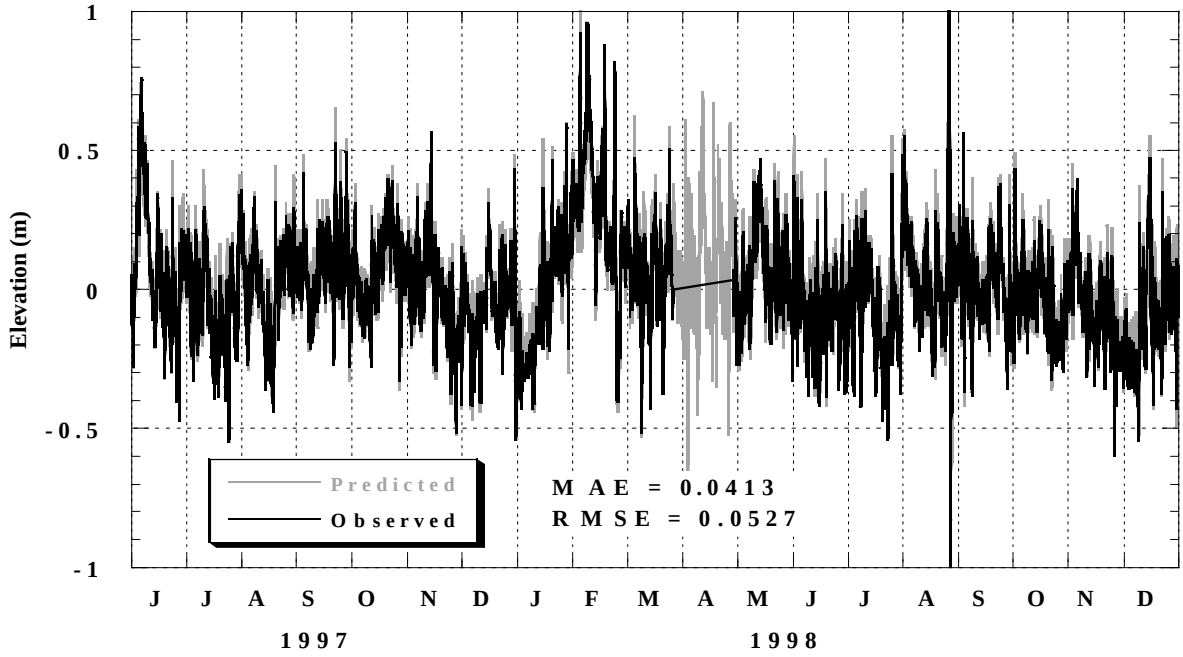

Figure 7. Model predicted and observed water surface elevations in the Neuse River Estuary near New Bern, NC during 1997 and 1998. The model's output frequency is 1 day; the observed data frequency is 1 hour.

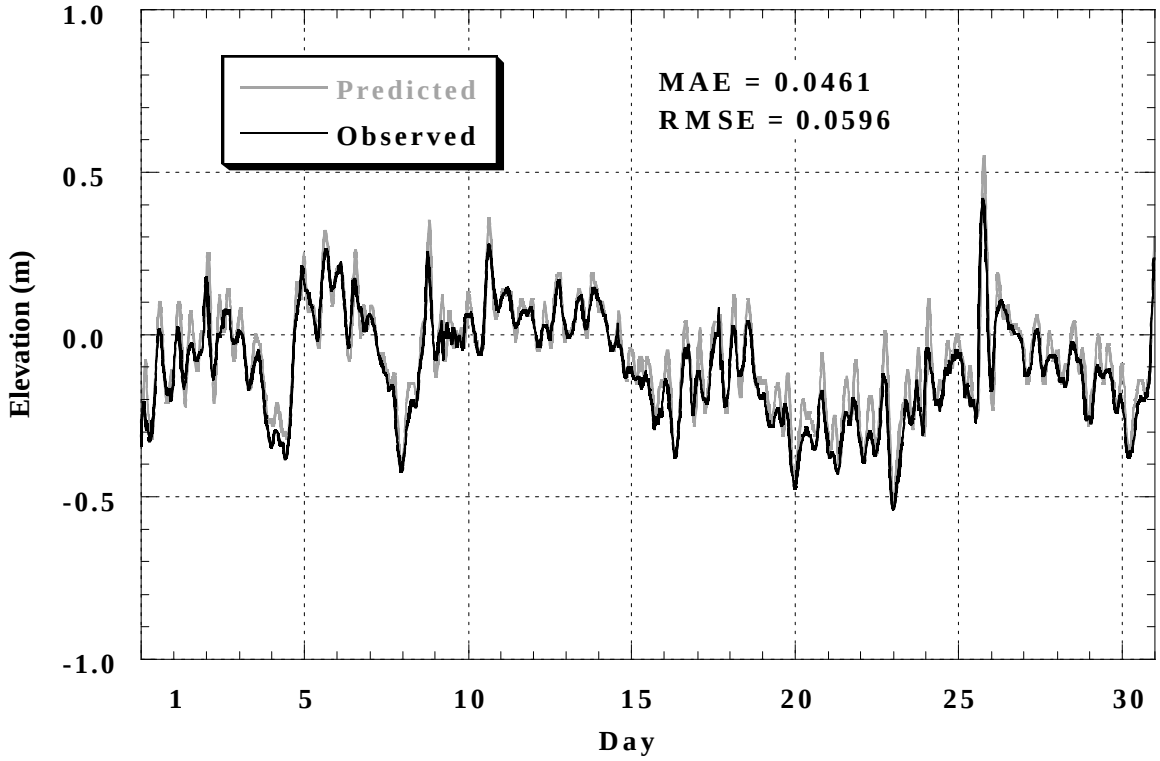

Figure 8. Model predicted and observed water levels in the Neuse River Estuary at New Bern, NC during July 1998.

A significant amount of variation also occurs at frequencies much less than one per day. No single frequency dominates the power spectrum. The model predictions show a similar pattern, but at frequencies above one per day the model overpredicts the degree of variation. The predictions also a peak in the power spectrum at two per day that is less pronounced in the observed data (Figure 9).

In early calibration runs the variation between the power spectra of model predictions and observations was quite a bit higher at one particular frequency (approx. 3.5 day^{-1}). A spurious peak at this frequency was observed in the model predictions. The magnitude of the peak increased for more upstream segments. The time period of the variations was also found to be roughly equal to twice the time necessary for a gravity wave to traverse the modeled region. This suggests that the peak was a result of reflections of wave energy within the model, perhaps as a result of the downstream boundary elevation specification. The magnitude of the peak was found to decrease as the boundary roughness increased. At the Manning's "n" value used (0.025) the magnitude of the peak was considered to be acceptably small.

During calibration, comparisons of near-surface and near-bottom salinity were performed using observed data from the MODMON monitoring program that collected on a weekly basis vertical profiles of salinity at 10 - 17 stations (see Figure 5 for station locations). Here we show time history comparisons for one station that is representative of the upper estuary (New Bern, Figure 10) and another station that is representative of the middle and lower estuary (Cherry Point, Figure 11). In general the model tracked well the seasonal variation in salinity. Throughout the latter half of 1997 salinities increased in the estuary. The surface waters at New Bern (Figure 10) were generally fresher than the surface water at Cherry Point (Figure 11). The entire estuary was stratified from mid-June onward, with surface to bottom salinity differences ranging from 2 - 8 g/l (Figure 10, 11). The degree of stratification, however, was quite variable. At a number of times during 1997 (e.g., late August, late October) the difference between top and bottom salinities decreased markedly. Each of these features of the observed salinity distributions were also found in the model predictions.

Much of the calibration effort for the circulation model focused on efforts to improve the model's prediction of vertical stratification. Initially, the model predicted much stronger stratification than was seen in the observed data. This was particularly true in the lower estuary, whereas upper estuary predictions were often under stratified. Through tuning of parameters in the turbulence model, it was possible to find a balance between underprediction of stratification in the upper estuary, and overprediction of stratification in the middle and lower estuary. Statistical measures of calibration were similar at New Bern and Cherry Point, with mean absolute errors (MAE) between predictions and observations of 1.21 and 2.00 g/l, respectively. These errors represent approximately 20% of the mean salinity values at these two locations. For the entire estuary, based on a comparison to 7,629 observed salinities, the model predicted 88.5% of the observed variation in salinity. The mean absolute error between predictions and observations was 1.26 g/l, which was 21% of the mean observed salinity during the time period.

Temperature predictions and observations showed similar patterns. Only slight differences were seen in top and bottom temperatures at New Bern (Figure 12) and Cherry Point (Figure 13). In

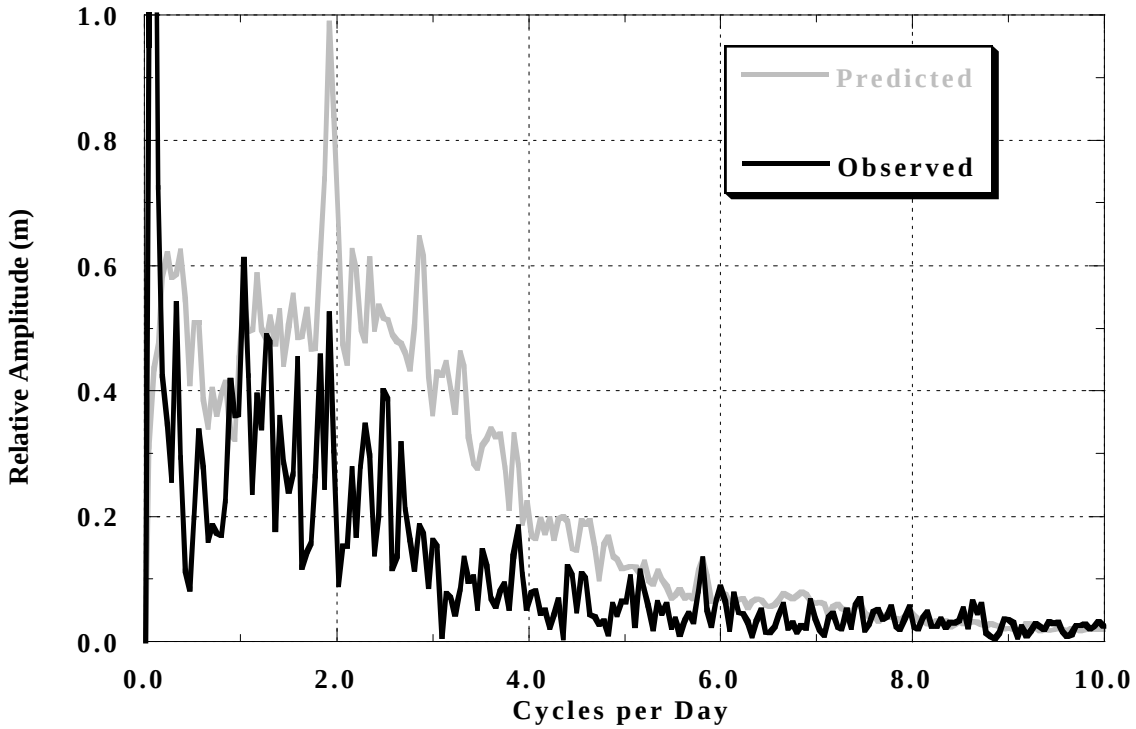

Figure 9. Relative amplitudes (m) of water surface elevation fluctuations based on model predictions and observations in the Neuse River Estuary near New Bern, NC during June through October 1997

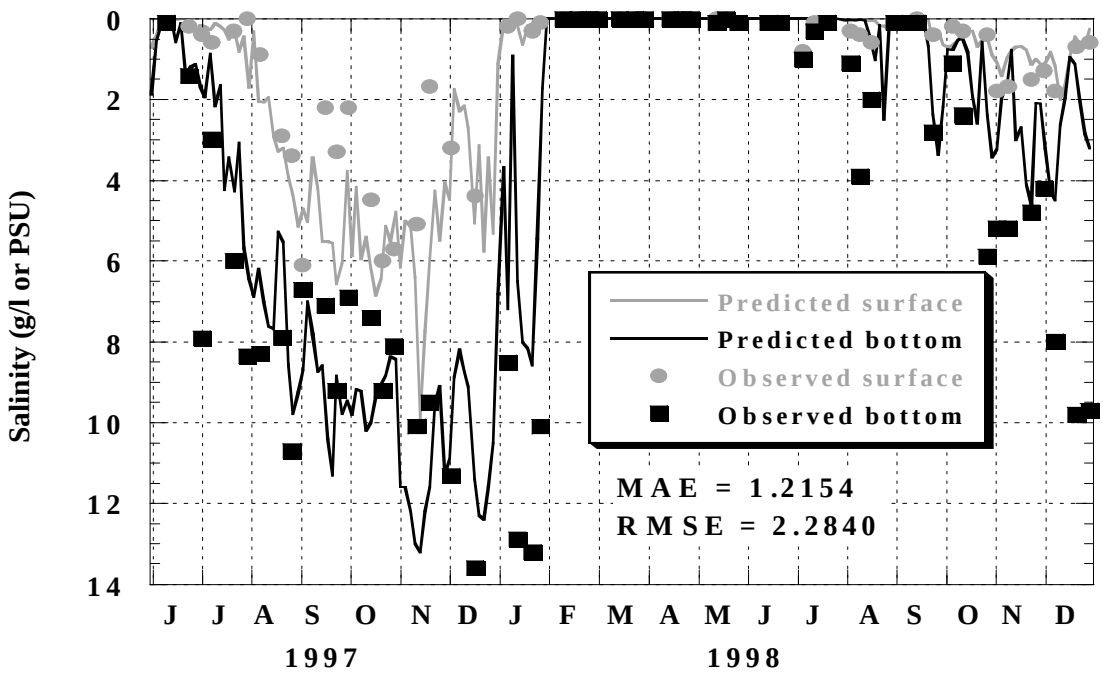

Figure 10. Model predicted (solid lines) and observed (symbols) salinities (g/l or PSU) for near-surface and near-bottom mid-channel waters in the Neuse River Estuary near New Bern, NC during 1997 and 1998.

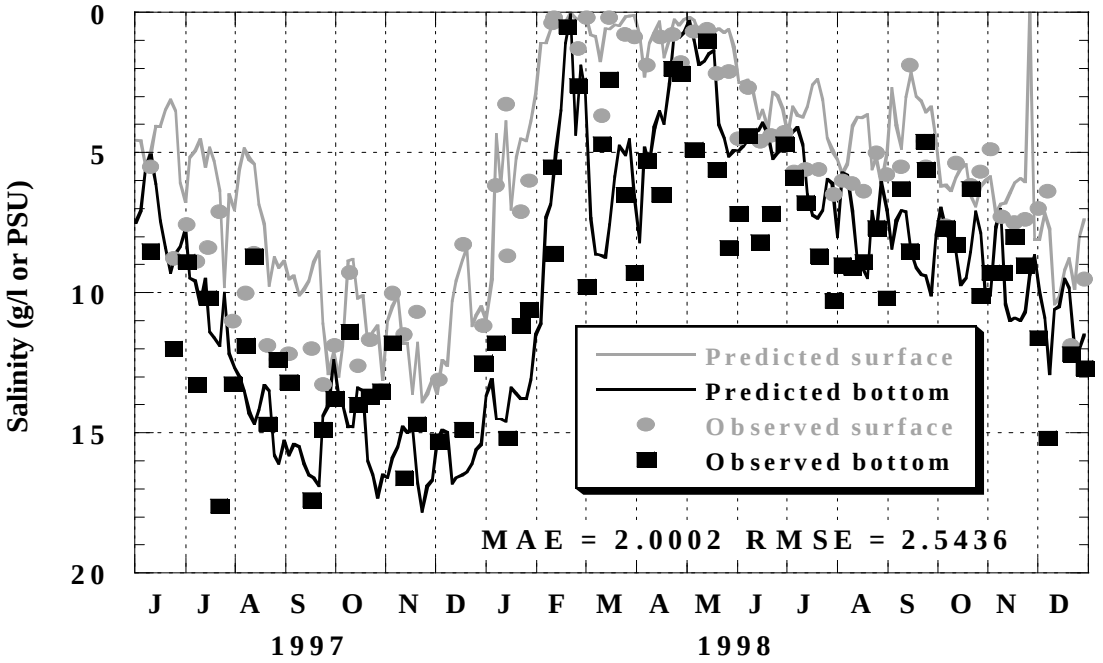

Figure 11. Model predicted (solid lines) and observed (symbols) salinities (g/l or PSU) for near-surface and near-bottom mid-channel waters in the Neuse River Estuary near Cherry Point, NC during 1997 and 1998.

both 1997 and 1998, the water temperatures reached a maximum value of approximately 30°C by early August. The minimum water temperature of approximately 8°C occurred in mid-January 1998. Surface waters were slightly warmer than bottom waters except for late fall and winter (Figures 12, 13). The mean absolute errors between observed and predicted temperatures were similar for New Bern and Cherry Point, with MAE values of 0.95°C and 0.90°C respectively. These error values correspond to roughly 5% of the mean water temperature for the estuary.

Comparing cumulative frequency distributions for observations and model predictions is a useful method for assessing a model's calibration performance. This comparison allows all predictions and observed data to be considered. In addition, it allows for assessment of the model's ability to predict mean and extreme values. An examination of the predicted and observed cumulative frequency distributions for salinities shows that the median predicted salinities are approximately 1.0 g/l less than observed values (Figure 14). The model underpredicts salinities by about 1.0 g/l for cumulative frequencies less than 0.90, which corresponds to a salinity value of 13 ppth. The upper 10% of the observed and predicted salinity distributions show a better degree of agreement, with errors that are less than 0.5 g/l (Figure 14).

Another important consideration in assessing the hydrodynamic model's calibration performance is its ability to simulate episodes of relatively strong stratification that in the summertime could inhibit vertical transport of dissolved oxygen to the bottom waters, thereby producing anoxia in these waters. Luettich et al. (2000) have observed particular summertime stratification conditions that may be associated with fish kills in the Cherry Point area. One such fish kill episode occurred in July 1998. Through most of the month there was little difference in salinities measured by monitors moored near the surface and bottom of the water column (Figure 15, middle panel), but sustained winds from the southwest near mid-July lead to increases in stratification by enhancing the estuarine circulation. The predicted salinities show a similar evolution, although stratification develops sooner (Figure 15, bottom panel). Near the end of the month a period of strong winds from the northeast is thought to have laterally transported anoxic bottom waters to the shallow flats on the northern shore of the estuary (Luettich et al. 2000), which produced a fish kill by trapping fish in the anoxic water volume. This wind reversal also lead to a breakdown in the salinity stratification (Figure 15, middle panel) by producing upstream directed surface currents that oppose the estuarine circulation. This connection between wind direction and surface currents can be seen in both the observed and predicted surface currents (Figure 16, middle and bottom panel). Winds from the southwest were associated with downstream surface currents, whereas winds from the northeast produced generally upstream surface currents (Figure 16). More information on predicted and observed dissolved oxygen concentrations at Cherry Point can be found in the following section.

4.1.2 Water Quality Model Calibration

During the water quality calibration, all constituents were examined qualitatively, with a quantitative calibration that focused on nutrients, chlorophyll-a concentrations, and dissolved oxygen. The objective of the calibration was to minimize the differences between observed and predicted concentrations of nitrate-nitrite, dissolved oxygen, and chlorophyll-a. Observations of

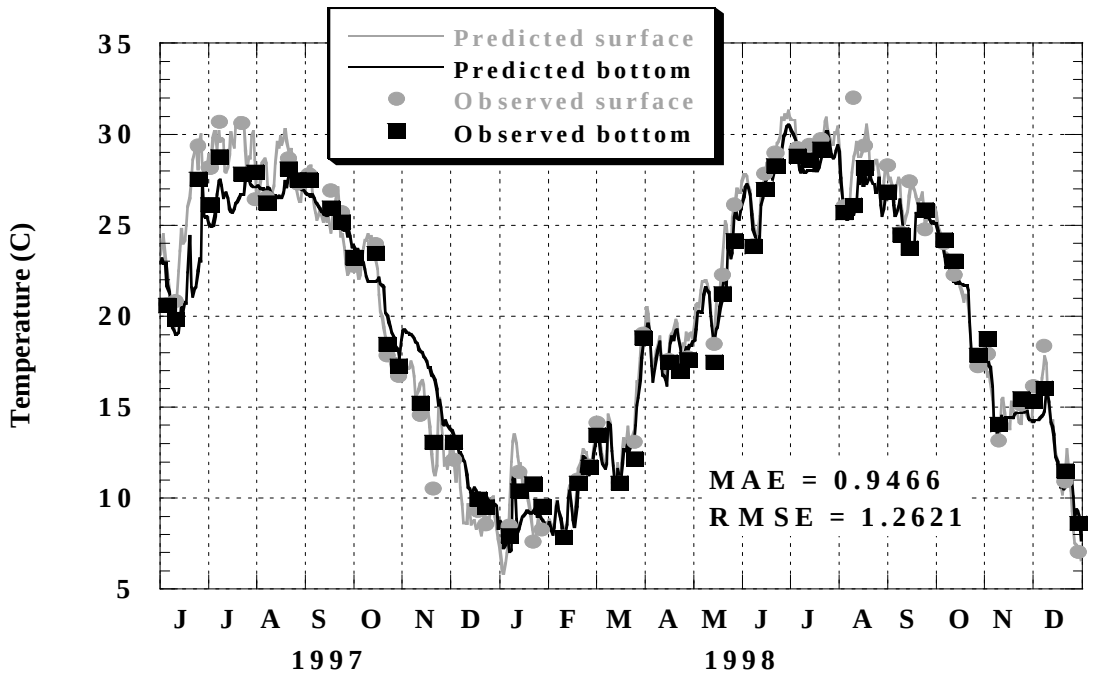

Figure 12. Model predicted (solid lines) and observed (symbols) temperatures (°C) for near-surface and near-bottom mid-channel waters in the Neuse River Estuary near New Bern, NC during 1997 and 1998.

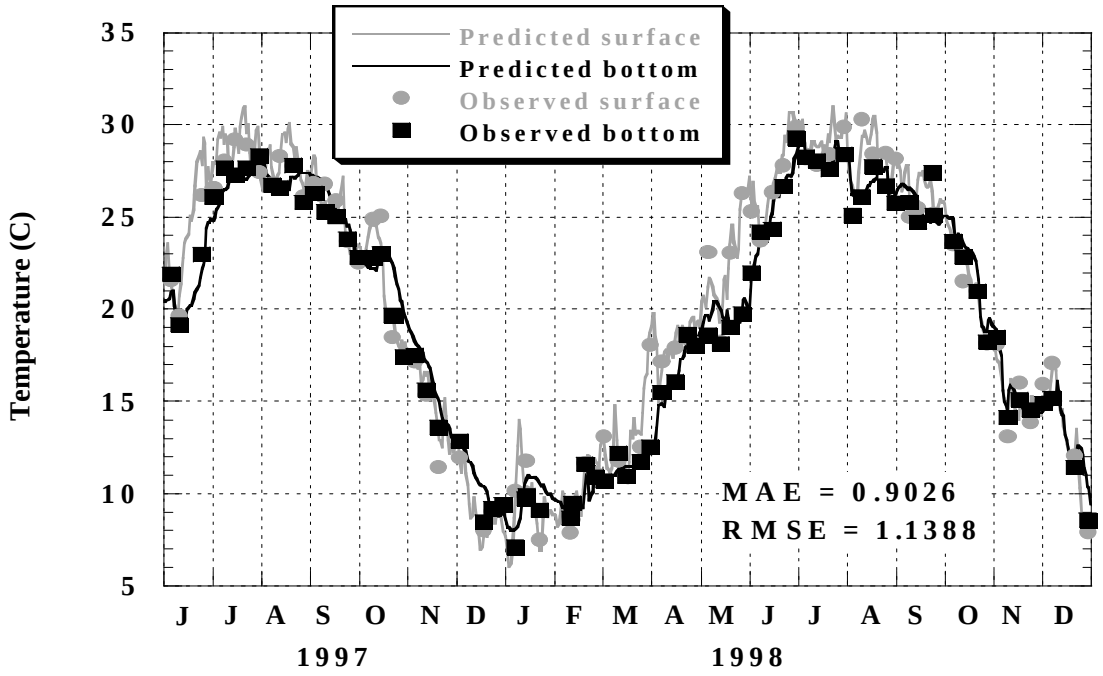

Figure 13. Model predicted (solid lines) and observed (symbols) temperatures (°C) for near-surface and near-bottom mid-channel waters in the Neuse River Estuary near Cherry Point, NC during 1997 and 1998.

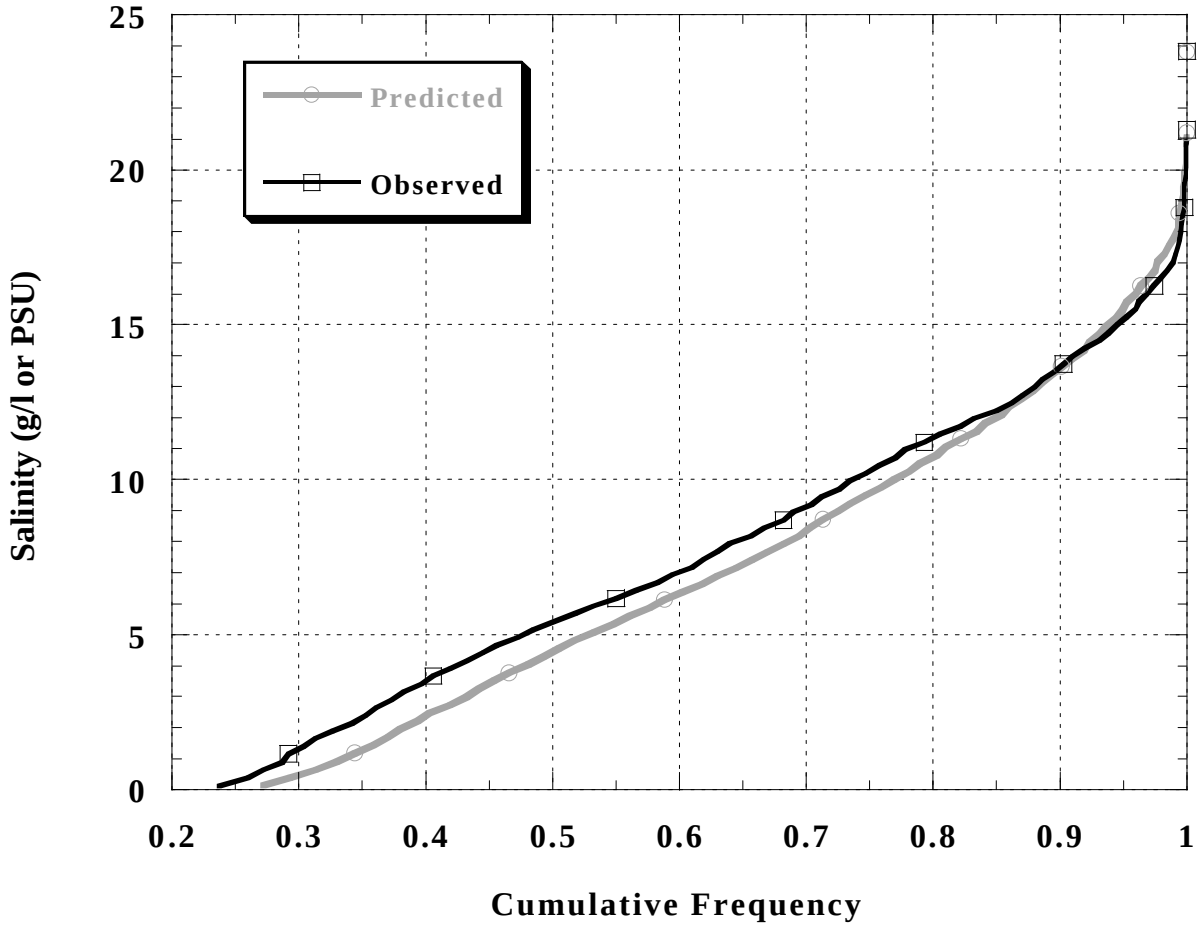

Figure 14. Cumulative frequency distributions for predicted and observed salinities in the mid-channel waters of the Neuse River Estuary during 1997 and 1998.

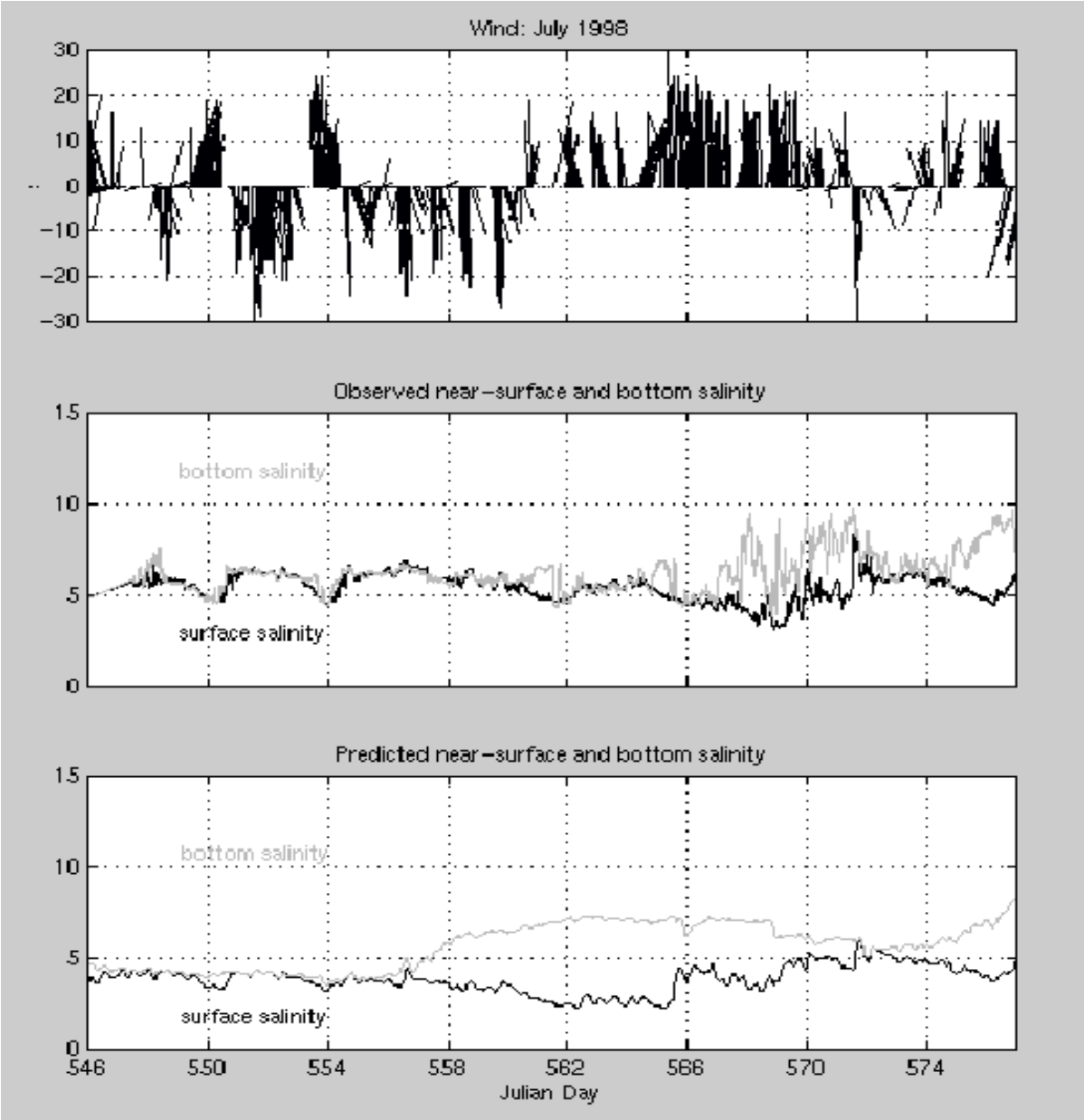

Figure 15. Wind speeds (top panel, mi/hr.), observed top and bottom salinities (middle panel, PSU), and predicted top and bottom salinities (bottom panel, g/l) in the mid-channel waters of the Neuse River Estuary near Cherry Point, NC during July, 1998 (Julian Day 546 = July 1, 1998).

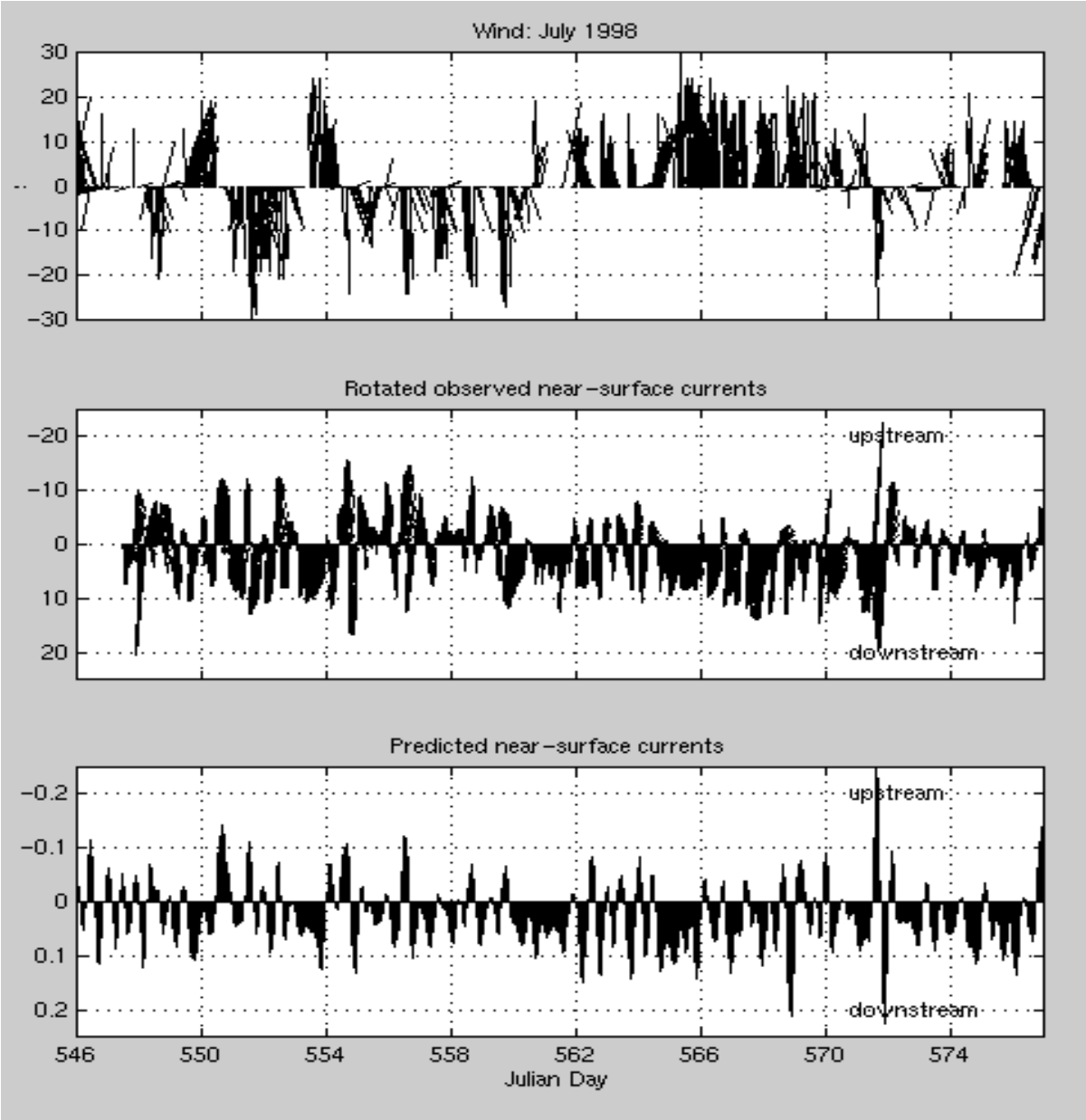

Figure 16. Wind speeds (top panel, mi/hr.), observed observed near-surface currents (middle panel, cm/s), and model predicted near-surface currents (bottom panel, m/s) in the mid-channel waters of the Neuse River Estuary near Cherry Point, NC during July, 1998 (Julian Day 546 = July 1, 1998).

these constituents in surface and bottom waters were available from the MODMON monitoring program (Luettich et al. 2000). Model parameters were adjusted to maximize the correlation between model predictions and observations, and to minimize the difference betweeb mean observations and predictions. Certain model parameters were not calibrated, but were determined using data from the estuarine monitoring program. For instance, the stoichiometric carbon to nitrogen ratio in the model's three algal groups was determined by regressing observed particulate organic carbon against observed particulate organic nitrogen (Figure 17). A similar procedure was used to establish the carbon to chlorophyll ratio for the model's three algal organic matter constituents (Figure 18).

As was mentioned earlier, during model development it was decided that multiple phytoplankton constituents would be needed to adequately simulate the behavior of the community. Using measurement of accessory pigments, the MODMON monitoring (Luettich et al. 2000) included quantification of five algal groups (diatoms, dinoflagellates, chlorophytes, cryptophytes, and blue-green algae). In the model these five groups were coalesced into three groups that were assumed to have three distinct growth characteristics. The first group, diatoms and dinoflagellates, were assumed to have a lower temperature optima than the two remaining groups (Figure 19). The blue-green algae were assumed to be fast growing, with a high temperature optima. The last group, chlorophytes and cryptophytes were characterized by their relatively low maximum growth rate and intermediate temperature optima. Other differences in the behavior of these groups were established during calibration, such as nutrient half-saturation constants, sinking speeds, and respiration rates. Many other parameters related to the cycling and transformation of water quality constituents were also established during calibration. A summary of the calibrated water quality parameters is provided in Appendix A.

4.1.3 Water Quality Predictions

The calibrated model was utilized to perform simulations of water quality conditions from June 1, 1997 until December 31, 1998 for a base case, described here, and for three additional cases having reduced inorganic nutrient loading. Not surprisingly, both the model predictions and the observed data showed significant temporal, longitudinal, and vertical variations in salinity, nutrient, dissolved oxygen, and chlorophyll-a concentrations. While the temporal variability in model predictions was important, there were some typical spatial patterns for some key constituents. For instance, spatial salinity patterns showed the classic character of the partially mixed estuary. Salinities increased in the downstream direction, and with increasing depth (Figure 20). The upper estuary was generally less stratified than the middle and lower estuary. Relatively high nitrate + nitrate concentrations were predicted to be in the fresh surface waters of the upper estuary (Figure 21). These concentrations decreased both vertically downward and with increasing distance downstream, in qualitative agreement withe earlier monitoring studies (Christian et al. 1991, Paerl et al. 1995). The highest predicted chlorophyll-a concentrations were typically in the surface waters somewhere between New Bern and Cherry Point (Figure 22). Minimum dissolved oxygen concentrations (Figure 23) were always in the bottom waters

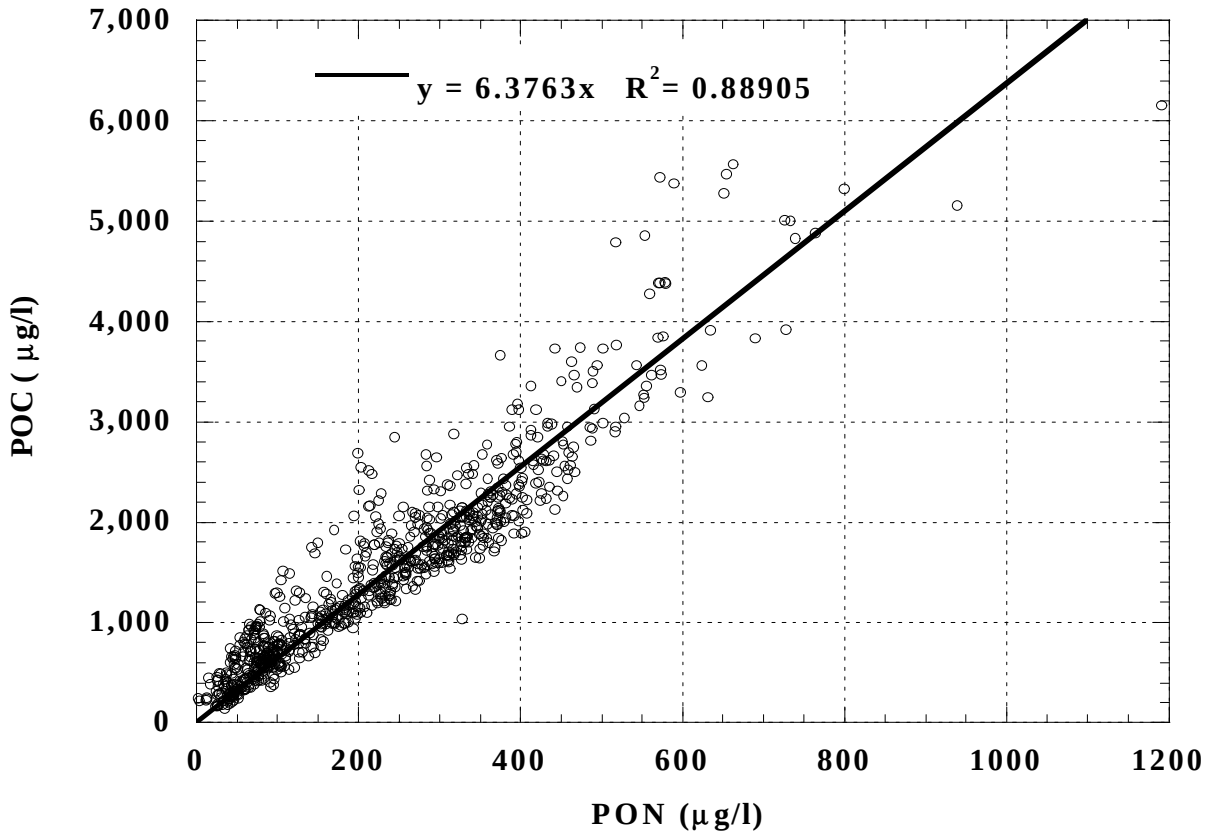

Figure 17. Observed particulate organic carbon (µg/l) vs. particulate organic nitrogen (µg/l) in the mid-channel waters of Neuse River Estuary during 1997 and 1998.

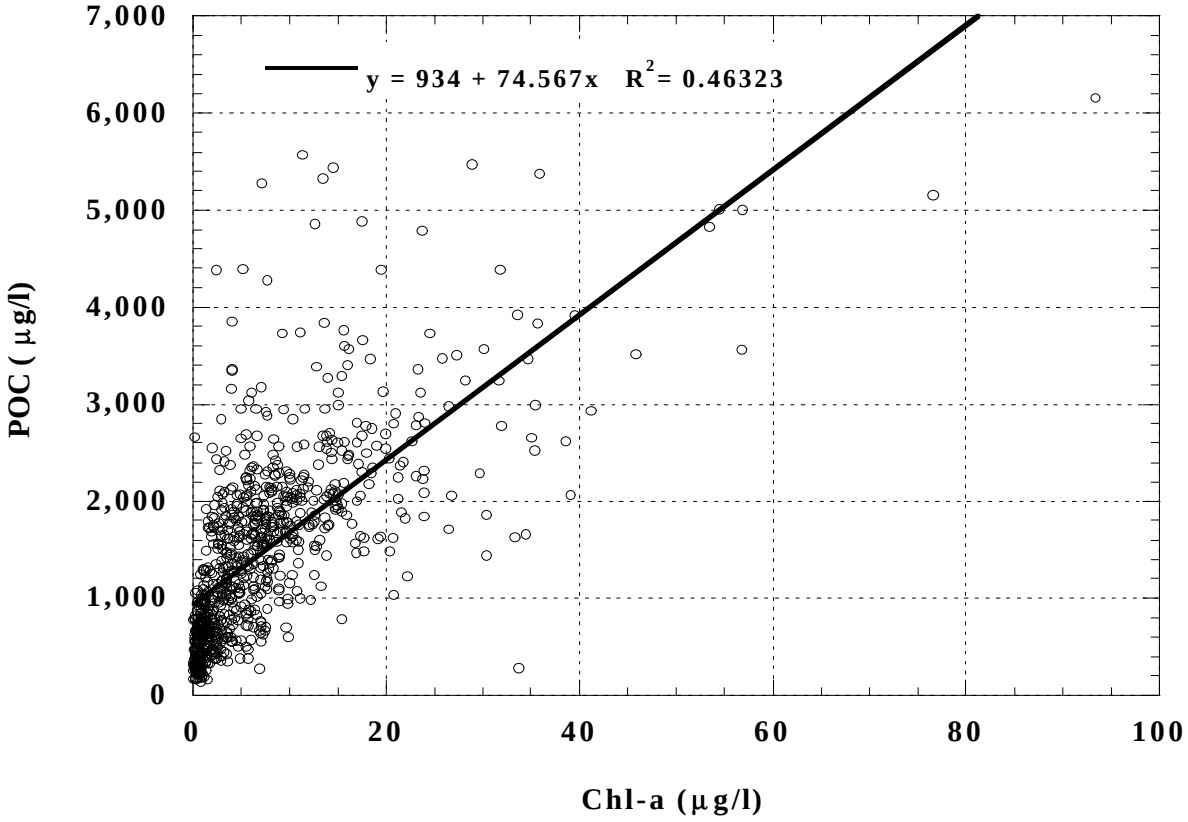

Figure 18. Observed particulate organic carbon concentrations (µg/l) vs. observed chlorophyll-a concentrations (µg/l) in mid-channel waters of the Neuse River Estuary during 1997 and 1998.

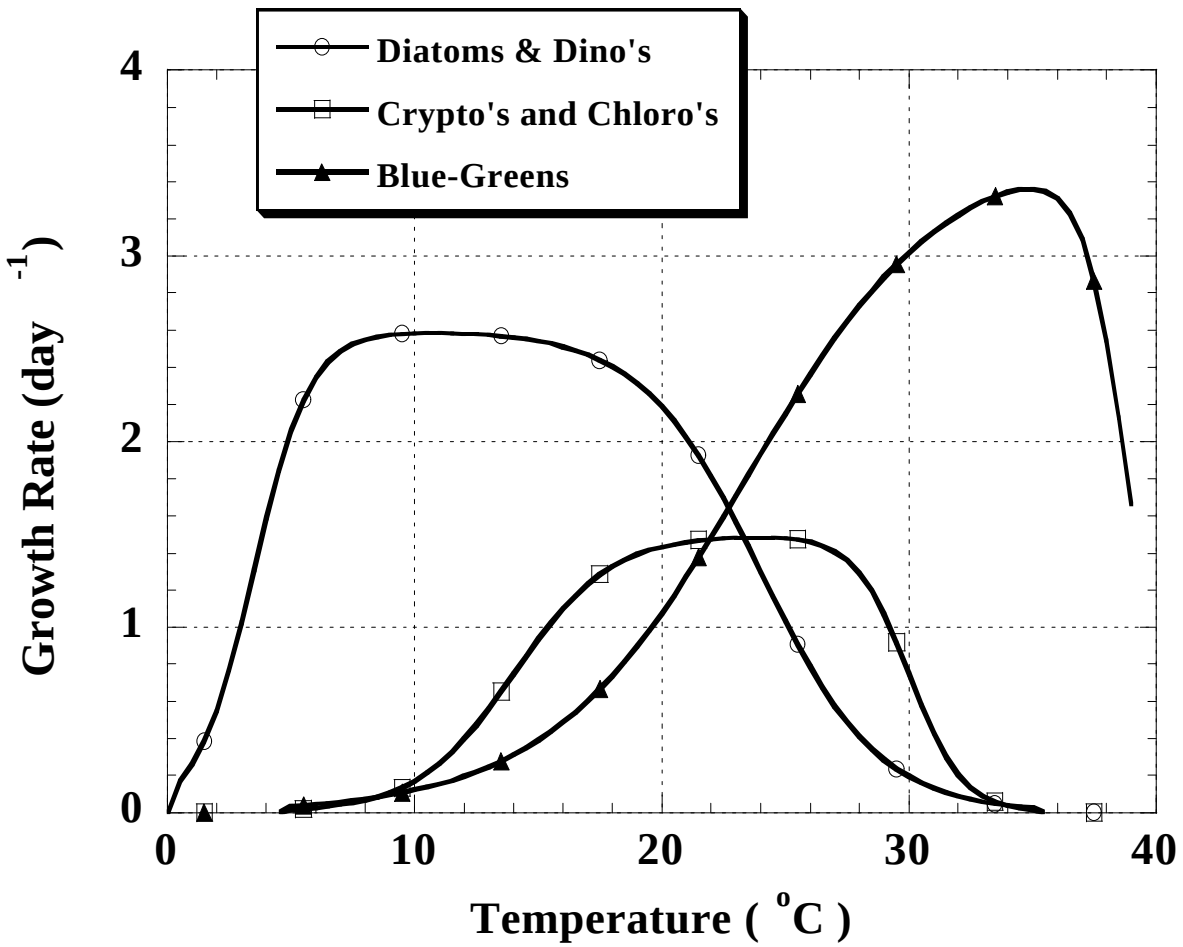

Figure 19. Calibrated growth rates (day^{-1}) vs. temperature for the three phytoplankton groups used to model the phytoplankton community in the Neuse Estuary Eutrophication Model.

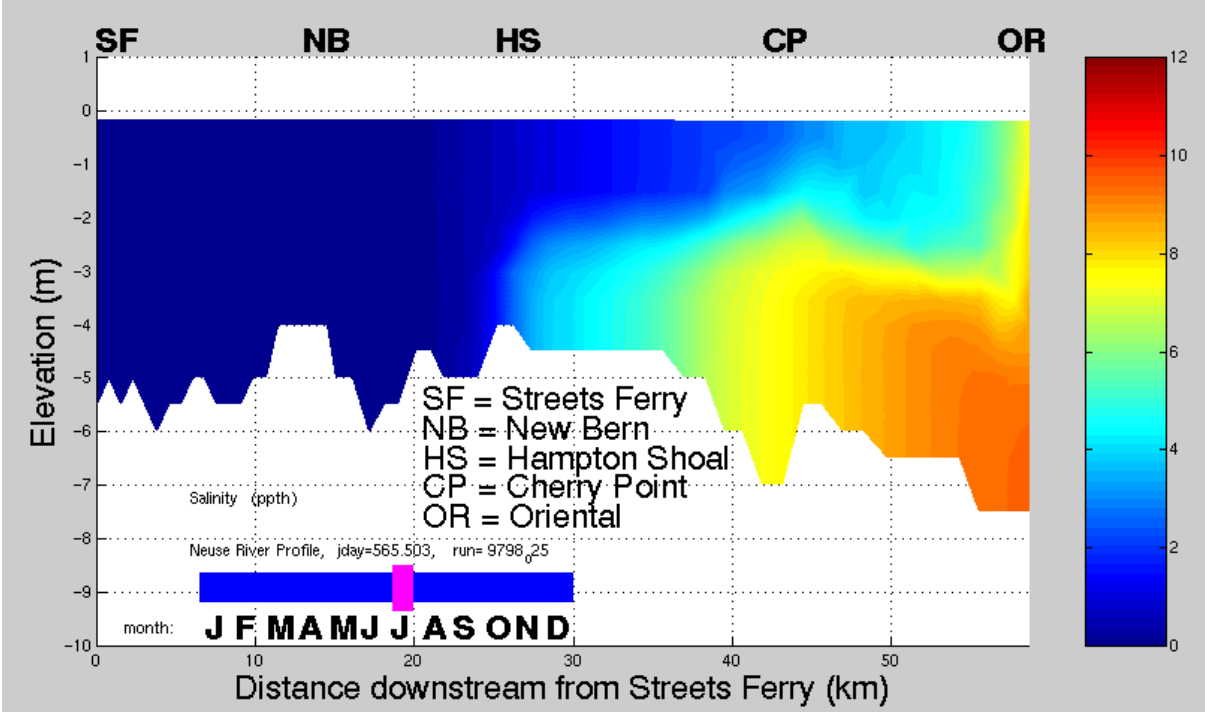

Figure 20. Model predicted longitudinal and vertical variations in salinity (g/l) in the Neuse River Estuary on July 20, 1998.

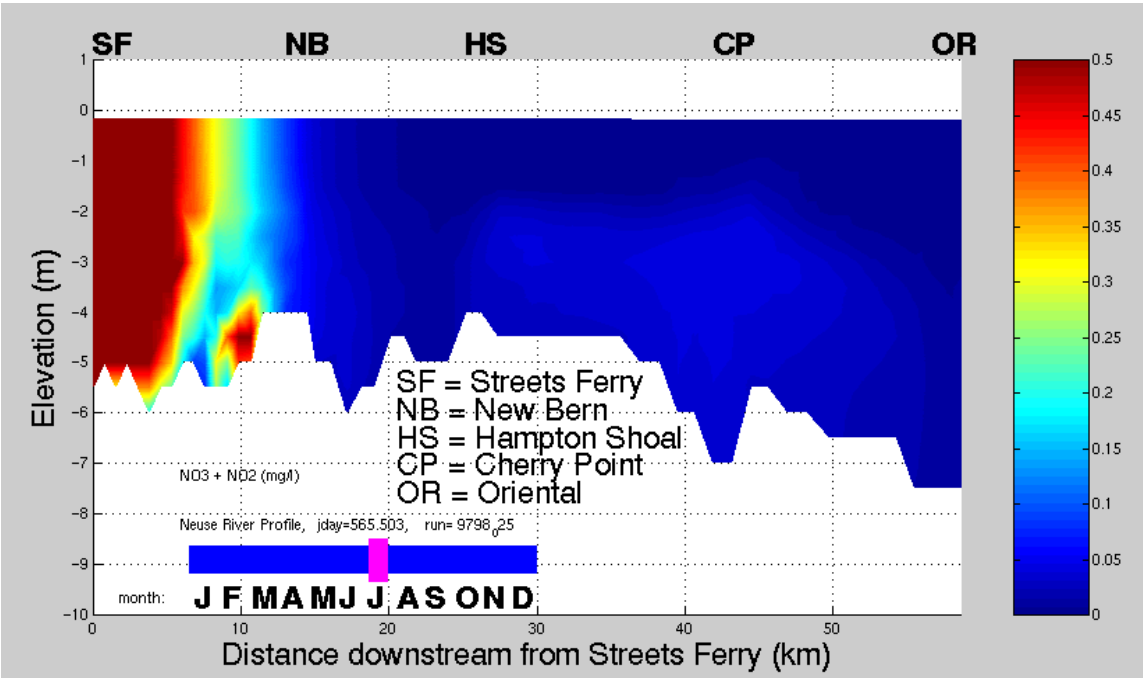

Figure 21. Model predicted longitudinal and vertical variations in nitrate + nitrite concentrations (mg N/l) in the Neuse River Estuary on July 20, 1998.

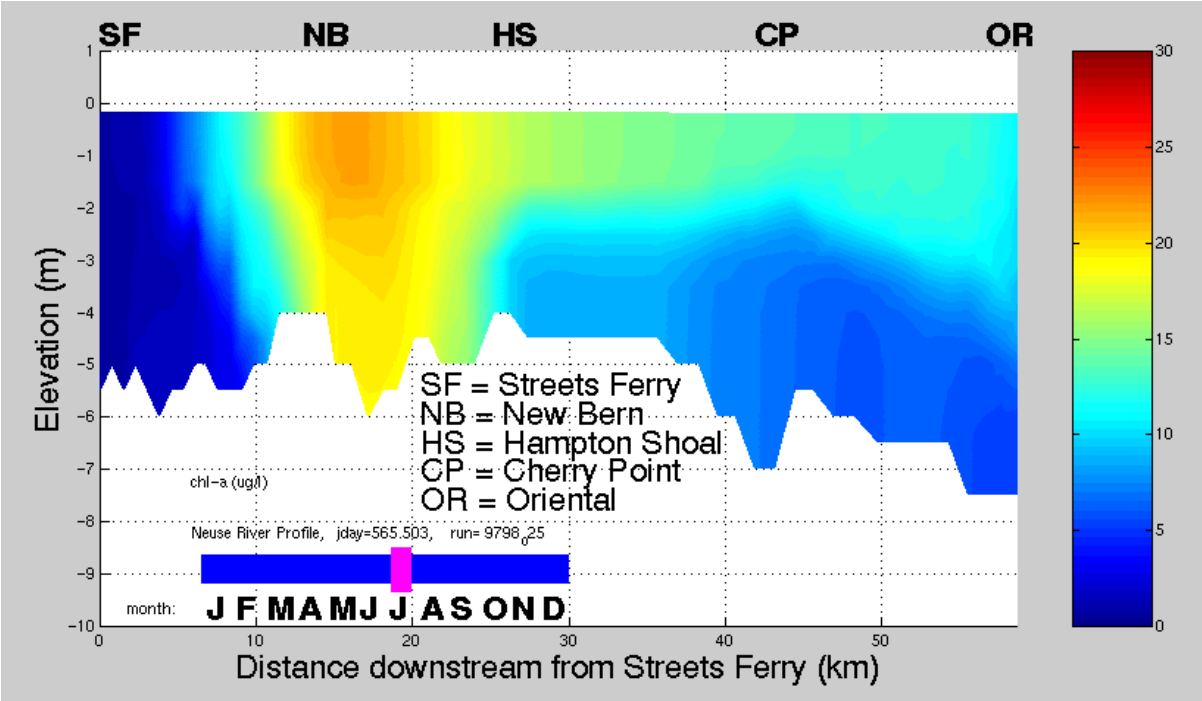

Figure 22. Model predicted longitudinal and vertical variations in chlorophyll-a concentrations (µg/l) in the Neuse River Estuary on July 20, 1998.

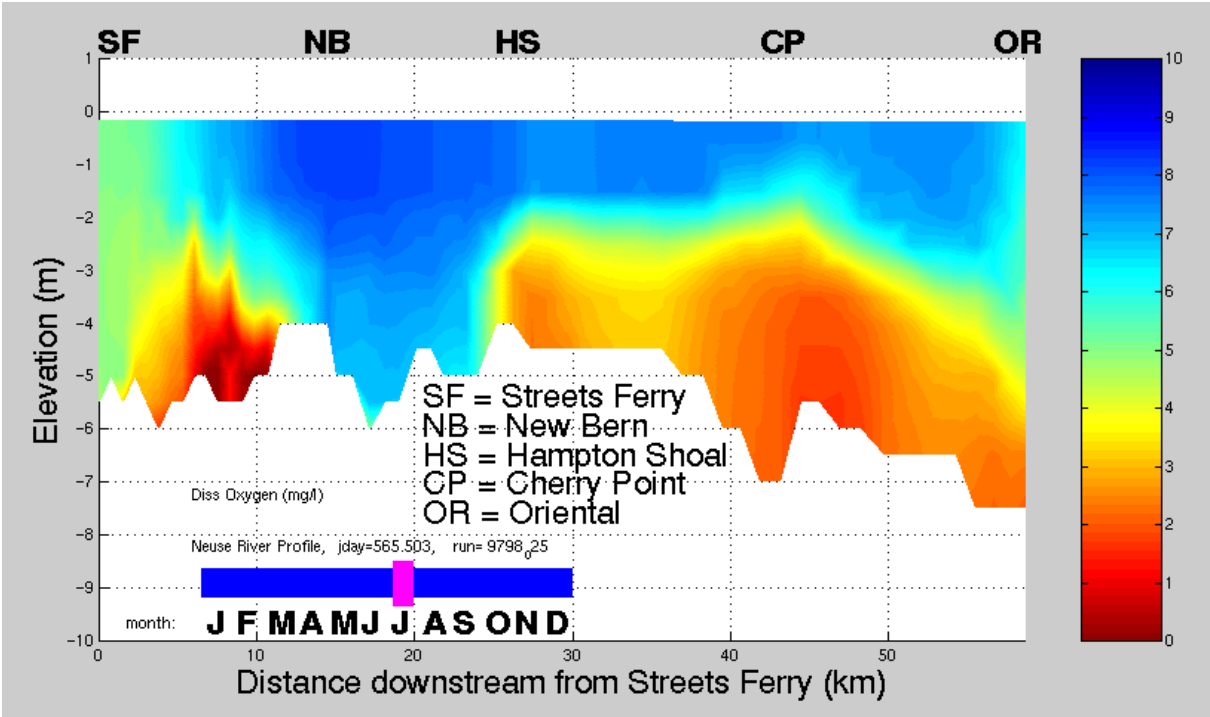

Figure 23. Model predicted longitudinal and vertical variations in dissolved oxygen concentrations (mg/l) in the Neuse River Estuary on July 20, 1998.

during the summer, with local minima generally in the relatively deep waters above New Bern and near Cherry Point.

Time histories comparisons of model predictions and observations at particular locations revealed interesting information about the temporal evolution in water quality conditions. Surface water concentrations of nitrate + nitrite were much higher and less variable at New Bern (Figure 24) than at Cherry Point (Figure 25). Nitrate + nitrite concentrations at Cherry Point were less than 0.05 mg/l for all but the high flow period from January through April 1998. The model predictions of nitrate+nitrite concentrations generally agreed well the observations, although the surface concentrations at Cherry Point during the high flow period were generally underpredicted (Figure 25). Mean absolute errors between predictions and observations were higher at New Bern (MAE = 0.161 mg/l) than at Cherry Point (MAE = 0.051 mg/l). Model predictions of surface water ammonia concentrations at New Bern (Figure 26) and Cherry Point (Figure 27) agreed well with observations, but the model consistently overpredicted 1998 bottom water concentrations at Cherry Point. The model also consistently overpredicted orthophosphate concentrations at both New Bern (Figure 28) and Cherry Point (Figure 29). Surface and bottom concentrations of orthophosphate were similar to one another in both the observed data and the model predictions.

Comparisons of model predicted and observed chlorophyll-a time histories revealed important information about the model's prediction capabilities. While the model generally tracked the observed seasonal and vertical variation in chlorophyll-a concentrations at both New Bern (Figure 30) and Cherry Point (Figure 31), it on several occasions failed to predict bloom conditions seen in the observed data. For instance, during 1998 observed chlorophyll-a concentrations were above 30 µg/l in July and August at New Bern (Figure 30) and during May, July, August, and September at Cherry Point (Figure 31), but model predictions during these months never exceeded 20 µg/l. The model had similar problems in predicting dissolved oxygen concentrations. At New Bern, bottom water anoxia was observed at several times during August and November 1998, but was not predicted at those times by the model (Figure 32). The model did predict, however, the persistent bottom water anoxia observed in 1997. At Cherry Point, the model also predicted persistent bottom water anoxia during 1997 (Figure 33), yet the observations indicated intermittent anoxia. For 1998, intermittent summertime anoxia is evident in both the model predictions and observations (Figure 33).

While the model failed to predict particular extreme events at the exact time and place within the estuary, it did simulate the overall spatial and temporal patterns found in these constituents. For instance, in both model predictions (Figure 34) and observations (Figure 35) of surface nitrate + nitrite concentrations, values are above 0.6 mg/l in the upper 10 km of the estuary for all times except for mid-February to mid-April and early September 1998. At all times nitrate + nitrite concentrations decrease markedly downstream, and are below 0.1 mg/l for all times except the high flow period from January through April 1998. In both model predictions (Figure 36) and observations (Figure 37) of surface water chlorophyll-a concentrations, relatively low concentrations are seen throughout the estuary in February and March 1998. Highest overall concentrations are seen in the summer months, and local maxima are observed in the middle estuary. Not surprisingly, the summer months also have the lowest bottom water dissolved

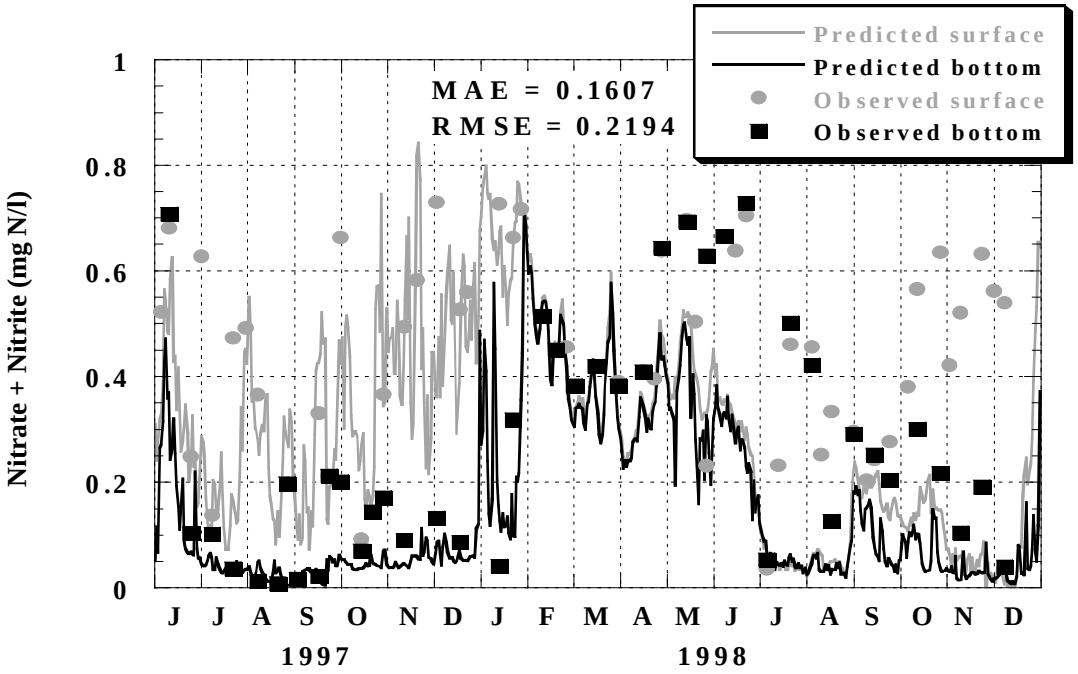

Figure 24. Model predicted (solid lines) and observed (symbols) nitrate + nitrite concentrations (mg N/l) for near-surface and near-bottom waters in the Neuse River Estuary near New Bern, NC during 1997 and 1998.

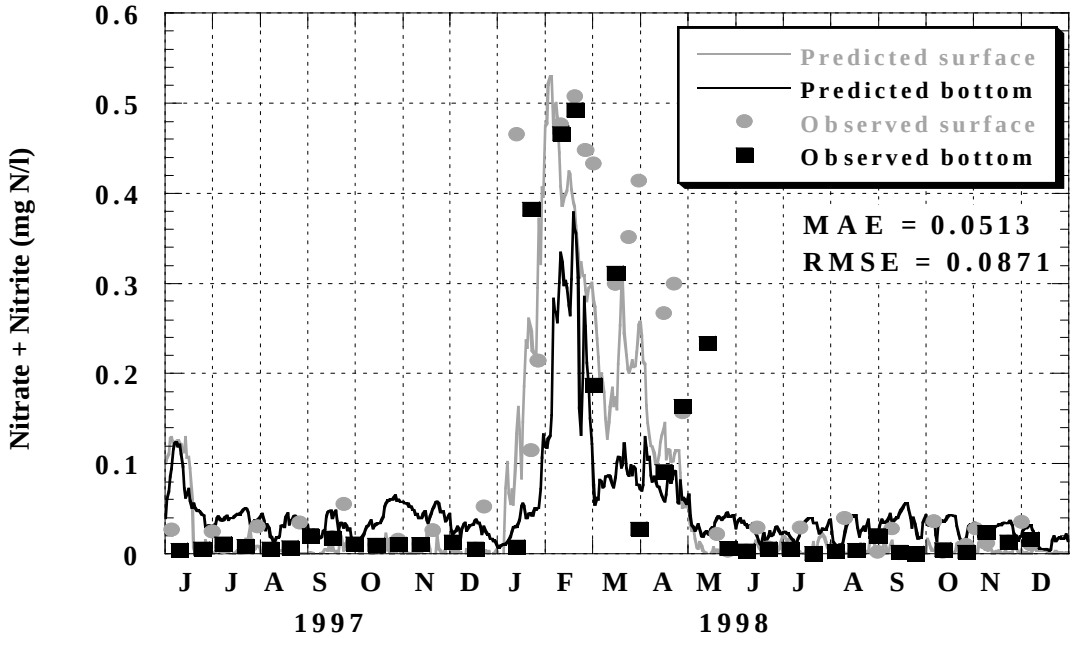

Figure 25. Model predicted (solid lines) and observed (symbols) nitrate + nitrite concentrations (mg N/l) for near-surface and near-bottom waters in the Neuse River Estuary near Cherry Point, NC during 1997 and 1998.

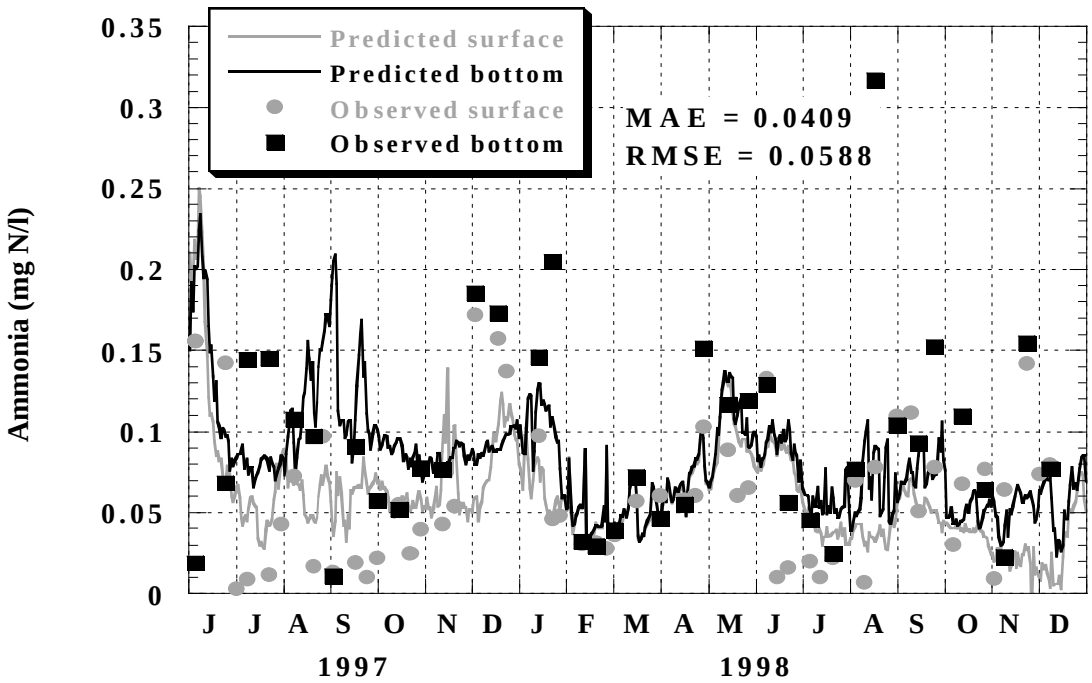

Figure 26. Model predicted (solid lines) and observed (symbols) ammonia concentrations (mg N/l) for near-surface and near-bottom waters in the Neuse River Estuary near New Bern, NC during 1997 and 1998.

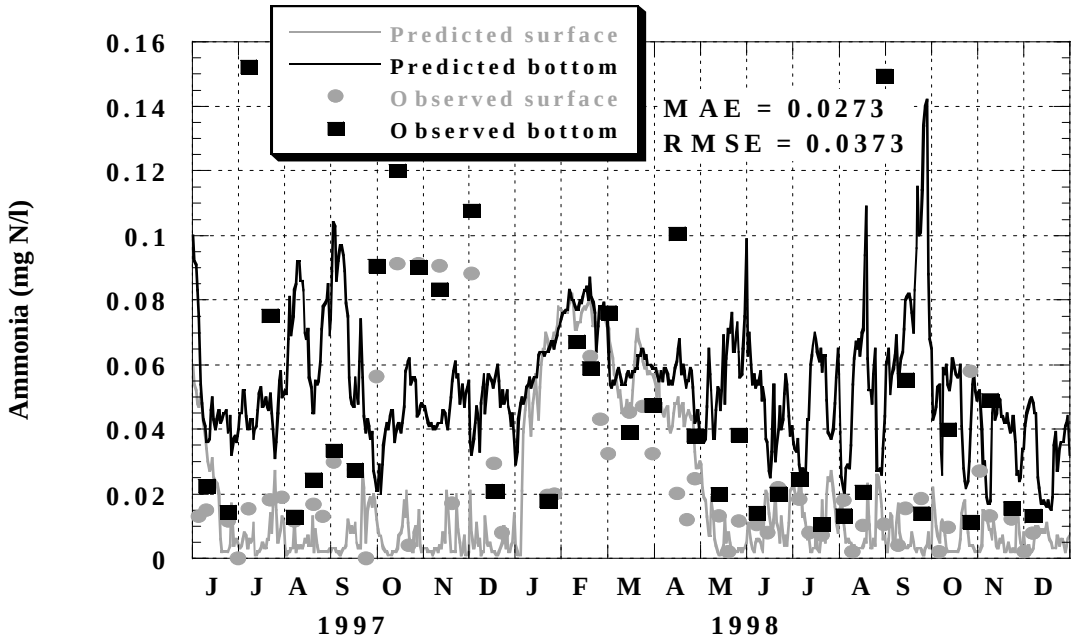

Figure 27. Model predicted (solid lines) and observed (symbols) ammonia concentrations (mg N/l) for near-surface and near-bottom waters in the Neuse River Estuary near Cherry Point, NC during 1997 and 1998.

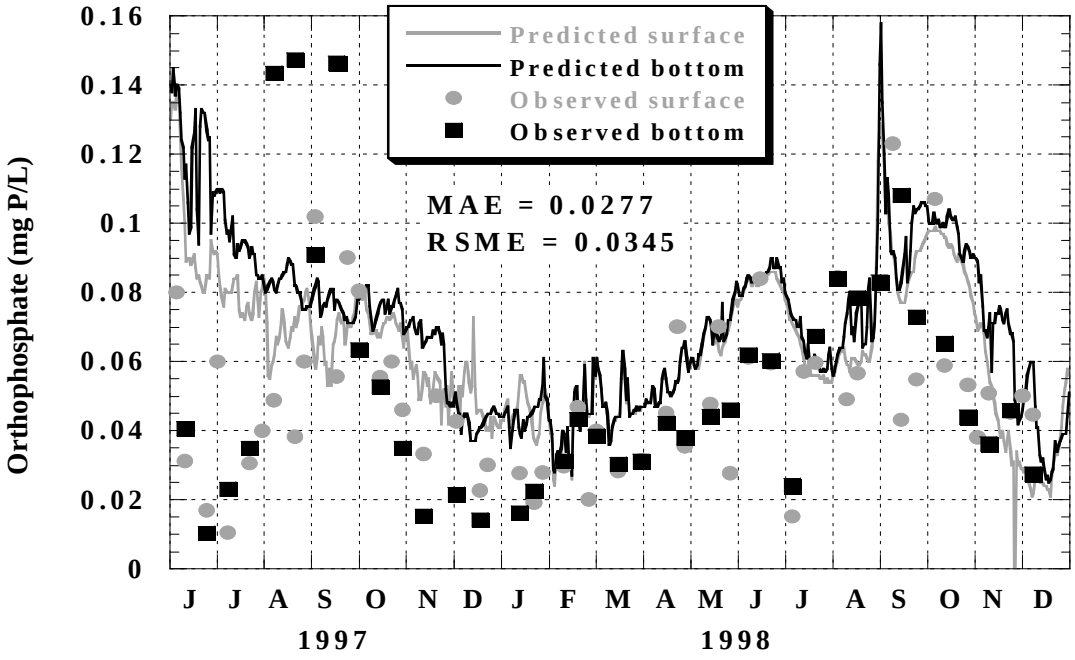

Figure 28. Model predicted (solid lines) and observed (symbols) orthophosphate concentrations (mg P/l) for near-surface and near-bottom waters in the Neuse River Estuary near New Bern, NC during 1997 and 1998.

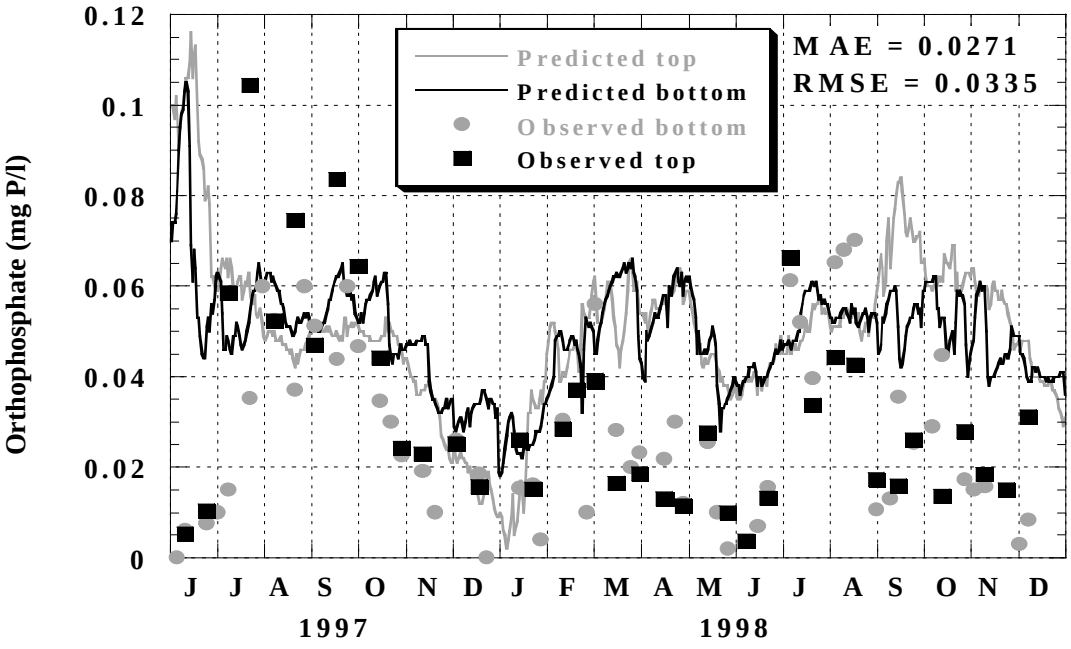

Figure 29. Model predicted (solid lines) and observed (symbols) orthophosphate concentrations (mg P/l) for near-surface and near-bottom waters in the Neuse River Estuary near Cherry Point, NC during 1997 and 1998.

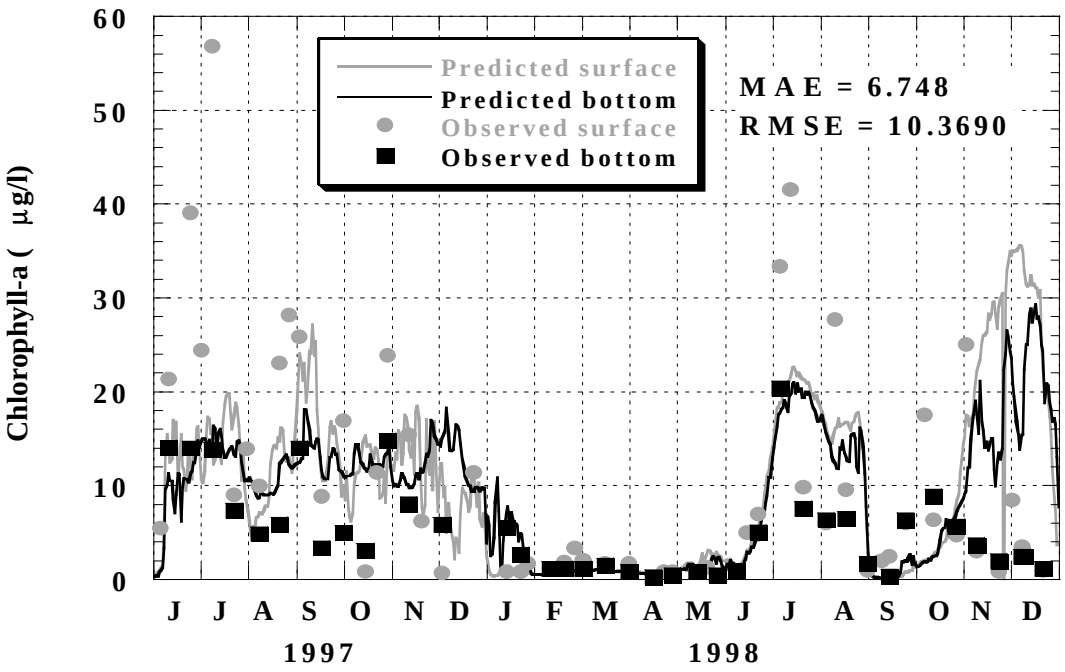

Figure 30. Model predicted (solid lines) and observed (symbols) chlorophyll-a concentrations (µg/l) for near-surface and near-bottom waters in the Neuse River Estuary near New Bern, NC during 1997 and 1998.

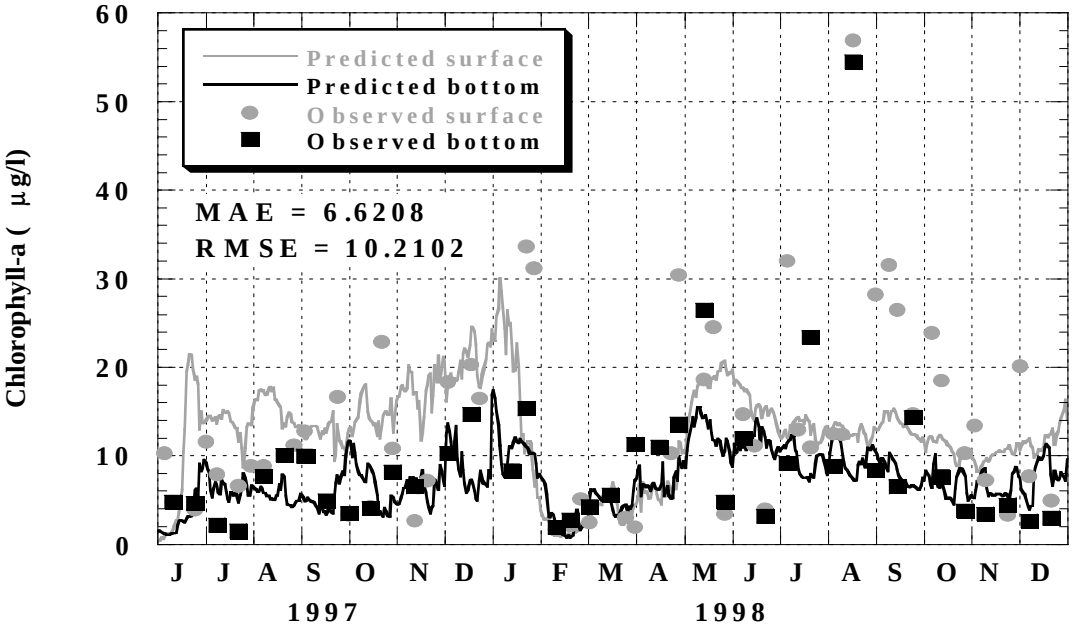

Figure 31. Model predicted (solid lines) and observed (symbols) chlorophyll-a concentrations (µg/l) for near-surface and near-bottom waters in the Neuse River Estuary near Cherry Point, NC during 1997 and 1998.

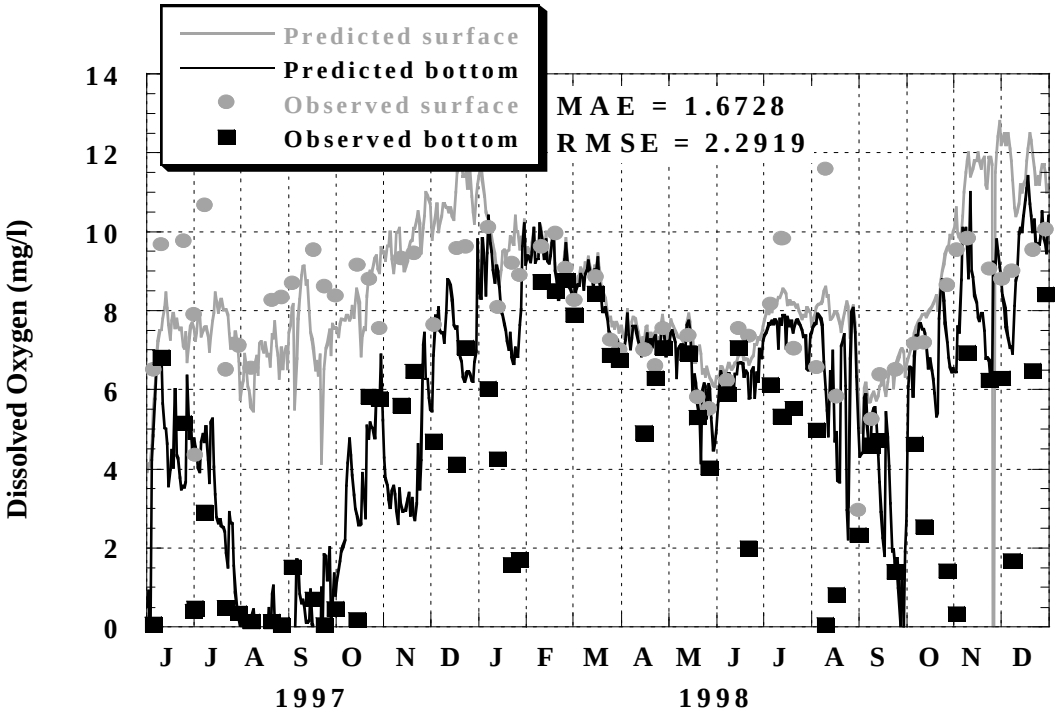

Figure 32. Model Predicted (solid lines) and observed (symbols) dissolved oxygen concentrations (mg/l) for near-surface and near-bottom waters in the Neuse River Estuary near New Bern, NC during 1997 and 1998.

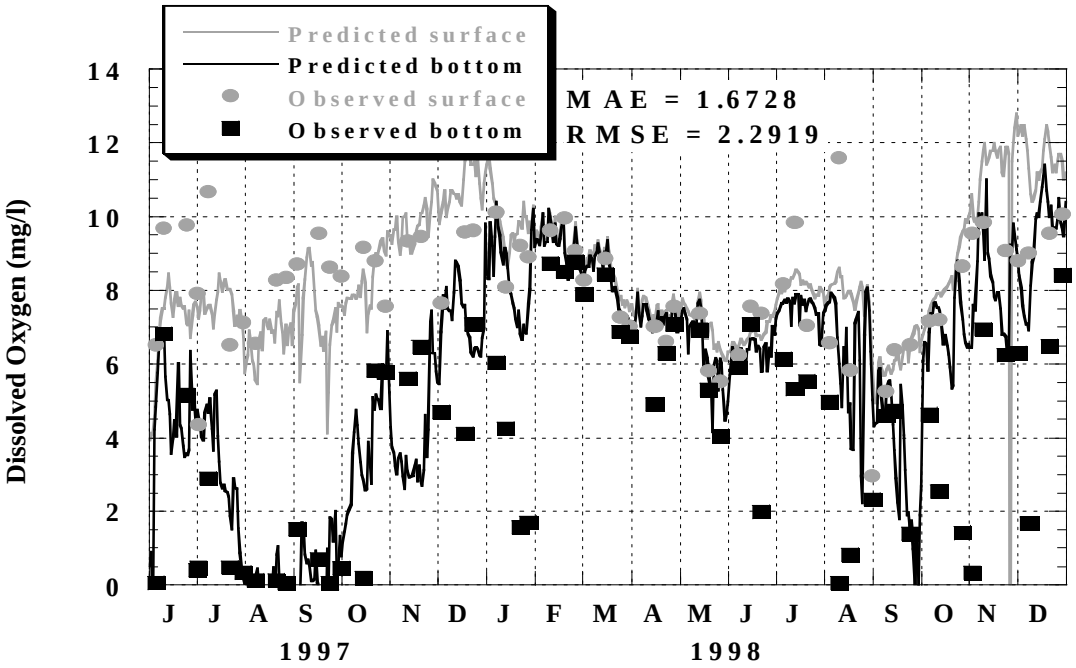

Figure 33. Model predicted (solid lines) and observed (symbols) dissolved oxygen concentrations (mg/l) for near-surface and near-bottom waters in the Neuse River Estuary near Cherry Point, NC during 1997 and 1998.

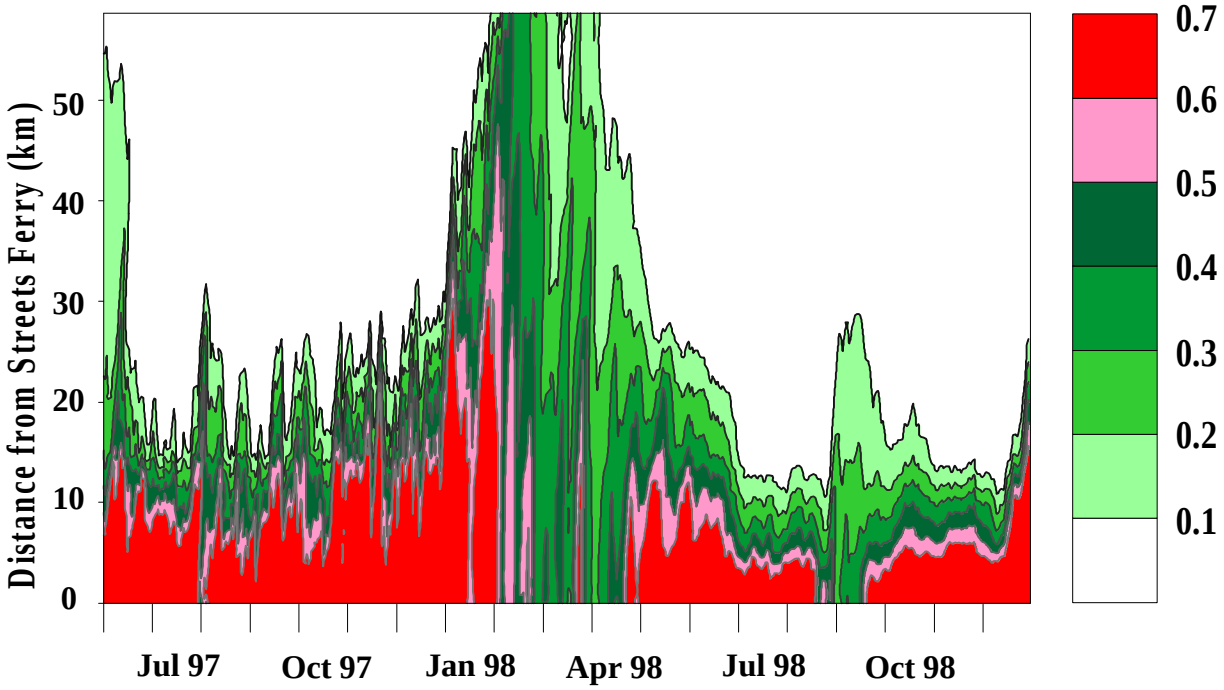

Figure 34. Predicted nitrate concentrations (mg/l) in the mid-channel surface waters of the Neuse River Estuary during 1997 and 1998.

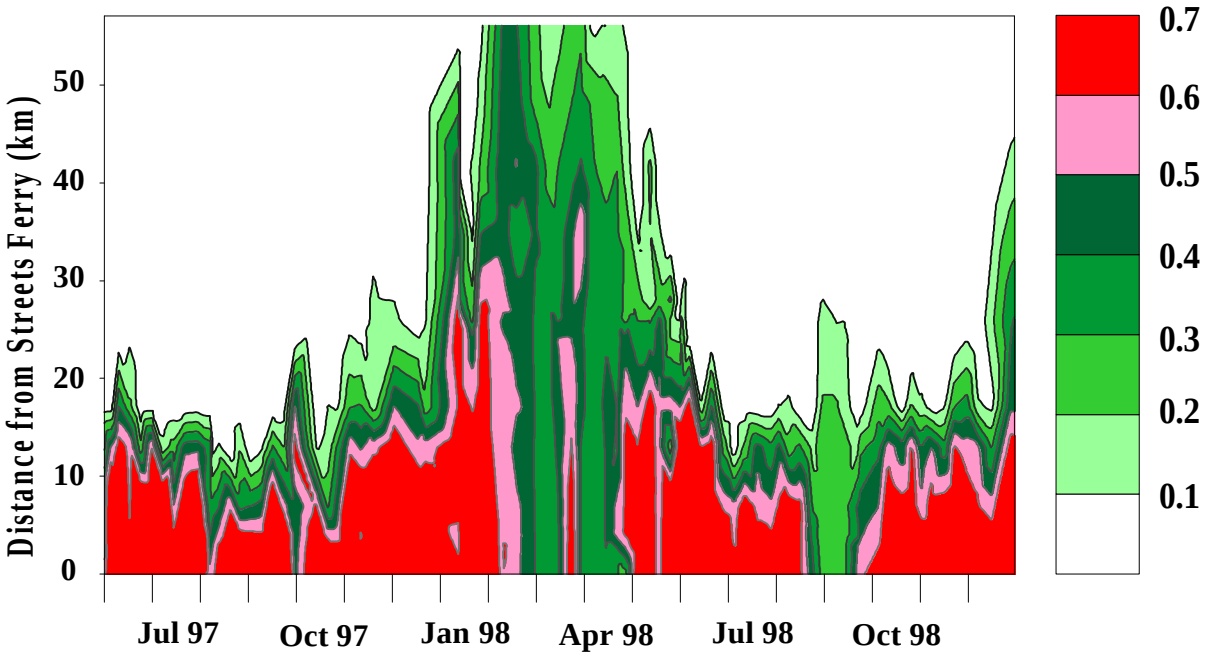

Figure 35. Observed nitrate concentrations (mg/l) in the mid-channel surface waters of the Neuse River Estuary during 1997 and 1998.

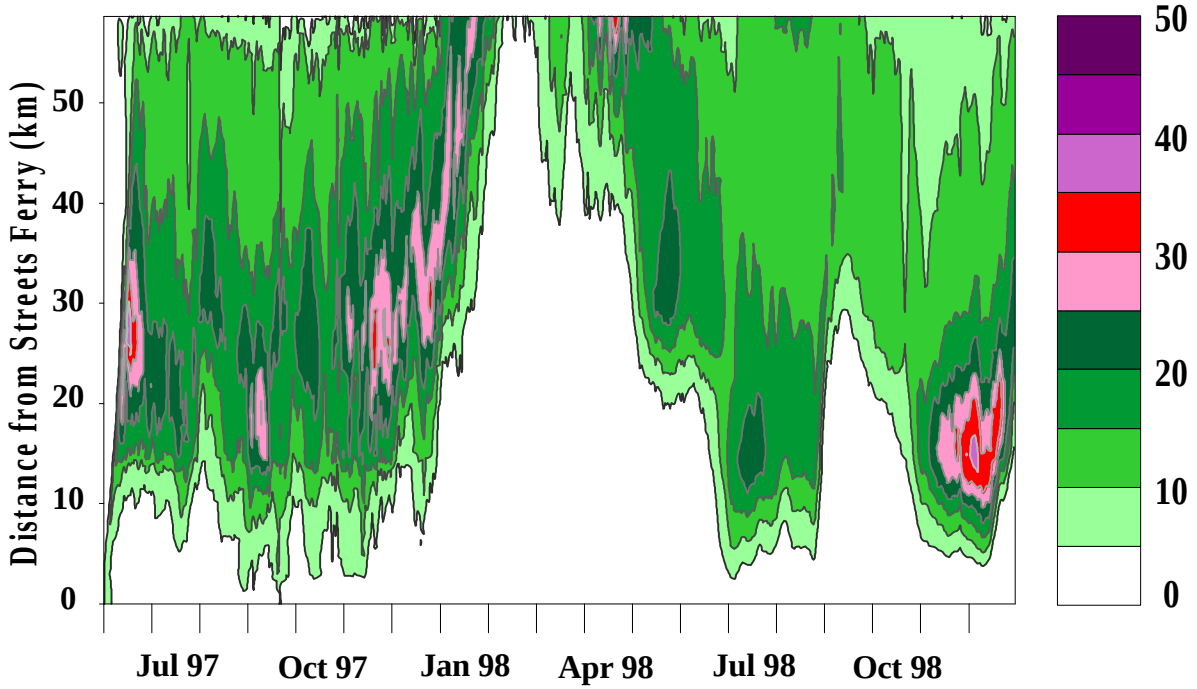

Figure 36. Predicted chlorophyll-a concentrations (µg/l) in the mid-channel surface waters of the Neuse River Estuary during 1997 and 1998.

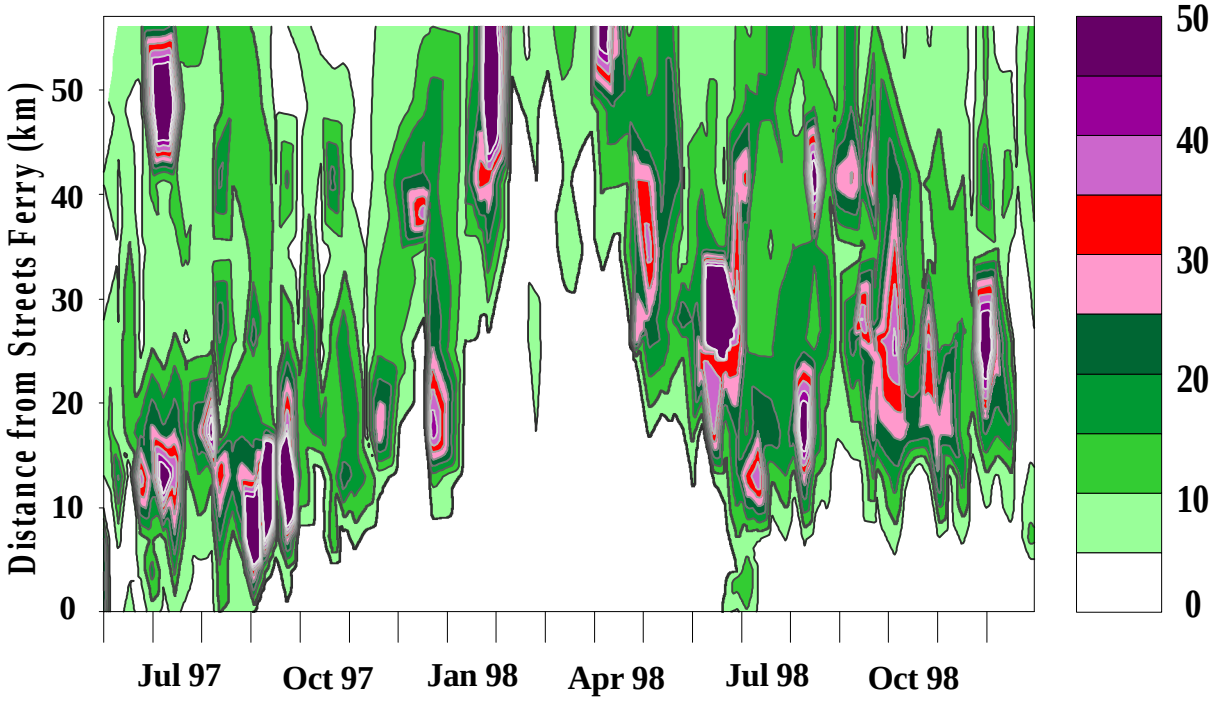

Figure 37. Observed chlorophyll-a concentrations (µg/l) in the mid-channel surface waters of the Neuse River Estuary during 1997 and 1998.

concentrations in both the model predictions (Figure 38) and observations (Figure 39). In both cases bottom water anoxia is both more widespread and persistent in 1997 as compared to 1998. In addition, both model predictions and observations indicate that bottom water anoxia is most frequent in the middle estuary.

The model predictions can also be compared with measured material fluxes in the estuary. As part of the MODMON monitoring program, sediment oxygen demand (SOD) was measured from eight sediment cores taken from four transects located between MODMON stations 40 and 140 (Figure 5) during June and July 1997 (Luettich et al. 2000). Although properties such as sediment total organic carbon concentration and porewater nutrient concentration varied dramatically, measured sediment oxygen demand rates varied less so, from a high of 31.5 mmol O_2 m^{-2} d^{-1} (1.01 g O_2 m^{-2} d^{-1}) at station S42D (14 km downstream from Streets Ferry), to a low of from 16.7 mmol O_2 m^{-2} d^{-1} (0.534 g O_2 m^{-2} d^{-1}) at station S115F (40 km downstream from Streets Ferry). The two stations near New Bern had SOD rates that were approximately 25% higher than the other six sites. The model predicted that SOD was highest during the summer in the area just downstream of New Bern and in the deepest portion of the estuary near the downstream boundary (Figure 40). Model predictions of SOD in the times and places where measurements were taken were somewhat lower, ranging from 0.25 to 0.45 g O_2 m^{-2} d^{-1}. Like the data, the model predicted relatively little spatial variation in SOD rates through the estuary. Seasonal variation in SOD rates were significant, however, as predicted SOD rates for the winter were no more than 10% of the peak summertime values.

Calibration efforts also included comparison of model predicted and observed cumulative frequency distributions. Cumulative frequency distributions of predicted and observed orthophosphate concentrations (Figure 41) showed relationships similar to those seen for time histories of orthophosphate (Figures 28, 29). Predicted values were higher than observed by a significant amount (Figure 41). Overall, the mean predicted orthophosphate concentration was 40.2% higher than the mean observed concentration (Table 8). Mean absolute error was only slightly higher (54.7%, Table 8). For orthophosphate, the model predictions explained 22.6% of the observed variability. Mean errors in the two inorganic nitrogen constituents were much lower. The cumulative frequencies for predicted and observed ammonia concentration were very similar (Figure 42), and the normalized mean error was only 0.9% (Table 8). Predicted nitrate+nitrite concentrations were on average 10.9% lower than observed values, a deviation that can also be seen in the comparison of predicted and observed frequency distributions (Figure 43). Median predicted nitrate+nitrite concentrations are approximately 0.1 mg/l less than the observed median value, but the two distributions come together at both the low and high ends of the frequency distributions (Figure 43). Overall, the model explained 75.6% of the observed variability in nitrate+nitrite concentrations. Mean predicted chlorophyll was 2.6 less than the mean of the observed values (Table 8), although the median predicted chlorophyll was higher than the median observed value (Figure 44). The relatively infrequent high chlorophyll values (cumulative frequencies greater than 0.9) were significantly underpredicted by the model (Figure 44). The shapes of the two chlorophyll frequency distributions were significantly different, with the observed distribution skewed to higher values as compared to the model predictions. For dissolved oxygen, however, the shapes of the two frequency distributions were very similar

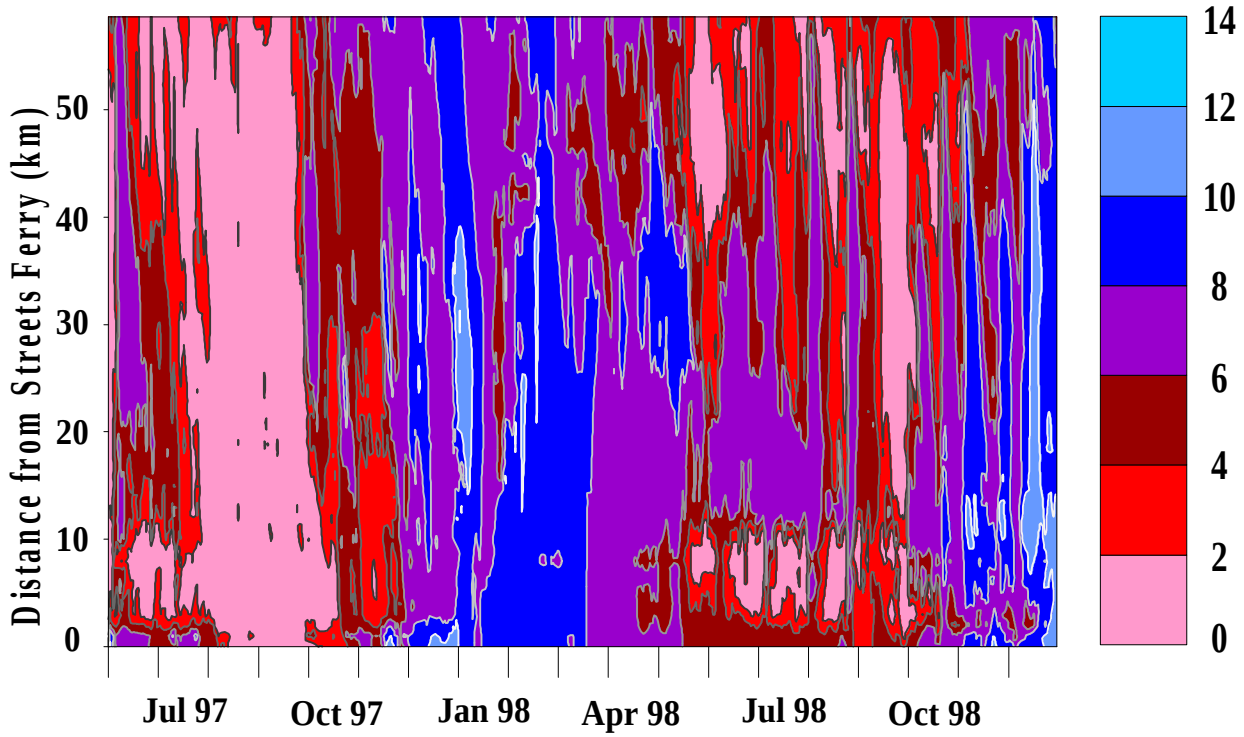

Figure 38. Predicted dissolved oxygen concentrations (mg/l) in the mid-channel surface waters of the Neuse River Estuary during 1997 and 1998.

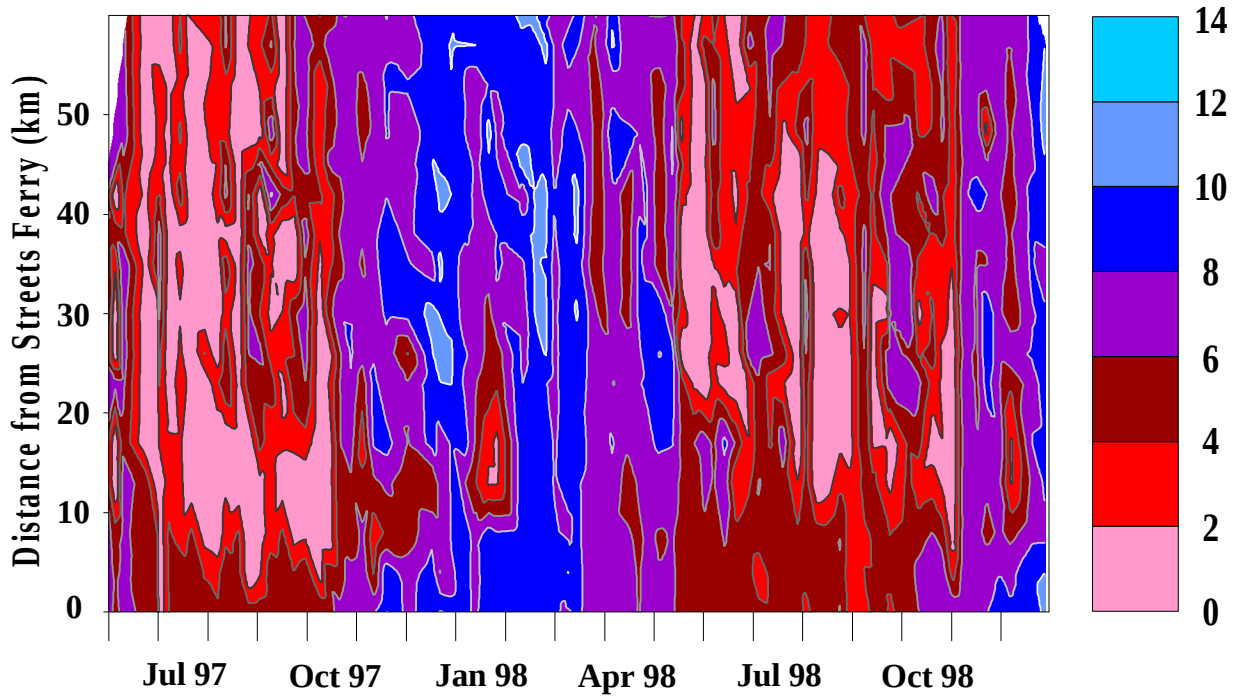

Figure 39. Observed dissolved oxygen concentrations (mg/l) in the mid-channel surface waters of the Neuse River Estuary during 1997 and 1998.

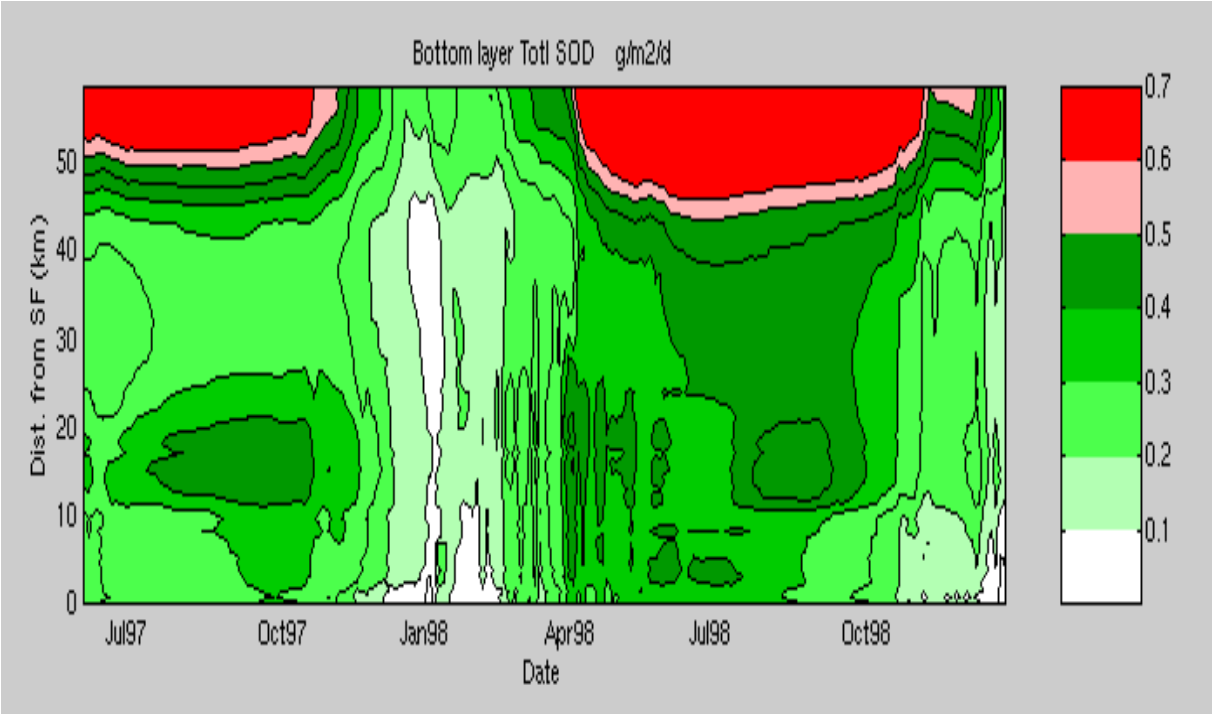

Figure 40. Predicted sediment oxygen demand ($g/m^2/d$) in the mid-channel bottom sediments of the Neuse River Estuary during 1997 and 1998.

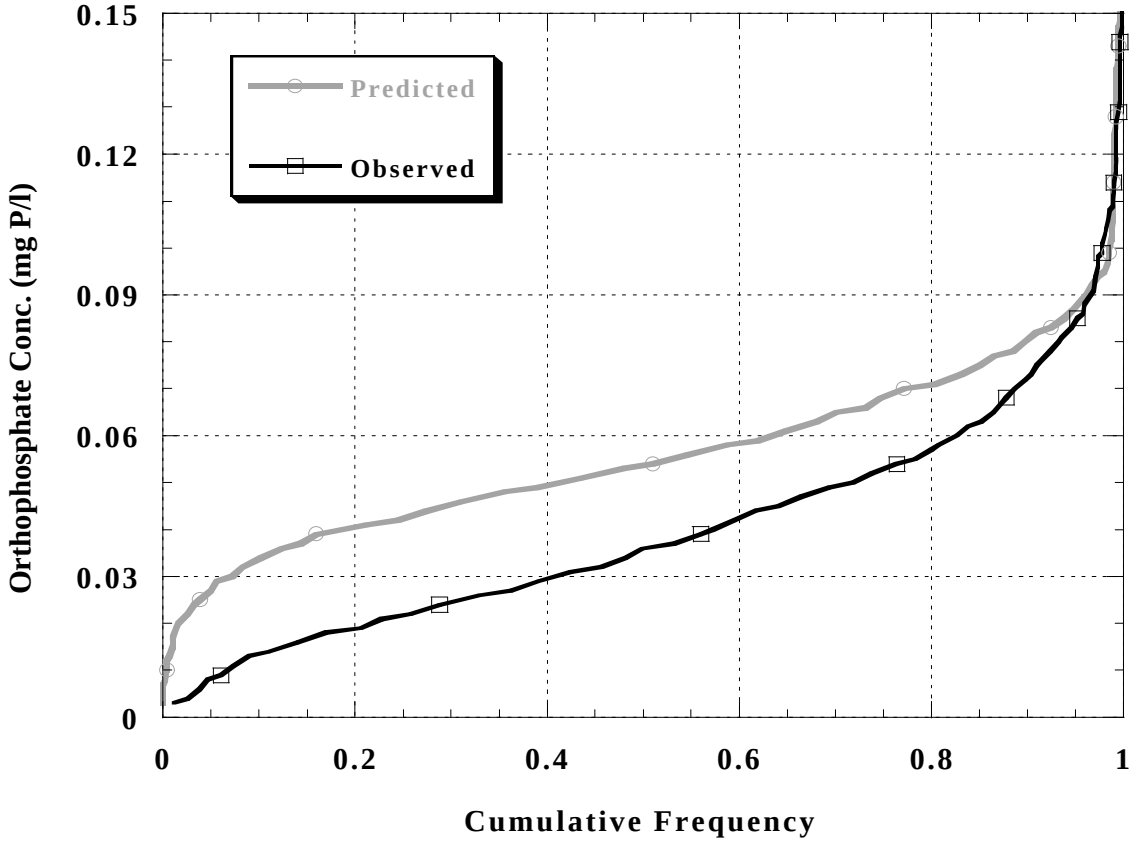

Figure 41. Cumulative frequency distribution of predicted and observed orthophosphate concentrations (mg/l) in the mid-channel waters of the Neuse River Estuary during 1997 and 1998.

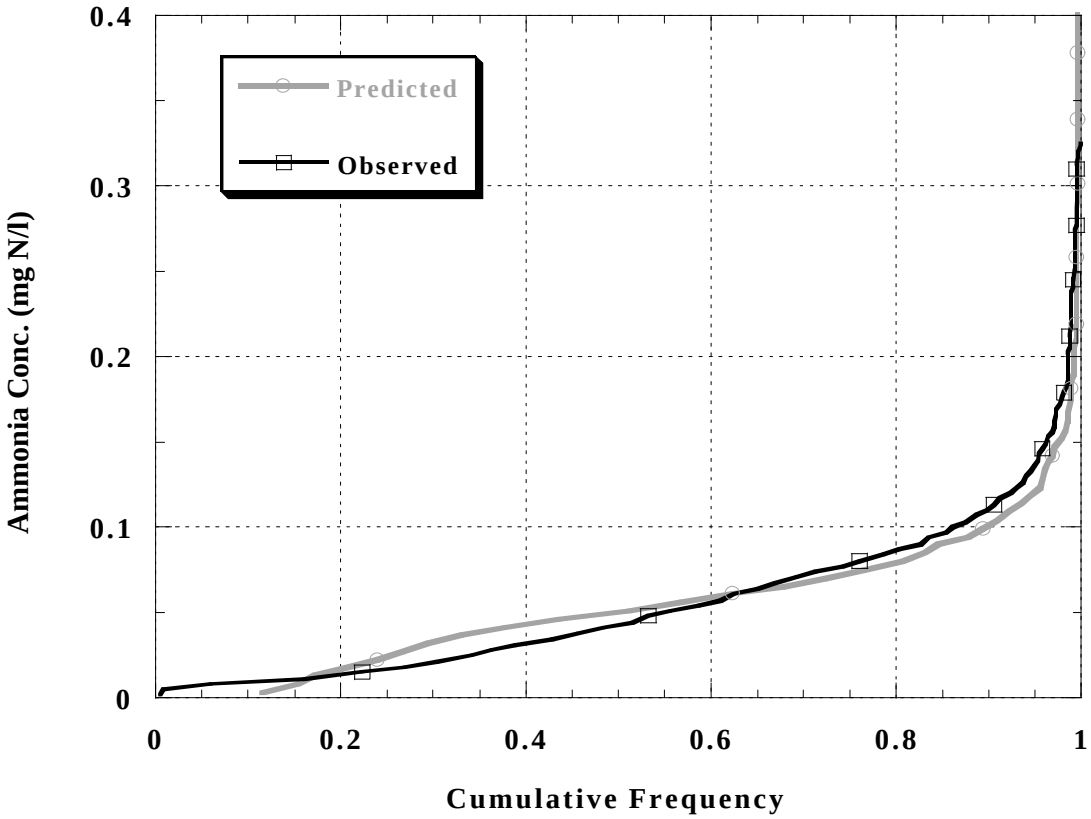

Figure 42. Cumulative frequency distribution of predicted and observed ammonia concentrations (mg/l) in the mid-channel waters of the Neuse River Estuary during 1997 and 1998.

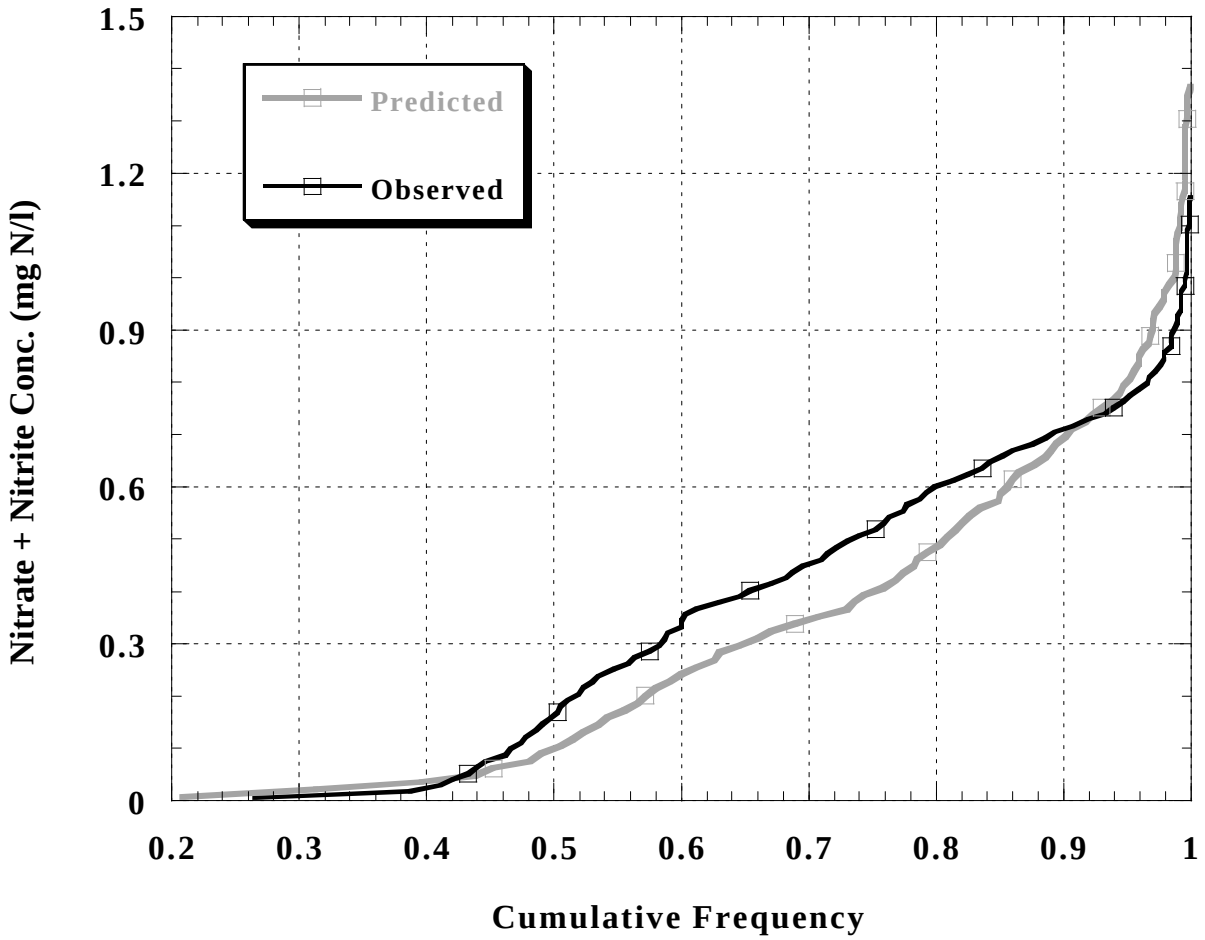

Figure 43. Cumulative frequency distribution of predicted and observed nitrate + nitrite concentrations (mg/l) in the mid-channel waters of the Neuse River Estuary during 1997 and 1998.

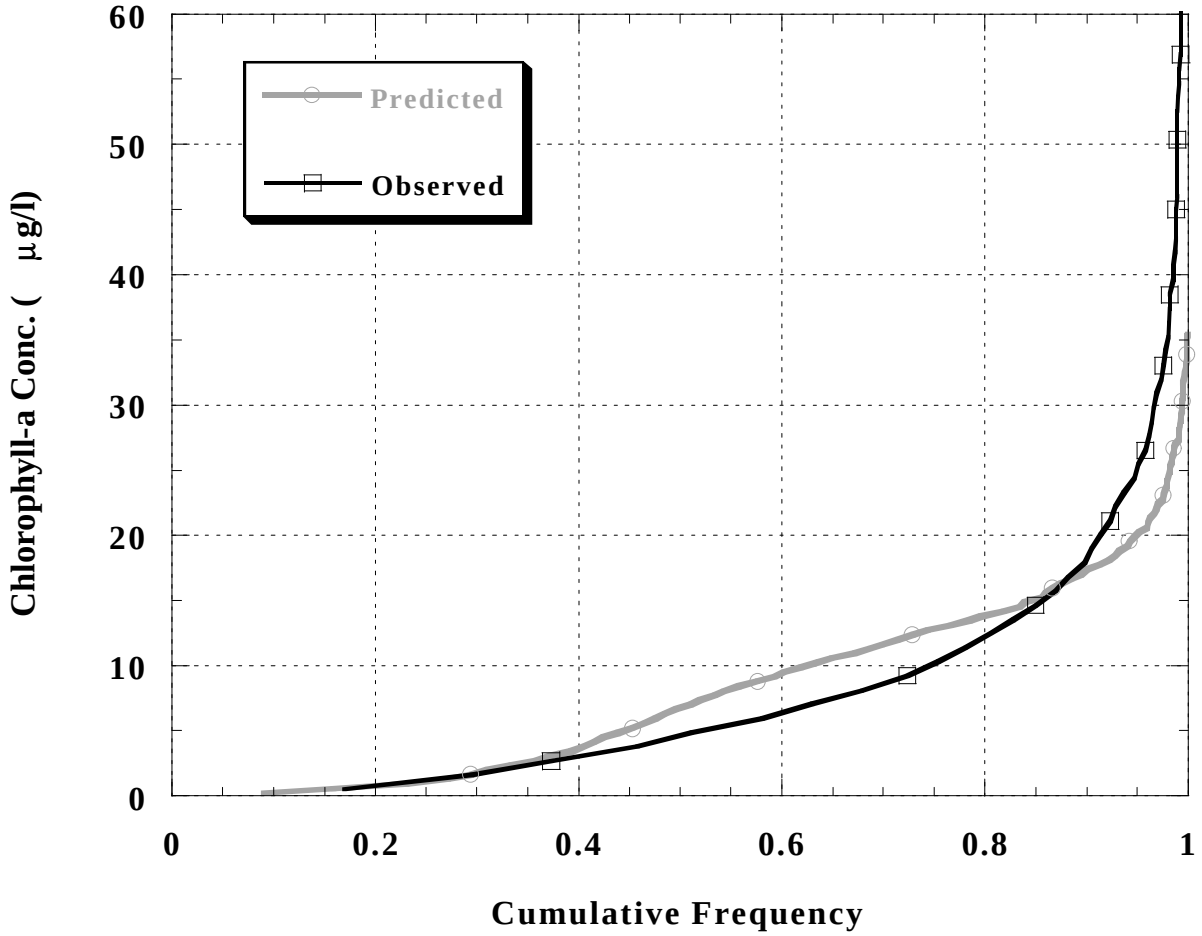

Figure 44. Cumulative frequency distribution of predicted and observed chlorophyll-a concentrations (µg/l) in the mid-channel waters of the Neuse River Estuary during 1997 and 1998.

(Figure 45). Overall, predicted mean dissolved oxygen concentrations were slightly lower than corresponding observed values (Table 8, Figure 45).

Table 8. Comparison of Model Predictions to Observed Data

Constituent	Mean Error (pred. - obs.)	Normalized Mean Error (%)	Mean Absolute Error	Normalized Mean Absolute Error (%)	Corre-lation r^2 (%)	No. of Data Points
Salinity (g/l or PSU)	-0.475	-7.8%	1.261	20.8%	88.5%	7,629
Nitrate + Nitrite (mg N/l)	-0.030	-10.9%	0.087	31.2%	75.6%	755
Ammonia (mg N/l)	0.001	0.9%	0.034	60.4%	11.7%	746
Orthophosphate (mg P/l)	0.016	40.2%	0.022	54.7%	22.6%	736
Chlorophyll-a (µg/l)	-0.209	-2.6%	5.308	65.0%	17.9%	1,025
Dissolved Oxygen (mg/l)	-0.394	-5.5%	1.400	19.6%	51.8%	9,154

4.2 Predictions of Water Quality Improvement

Because of the coupling in the water column between water column nutrients, phytoplankton biomass, organic matter, and dissolved oxygen, reductions in nutrient loading would be expected to affect all these constituents. In fact, detectable, though not necessarily significant changes were observed in all these constituents when model simulations were run that reduced inorganic nutrient loading to the estuary. In this section, however, we focus on the two of the most important descriptors of eutrophication status, chlorophyll-a and dissolved oxygen concentration.

As expected, reducing inorganic nutrient loading to the estuary resulted in lower chlorophyll-a concentrations and higher dissolved oxygen concentrations. The magnitude of the changes, however, was quite different for these two constituents. Two of the three inorganic nutrient loading reduction scenarios (-30% N, -30% N & P) produced lower chlorophyll concentrations for the estuary as a whole (Figure 46). Only very slight differences were seen in the reductions for these two cases with reduced inorganic nitrogen loading. Reducing just the loading of inorganic phosphorus had essentially no effect. The magnitude of decrease in predicted chlorophyll-a concentration was most pronounced for the upper end of the cumulative frequency distribution. Inorganic nitrogen loading reductions of 30% reduced the predicted mean chlorophyll-a concentrations by less than 1 µg/l, and reduced predicted chlorophyll-a concentrations at the 0.9 cumulative frequency level by approximately 2.5 µg/l (Figure 46).

Examination of the cumulative frequency distributions for predicted chlorophyll-a concentrations near Cherry Point indicated that the lower estuary would be much more affected by reduced

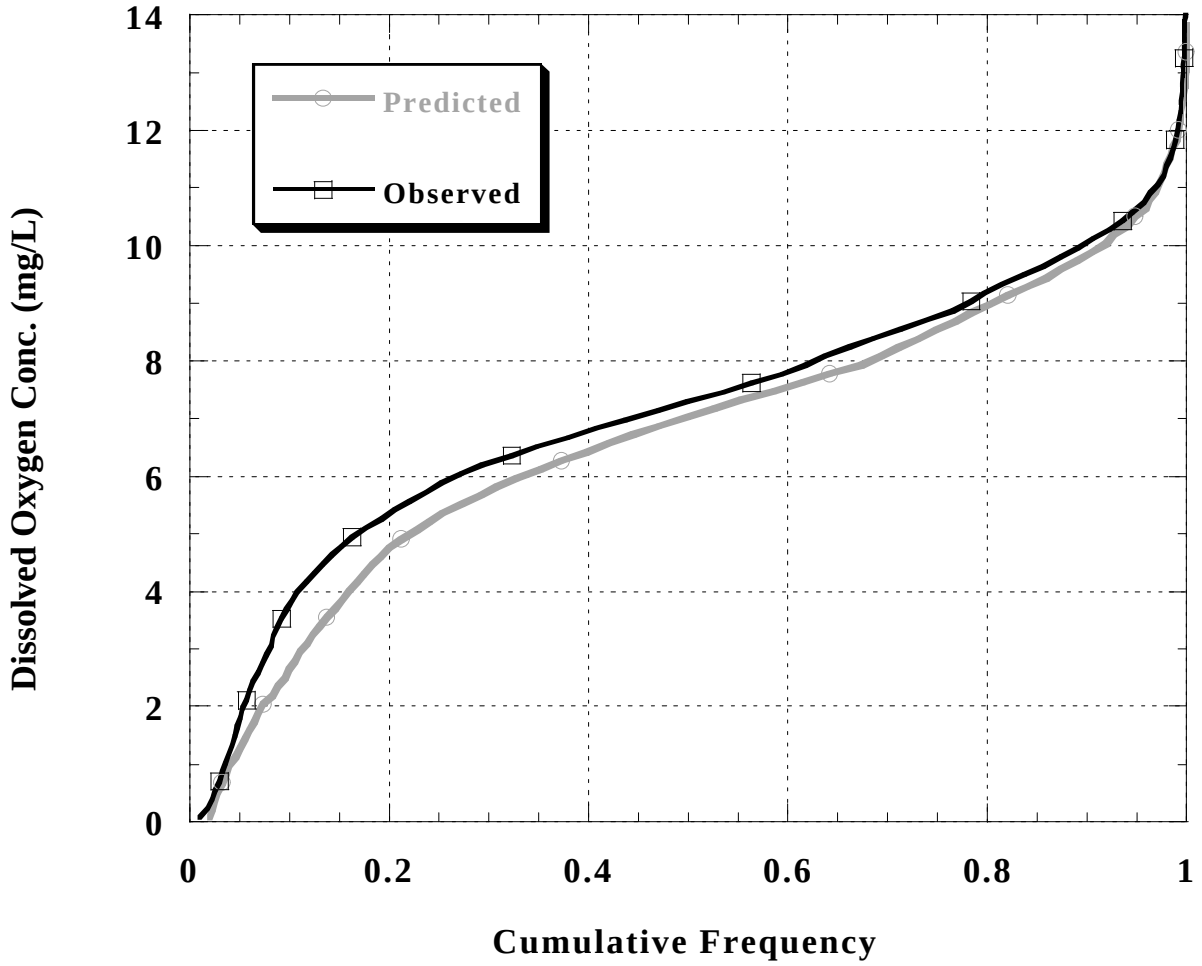

Figure 45. Cumulative frequency distribution of predicted and observed dissolved oxygen concentrations (mg/l) in the mid-channel waters of the Neuse River Estuary during 1997 and 1998.

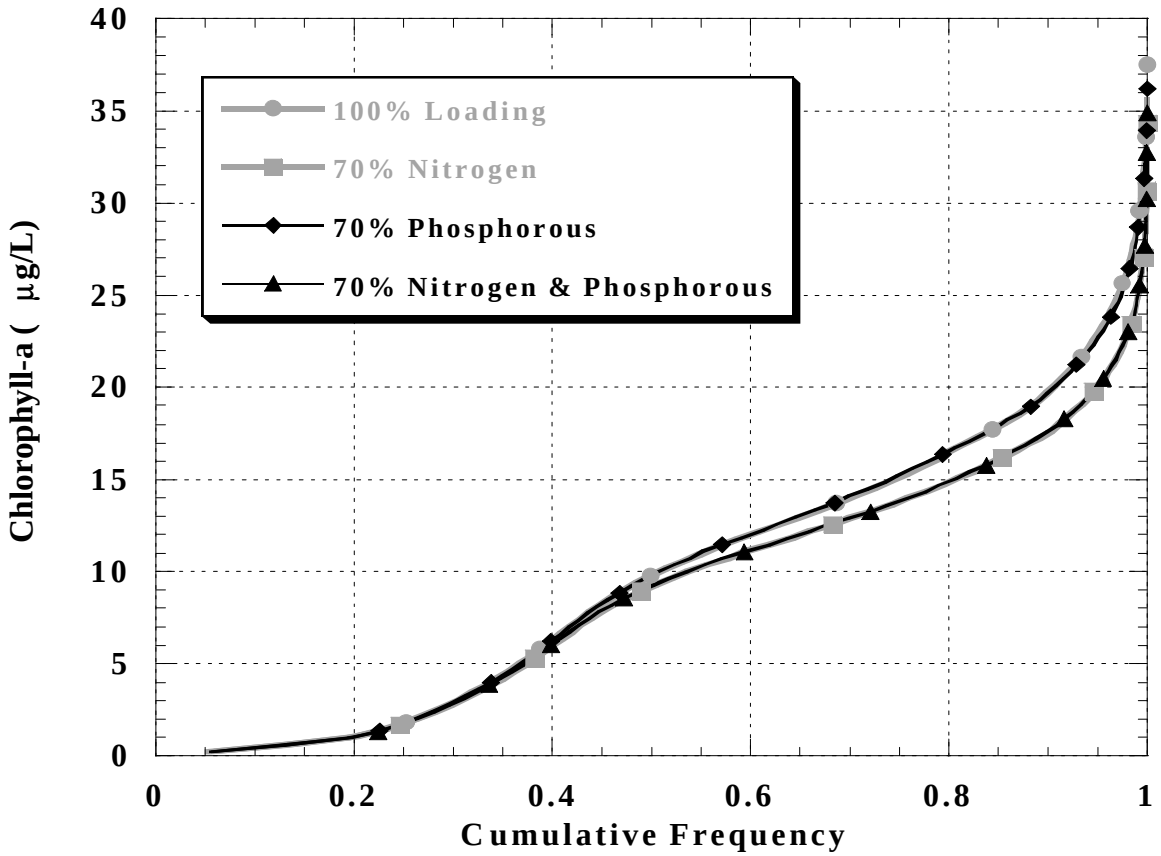

Figure 46. Comparison of 1997-1998 model predicted cumulative frequency distributions of chlorophyll-a concentrations in the Neuse River Estuary for a base case (100% loadings) and for three nutrient loading reduction scenarios.

nutrient loading than would the upper estuary. Again, reducing just inorganic phosphorus had little effect on the predicted chlorophyll-a frequency distribution. The two cases where inorganic nitrogen loading was reduced, however, showed significant decreases in predicted chlorophyll-a concentrations over most of the cumulative frequency range (Figure 47). The median predicted chlorophyll-a was reduced by 1.7 µg/l while the predicted chlorophyll-a concentration at the 0.9 cumulative frequency level was reduced by 2.9 µg/l. Nutrient reduction had little effect, however, on the lowest 20% of the frequency distribution, as all four nutrient reduction scenarios were nearly identical over this frequency range (Figure 47).

Reductions in predicted chlorophyll-a concentrations in the New Bern area, on the other hand, were found to be relatively minor when nutrient loading to the estuary was reduced. In this case all four scenarios produced nearly identical results at cumulative frequencies below 0.6 (Figure 48). At higher cumulative frequencies, chlorophyll-a concentrations were reduced somewhat for cases where inorganic nitrogen loading was reduced. At the 0.9 cumulative frequency level, predicted chlorophyll-a concentrations were reduced from by nearly 3 µg/l from 21.2 to 18.8 µg/l (Figure 48). As in previous cases, no additional effect was observed for reductions in both inorganic nitrogen and phosphorus.

Model predictions indicated that the dissolved oxygen concentrations would be increased only slightly in the short-term by reducing nutrient loading to the estuary. Cumulative frequency distributions of predicted dissolved oxygen for the entire modeled region (Figure 49) or for the model segments near New Bern (Figure 50) were practically identical for the base case scenario and the three nutrient reduction scenarios. An additional scenario was run that sought to simulate the reduction in sediment organic matter concentrations that would result over the longer term from nutrient load reductions. A case was run in which both inorganic nitrogen and phosphorus loading were reduced by 30%. Predicted sediment organic matter concentrations at the end of the 19 month simulation period were saved and used as the initial conditions for a subsequent run. This process was repeated two times, such that sediment organic matter concentrations used as initial conditions represented approximately five years (57 months) of inorganic nutrient load reduction. This case did produce a small, but detectable increase in predicted dissolved oxygen concentrations over the lower half of the cumulative frequency range (Figure 51). The percentage of time and locations with predicted dissolved oxygen concentrations of 0.0 mg/l decreased from 8.0% to 4.5%. At a cumulative frequency of 0.2, the “cleaner sediment” case had a predicted dissolved concentration of 3.5 mg/l whereas the base case had a predicted dissolved oxygen concentration of 2.9 mg/l (Figure 51).

4.3 Model Verification Attempt

It is standard practice in modeling studies to perform a model verification exercise. This is typically done by running the calibrated model using a second independent data set, with parameters set to values determined through calibration to the first data set. The model is considered to be “verified” (the term “validation” is also used) if model predictions for this second time period match the corresponding observed data sufficiently well. Ideally, the second data set

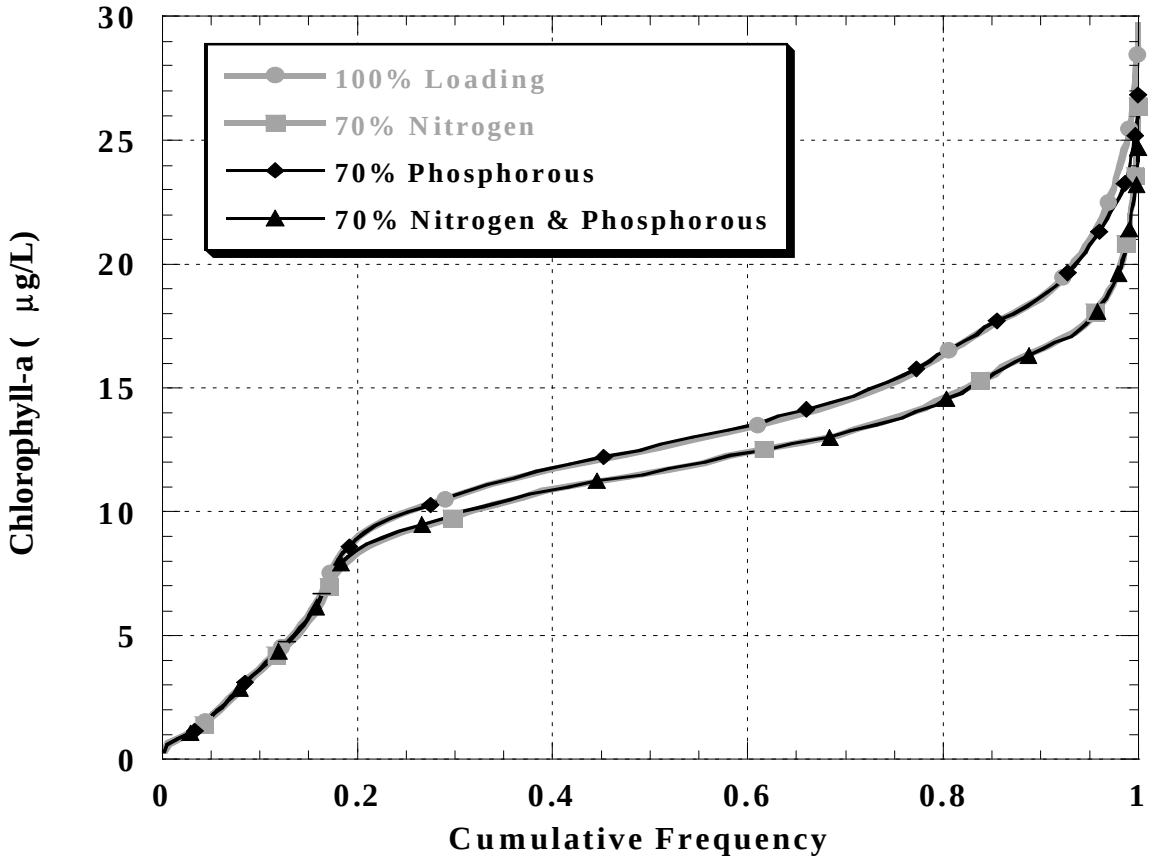

Figure 47. Comparison of 1997-1998 model predicted cumulative frequency distributions of chlorophyll-a concentrations in the Neuse River Estuary near Cherry Point, NC for a base case (100% loadings) and for three nutrient loading reduction scenarios.

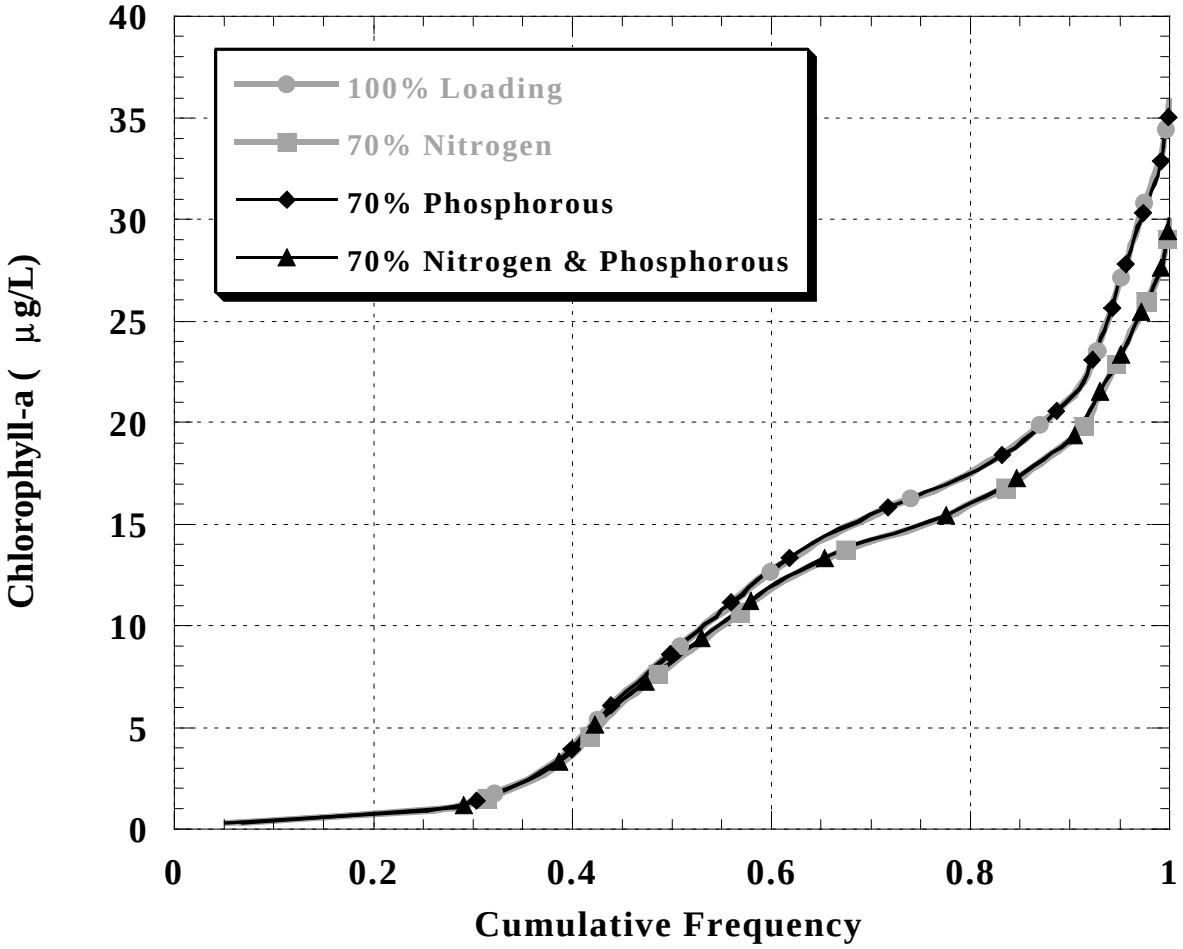

Figure 48. Comparison of 1997-1998 model predicted cumulative frequency distributions of chlorophyll-a concentrations in the Neuse River Estuary near New Bern, NC for a base case (100% loadings) and for three nutrient loading reduction scenarios.

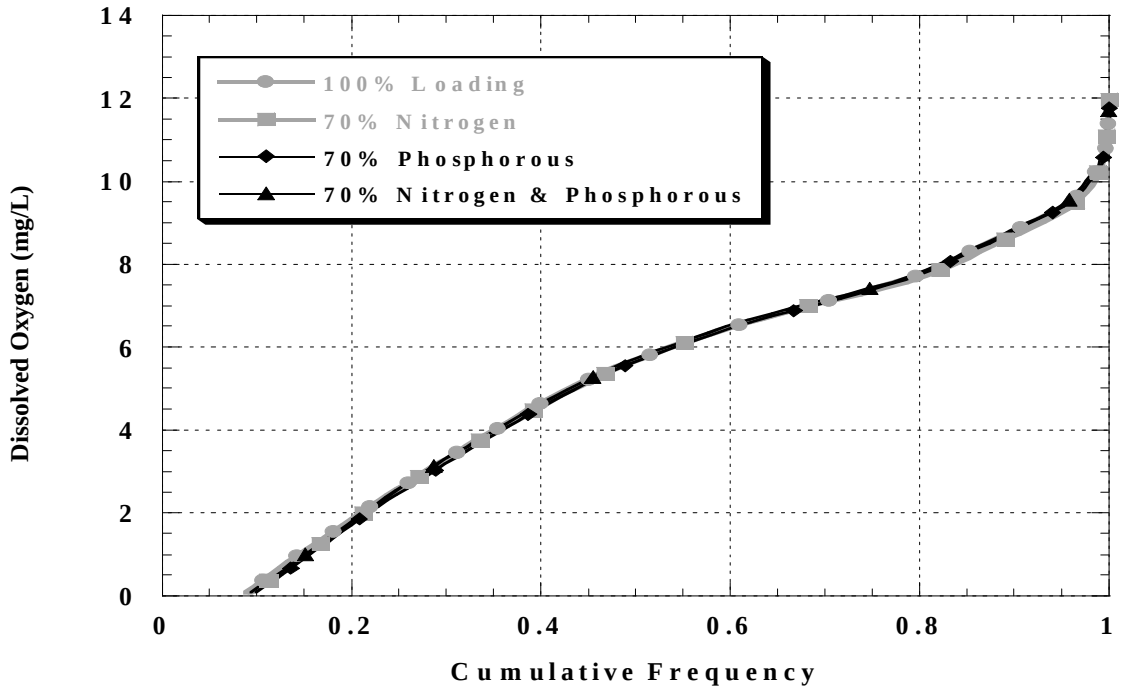

Figure 49. Comparison of 1997-1998 model predicted cumulative frequency distributions of dissolved oxygen concentrations in the Neuse River Estuary for a base case (100% loadings) and for three nutrient loading reduction scenarios.

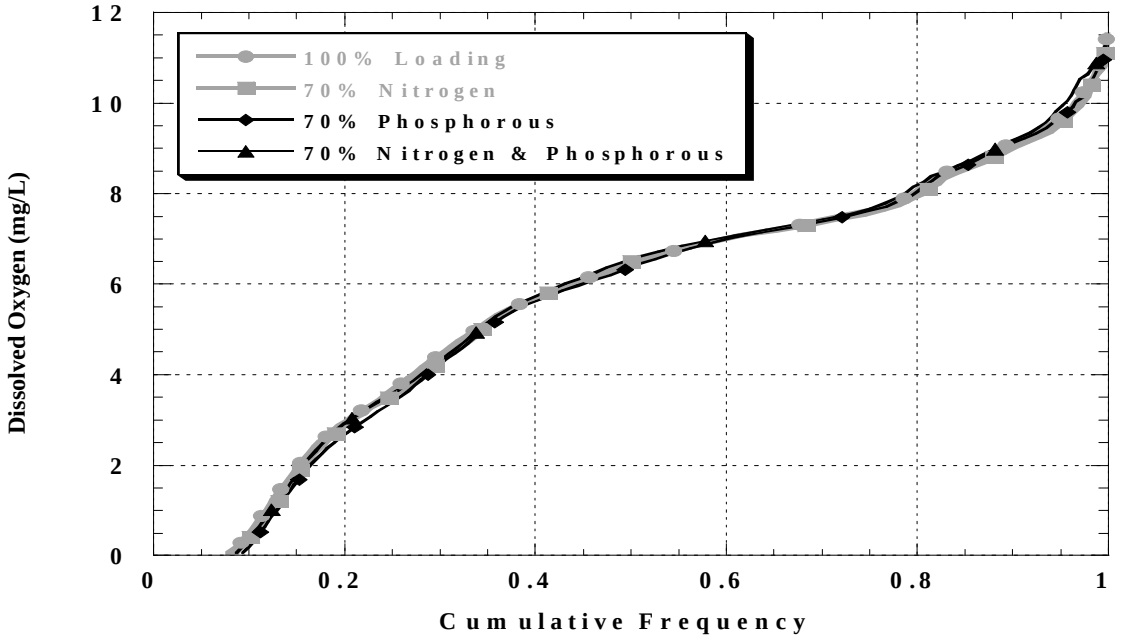

Figure 50. Comparison of 1997-1998 model predicted cumulative frequency distributions of dissolved oxygen concentrations in the Neuse River Estuary near New Bern, NC for a base case (100% loadings) and for three nutrient loading reduction scenarios.

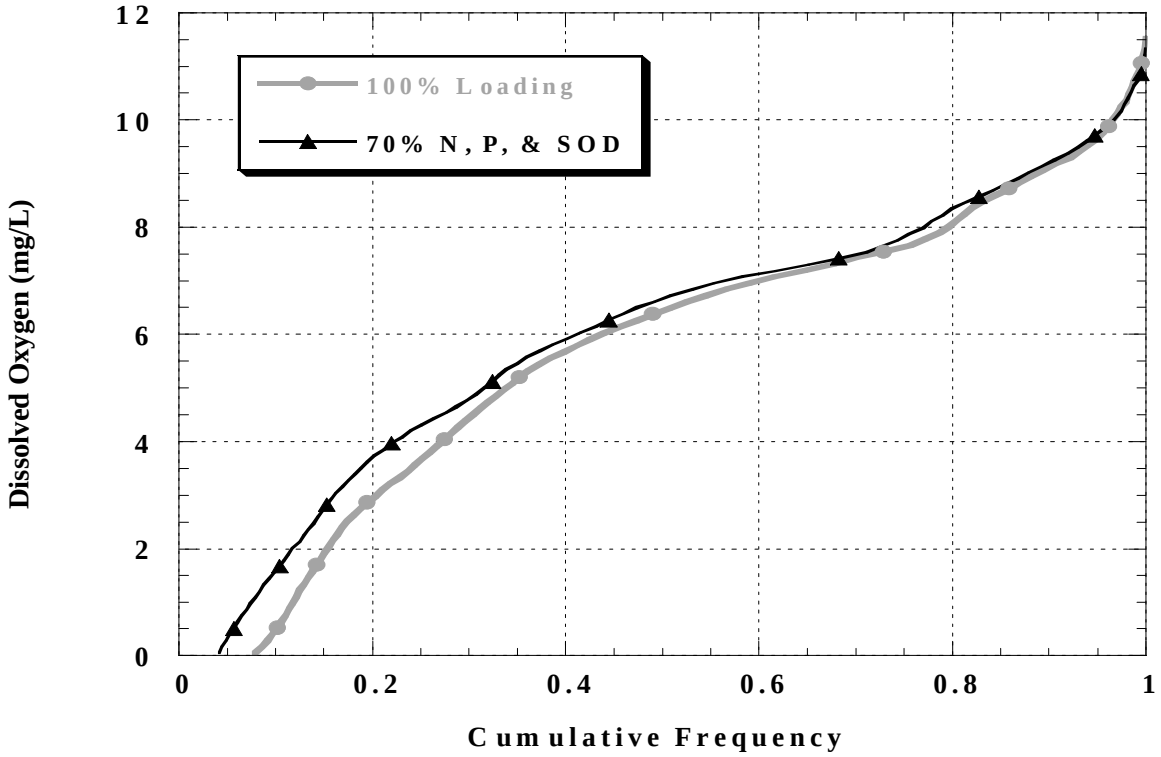

Figure 51. Comparison of 1997-1998 model predicted cumulative frequency distributions of dissolved oxygen concentrations in the Neuse River Estuary near New Bern, NC for a base case (100% loadings) and for a case with reduced nutrient load and reduced sediment organic carbon.

should be sufficiently different from the first set to provide a good test of the model's predictive capabilities, but exactly how verification should be performed, or if it needs to be done at all are matters of some controversy. In this study, model verification was attempted using the 1991 data as the second data set. It was eventually decided, however, that the quality of the 1991 water quality data set was not sufficient for model verification. In addition, the need to estimate the downstream boundary condition (see Section 3 for details) for salinity was considered a serious flaw that made verifying the model's conservative transport parameters difficult. Nonetheless, an analysis was performed to "verify" the elevation and salinity predictions of the model.

The model was run to predict water levels, water velocities, and salinities in the estuary for the period from March 1, 1991 through September 28, 1997. Predicted water levels at New Bern were compared corresponding observed values. Overall, the model predicted 1991 water surface elevations just as well as it predicted elevations in 1997 and 1998. The mean absolute error (MAE) for water surfac**e** elevations during July 1991 was 0.031 m (Figure 52), whereas the MAE for water surface elevations in July 1998 was 0.046 m (Figure 8). The model's salinity prediction capabilities using the 1991 data set also proved to be comparable to the predictive capability using the 1997-1998 data set. For July 1991 the mean absolute error between model predictions and observations for surface and bottom salinities at Cherry Point was 1.39 g/l (Figure 53). This compares to a MAE for surface and bottom salinities at Cherry Point using the entire 1997-1998 data set of 2.00 g/l (Figure 11). Because of the limitations of the observed data set, no additional model/data comparisons are possible, thus these comparisons are considered to constitute a "model verification attempt." The attempt, does indicate, however, that model runs using an independent data set can produce fits between predictions and observations that are comparable to the data set used for calibration.

4.4 Uncertainty Analysis

4.4.1 Feasible Parameter Vectors

As described earlier, 2187 candidate parameter vectors were created by choosing one of three levels for each one of seven variable parameters (Table 7). Of the 2187 candidate parameter vectors, 220 were considered to be feasible. Each of these 220 parameter vectors produced a model that fit the observed data set at least as well as the base case described previously. By definition the base case had all seven variable parameters set to level one. The distribution of parameter levels within the set of feasible parameter vectors (Figure 54) varied by parameter. For instance, for four of the seven variable parameters (carbon to chlorophyll ratio, maximum growth rate, settling velocity, P half saturation constant), each of the three parameter levels were nearly equally represented in the set of feasible parameter vectors (Figure 54). For two of the remaining three parameters (phytoplankton N fraction, N half saturation constant), only levels one and three produced feasible parameter vectors. Level two, where the parameter was set to a value below that for the base case, produced no feasible parameter vectors for these two parameters. The last variable parameter (labile POM decay rate) had only one of the 220 feasible parameter vectors with a level two value (Figure 54).

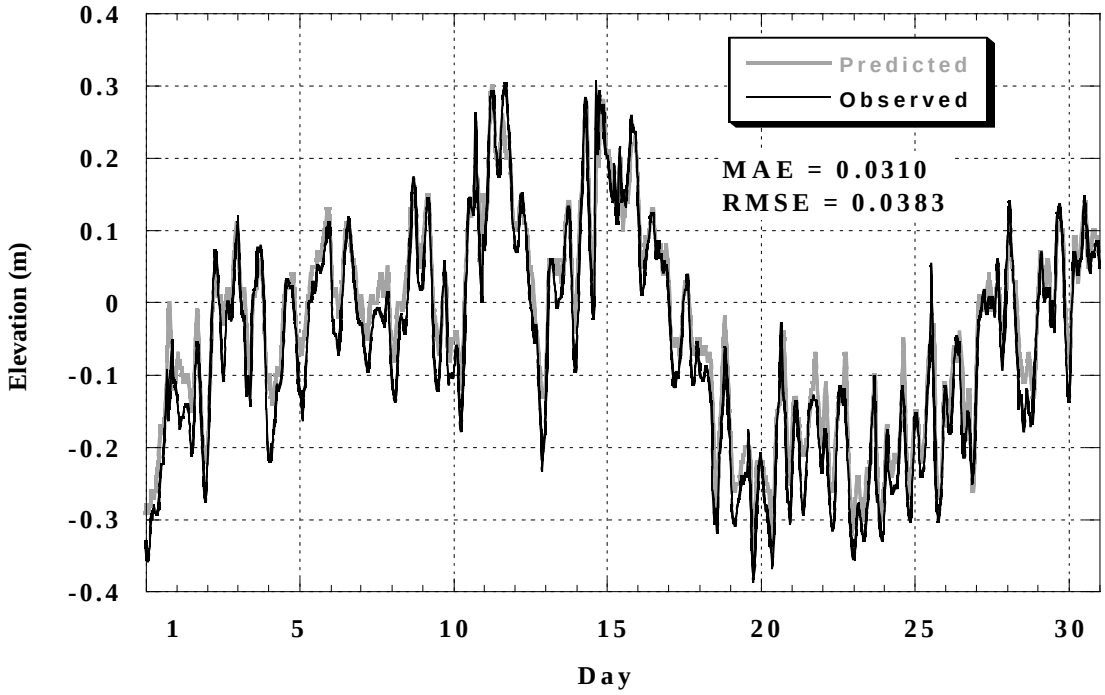

Figure 52. Model computed and observed water levels in the Neuse River Estuary at New Bern, NC during July 1991.

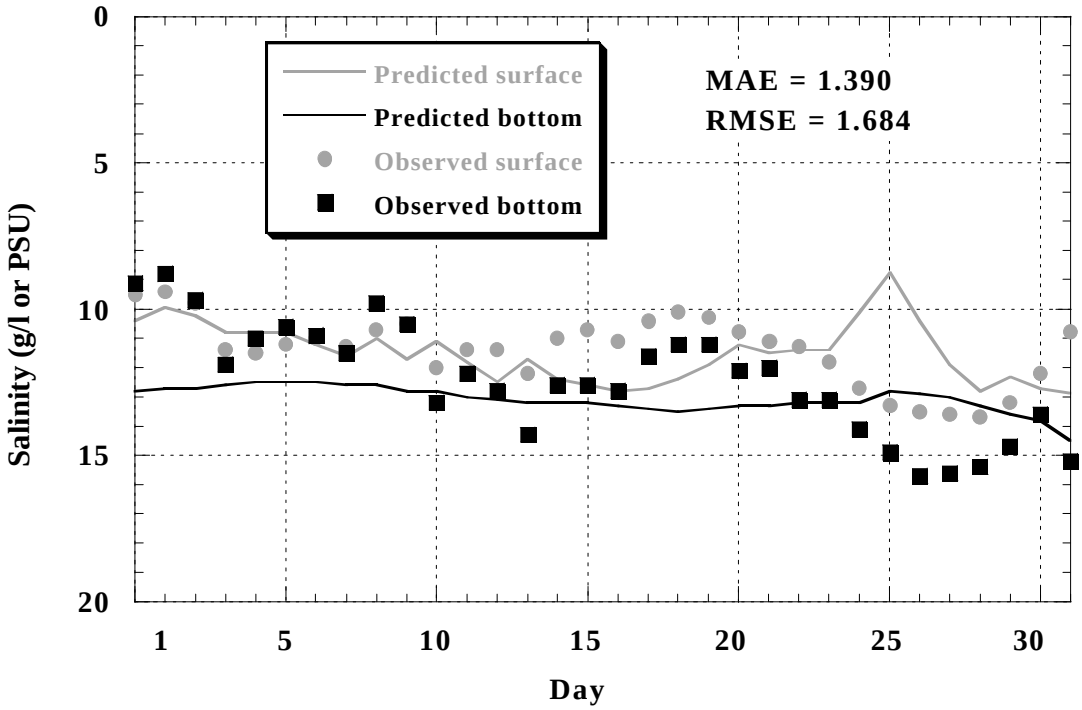

Figure 53. Model computed and observed salinities in the Neuse River Estuary at Cherry Point, NC during July 1991.

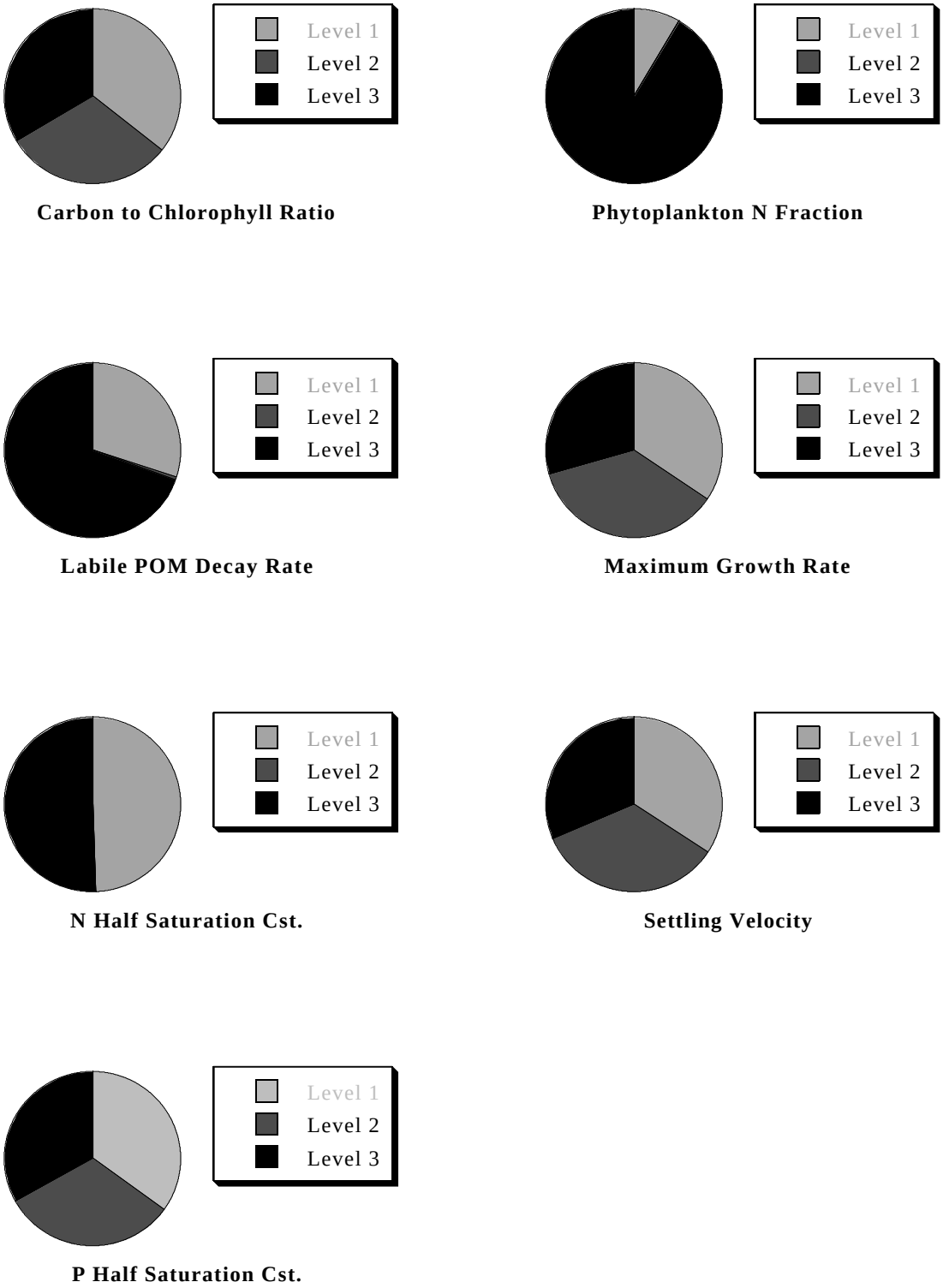

Figure 54. Distribution of parameter levels (see Table 7 for values) of the seven variable parameters for the 220 feasible parameter vectors. The base case had all seven variable parameters at level 1.

4.4.2 Variability of Predicted Water Quality Conditions

All 220 of the feasible parameter vectors were used for a standard inorganic nutrient loading run and for a run with inorganic nutrient loading (N and P) reduced by 30% from the standard value. As expected, a range of chlorophyll-a concentrations were predicted by the set of feasible parameter vectors, with reduced chlorophyll-a concentrations predicted for the reduced nutrient loading case (Figures 55 and 56). Surprisingly, the base values for median and maximum chlorophyll-a concentration were above the range representing 95% of the predicted values (Figure 55 and 56). Whereas median chlorophyll for the base case was 10.0 µg/l (Figure 47), 95% of the 220 runs had median predicted chlorophyll-a concentrations between 5.5 and 8.0 µg/l (Figure 55). This situation also existed for the predicted chlorophyll-a concentrations at Cherry Point. The base case median value (12.3 µg/l) was greater than the range of predicted median chlorophyll-a concentrations (6.5 to 8.7 µg/l) determined through the uncertainty analysis.

The uncertainty in predictions of chlorophyll-a concentration was dependent on the statistic describing the predictions. Uncertainty in predictions of median chlorophyll was less than for predictions of maximum chlorophyll. While the range in predicted median chlorophylls was only 2.5 µg/l for the entire estuary and 2.2 µg/l for the Cherry Point area, the corresponding ranges in predicted maximum chlorophylls were 7.7 and 5.0 µg/l. A third statistic, the percentage of predicted values above 25 µg/l was used as an estimate of how often relatively high concentrations would be present. For the estuary as a whole this measure varied only very slightly (Figure 55). For the Cherry Point area, this statistic was always zero for both the 100% and 70% loading scenarios (Figure 56).

The 220 feasible parameter vectors differed only slightly in their predictions of dissolved oxygen concentrations in the estuary. Predicted median dissolved oxygen concentration was slightly higher in the entire estuary (Figure 57) than it was at Cherry Point (Figure 58). The range in predicted medians for the 220 cases was 0.15 mg/l for the entire estuary and 0.20 mg/l for the Cherry Point area. There was a significant amount of variation, however, in the predictions of anoxia incidence (defined as the percentage of concentrations below 2.0 mg/l). For the entire estuary, the incidence varied from 4.1% to 6.3% for the 100% loading cases, and from 4.0% to 6.2% for the 70% loading cases (Figure 57). For the Cherry Point area, the anoxia incidence varied from 4.2% to 7.9% for the 100% loading cases, and from 4.2% to 7.7% for the 70% loading cases (Figure 58).

4.4.3 Variability in Predictions of Water Quality Improvement

In all of the 220 cases tested, lower nutrient loading “improved” the water quality by reducing chlorophyll-a concentrations and increasing dissolved oxygen concentrations. There were some interesting differences, in the uncertainty of predictions of water quality improvement. There was a relatively low level of uncertainty with regard to predictions of reductions in median and maximum chlorophyll-a concentrations in the entire estuary (Figure 59). Median chlorophyll was predicted to decrease by 6.7% to 11%, whereas maximum chlorophyll concentration would decrease by 6.0% to 7.6% (Figure 59). Predictions of the magnitude of water quality

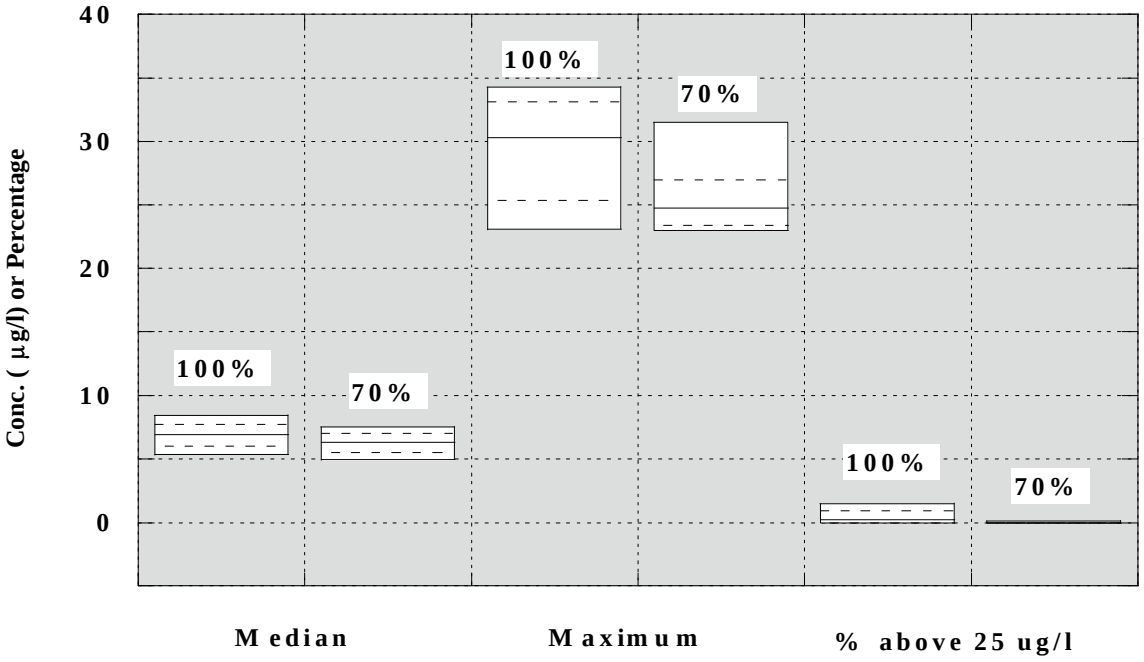

Figure 55. Distribution of median and maximum model predicted chlorophyll-a concentrations and the percentage above 25 µg/l in the Neuse River Estuary for 220 model runs using feasible parameter vectors with either 100% or 70% nutrient loading.

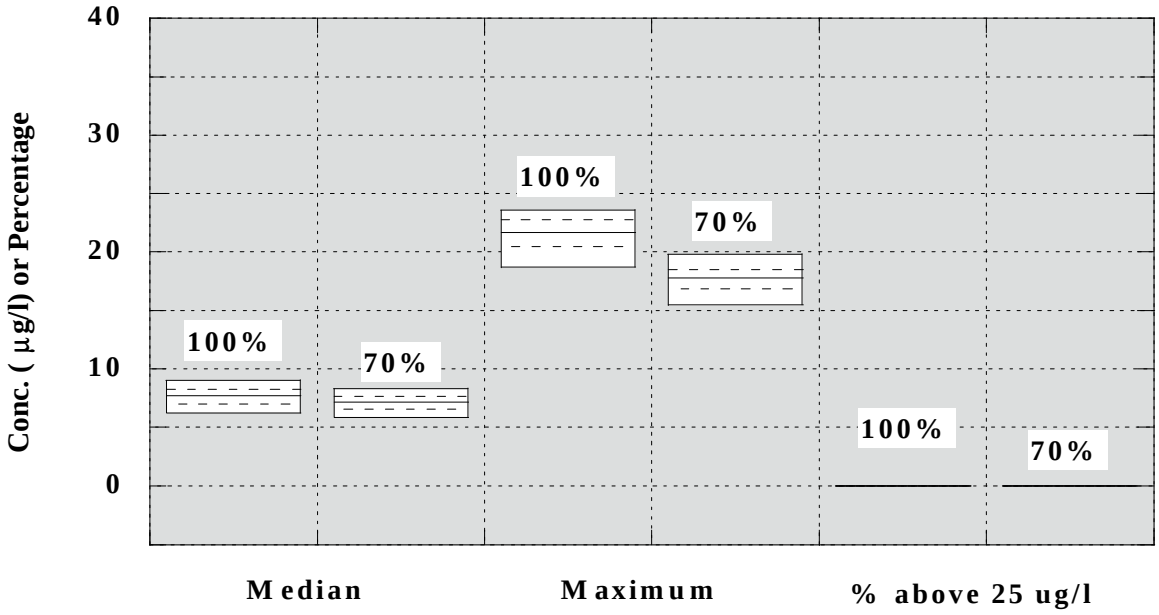

Figure 56. Distribution of median and maximum model predicted chlorophyll-a concentrations and the percentage above 25 µg/l in the Neuse River Estuary near Cherry Point, NC for 220 model runs using feasible parameter vectors with either 100% or 70% nutrient loading.

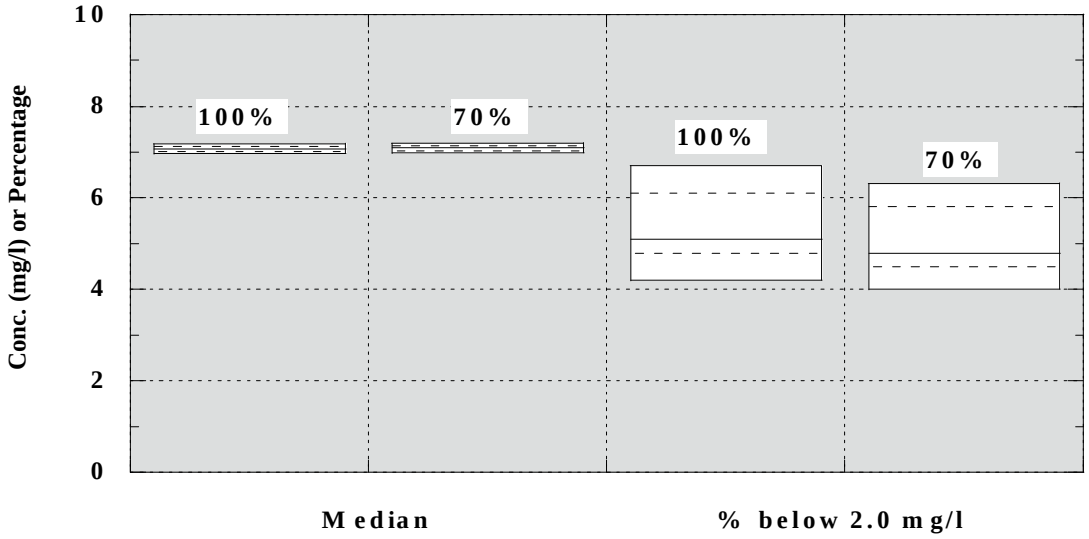

Figure 57. Distribution of median predicted dissolved oxygen concentrations and the percentage of concentrations below 2.0 mg/l in the Neuse River Estuary for 220 model runs using feasible parameter vectors with either 100% or 70% nutrient loading.

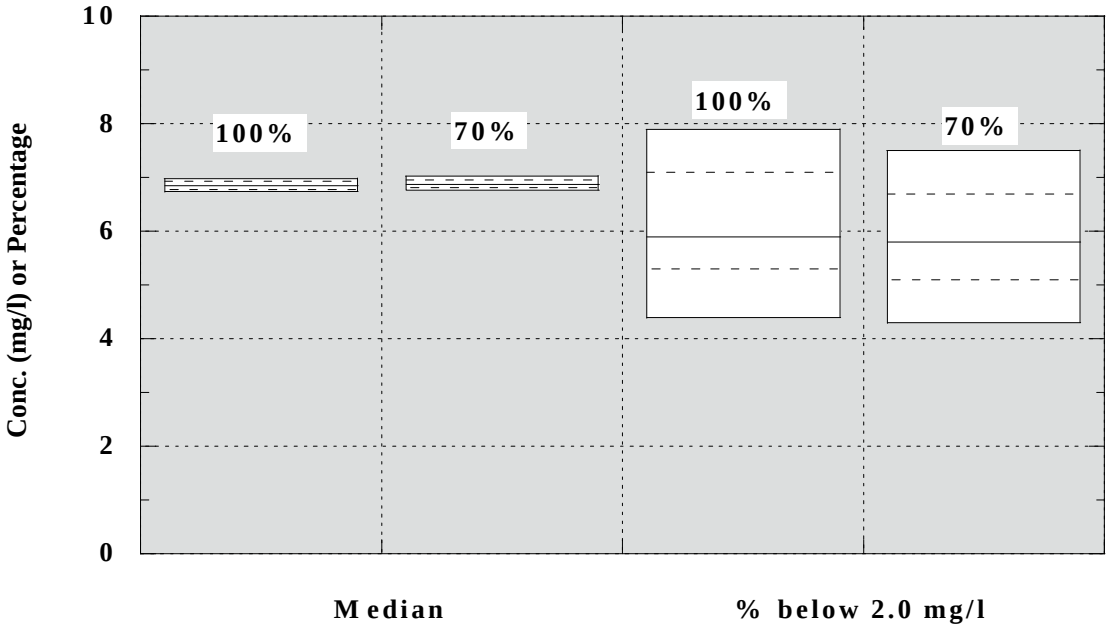

Figure 58. Distribution of median predicted dissolved oxygen concentrations and the percentage of concentrations below 2.0 mg/l in the Neuse River Estuary near Cherry Point, NC for 220 model runs using feasible parameter vectors with either 100% or 70% nutrient loading.

improvement in chlorophyll concentration at Cherry Point were larger but less certain. Median chlorophyll was predicted to decrease by 0.3% to 20%, whereas maximum chlorophyll concentration would decrease by 15% to 22% (Figure 59).

As seen earlier, increases in predicted dissolved oxygen concentration with reduced nutrient loading were slight. Median dissolved oxygen concentrations were essentially unchanged (Figure 60). Reduced nutrient loading did reduce the anoxia incidence somewhat. For the entire estuary, the fraction of dissolved concentrations below 2.0 mg/l was predicted to decrease by 2.3% to 11% with an inorganic nutrient load reduction of 30%. Once again, this prediction was less certain for the Cherry Point area than it was for the entire estuary. For the Cherry Point area, the fraction of dissolved concentrations below 2.0 mg/l was predicted to decrease by -5.5% to 13% with a 30% decrease in inorganic nutrient loading (Figure 60).

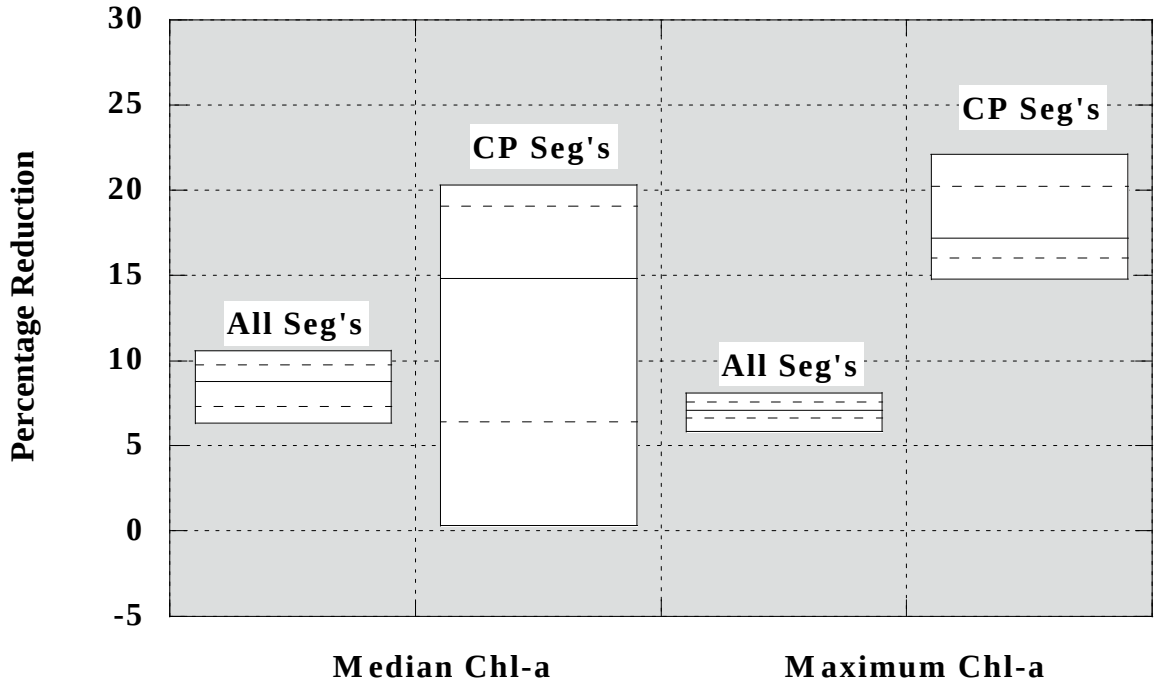

Figure 59. Distribution of predicted percent reduction in median, maximum, and fraction above 25 µg/l for mid-channel chlorophyll-a concentrations in the Neuse River Estuary using 220 model runs with feasible parameter vectors and a 30% nutrient load (N+P) reduction

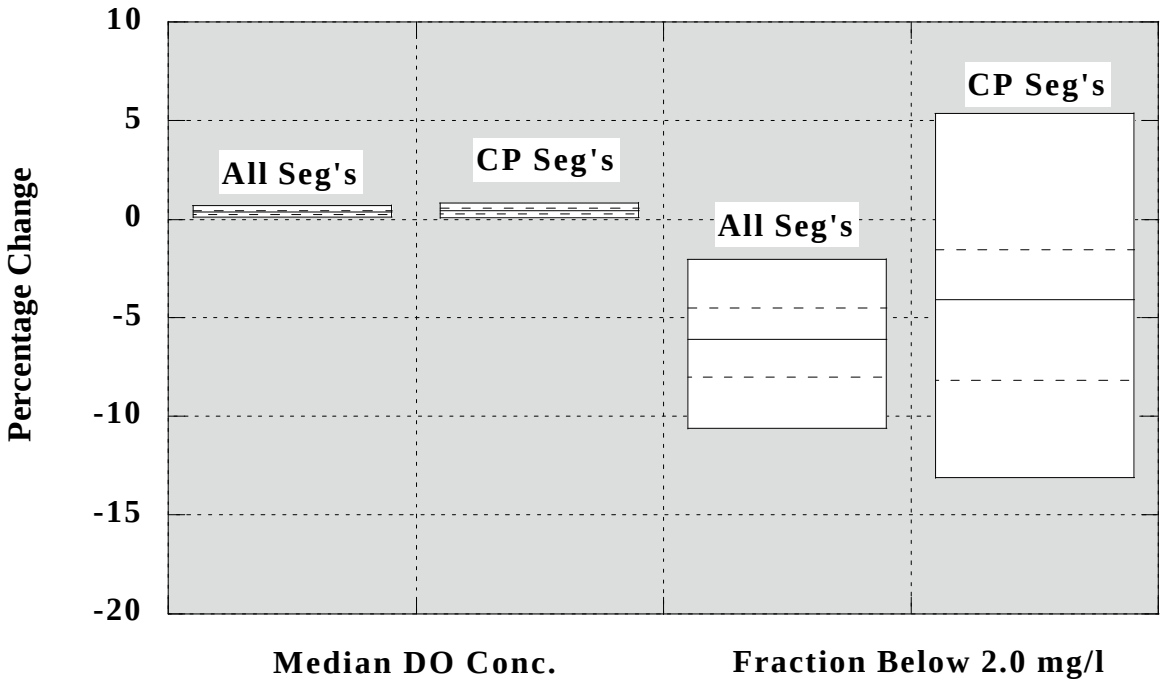

Figure 60. Distribution of predicted percent change in median and fraction below 2.0 mg/l for mid-channel dissolved oxygen concentrations in the Neuse River Estuary using 220 model runs with feasible parameter vectors and a 30% nutrient load (N+P) reduction

5. DISCUSSION AND CONCLUSIONS

5.1 Predicted Water Quality Improvement

Interesting differences were observed in the degree of water quality improvement for different areas of the estuary. A thirty percent inorganic nutrient loading reduction produced a larger reduction in phytoplankton biomass in the lower estuary (Figure 47) as compared to the upper estuary (Figure 48). This result seems to be due to the large differences in the concentration of nutrients in these two areas. The model predicted that nutrient concentrations decreased markedly downstream, so that nutrient concentrations in the New Bern area were typically above the phytoplankton's half-saturation constant for growth. Biomass accumulation in this area seemed often to be limited not by nutrients but by other factors such as water residence time, temperature, or light availability, thus reductions in nutrient concentrations did not have a significant effect on phytoplankton growth rates. Conditions in the Cherry Point area were significantly different, as nutrient limitation was much more frequent and pronounced, thus reductions in nutrient loading produced slower phytoplankton growth, and lower biomass levels.

Another interesting result was that reductions in inorganic nitrogen loading were much more effective in reducing phytoplankton biomass than were reductions in inorganic phosphorus loading. Reducing just inorganic nitrogen loading by 30% had an effect similar to reducing loadings of both inorganic nitrogen and phosphorus. This was true for the entire estuary (Figure 46), as well as the upper (Figure 48) or lower (Figure 47) estuary. Reducing just inorganic phosphorus loading produced essentially no change in the predicted phytoplankton biomass. This result agrees with the conclusions of earlier researchers (e.g. Paerl 1987) who have observed that phytoplankton primary production is usually nitrogen limited, and that the N:P ratio in the estuary varies from the upper to lower estuary (Paerl et al. 1995).

The model predictions differed very significantly in the extent to which nutrient loading reductions would produce changes in chlorophyll or dissolved oxygen concentrations. A 30 % nutrient loading reduction produced a 10% to 20% reduction in phytoplankton biomass (Figures 46, 47, 48) but produced a negligibly small increase in dissolved oxygen concentration (Figures 49, 50). This result is likely due, at least in part, to the longer time scale necessary for changes in benthic conditions as compared with water-column conditions. Once nutrient loading is reduced, it is expected that it would take years for a new equilibrium to be established between decomposition and deposition of sediment organic carbon. Once this new equilibrium was established, an additional amount of improvement in bottom water dissolved oxygen concentration would be expected. In this study, an attempt was made to simulate this process by running a scenario with both reduced nutrient load and reduced sediment organic carbon (Figure 51). While the upper end of the frequency range was unchanged for this case (Figure 51) , a lower frequency of anoxia was predicted. The frequency of dissolved oxygen concentrations below 2.0 mg/l was 12% for the reduced loading and sediment organic carbon case as compared with 16% for the base case. The results indicate the importance of sediment processes in determining bottom water dissolved oxygen concentrations. It also seems possible that physical processes such as the limitation of vertical transport during density stratification may be exerting an important control here, so that little sensitivity is observed to changes in nutrient loadings. Additional runs that allow for

simulation of longer time periods, and that include different physical forcings might be helpful in contributing additional information on the sensitivity of the bottom water dissolved oxygen concentrations to reductions in nutrient loading.

5.2 Prediction Uncertainty

An interesting result with regard to model prediction uncertainty of water quality improvement was that the degree of uncertainty was very dependent upon the endpoint being examined. For example, the uncertainty in the prediction of improvement in median chlorophyll was much less than the uncertainty in maximum chlorophyll improvement (Figures 55, 56). Whereas the range in predicted median chlorophyll was less than 5 µg/l, the range in predicted maximum chlorophyll was as high as 11 µg/l (Figure 55). Interestingly, the range in predicted maximum chlorophyll concentrations was significantly smaller for the Cherry Point area (Figure 56) than it was for the estuary as a whole (Figure 55). The dissolved oxygen predictions showed a similar relationship, with the median value being more certain than the predicted frequency of anoxia (Figures 57, 58). Different patterns were observed, however, for predictions of water quality improvement, which were determined by calculating the difference in predicted chlorophyll or dissolved oxygen concentration between the 100% and 70% loading cases. As for the 100% and 70% loading cases, predictions of improvement in dissolved oxygen concentrations were more certain for the predictions of median concentrations than for the frequency of anoxia (Figure 60). For the chlorophyll predictions, however, whole estuary predictions were significantly more certain than those for Cherry Point, both for the median concentrations, and for the maximum concentrations (Figure 59). In predicting the impact of reduced nutrient loading, it should be noted that the model is not able to predict precisely improvement in water quality parameters that relate to the "tails" of distributions of water quality parameters or to the predicted conditions at a particular location. In general, predictions of water quality improvement are most certain for median conditions or for conditions spatially averaged over the estuary.

An important, yet relatively subjective aspect of the uncertainty analysis procedure was the behavior specification. In this application, the calibrated base case was used as the basis for determining whether a parameter vector was feasible. Parameter vectors that produced calibration performance at least as good as the base case were considered to be feasible. Through this procedure, the feasibility criteria were set to be consistent with expectations of model performance and data quality. It was expected that the behavior specifications would be similarly selective in determining feasible parameter vectors, but this turned out not to be the case. The distribution of mean absolute errors was significantly different between the five constituents tested. The measures differed in selectivity, with the nutrient parameters generally being less selective than either dissolved oxygen or chlorophyll-a predictions in establishing feasible parameter vectors. The differences may be due to the model's differing sensitivity to changes in model parameters for different predicted constituents. It seems reasonable to select the specification of a feasible parameter vector based upon a traditional calibration exercise, as the judgement involved in this procedure considers the quality of the observed data, the model's ability to simulate various constituents, and the consequences of a particular level of calibration for various constituents. This may produce, however, behavior specifications that widely vary in their selectivity in producing feasible parameter vectors.

Having performed the uncertainty analysis, it becomes possible to go back and look at which parameter levels did and did not produce feasible parameter vectors (Figure 54, Table 9). The seven parameters considered to be variable differed quite significantly in this respect. Four parameters (carbon:chl ratio, maximum phytoplankton growth rate, P half-saturation constant for growth, and phytoplankton settling velocity) produced a similar number of feasible parameter vectors from each of the three parameter levels (Figure 54, Table 9). One parameter, the labile POM decay rate, had only a single feasible parameter vector from the second parameter level that was set to a value higher than the base case (see Table 7 for parameter values corresponding to each level). The remaining two parameters produced feasible parameters vectors from only two of the three parameter levels. Interestingly, both of these parameters (N half-saturation constants for growth and the N fraction in phytoplankton biomass) relate to the phytoplankton's nitrogen requirements. In addition it appears that there was some correlation between variables in this group, as the number of feasible parameter vectors for the various parameter levels is similar for these two parameters (Table 9).

Table 9. Parameter Levels for the 220 Feasible Parameter Vectors

Parameter Level	Parameter						
	Carbon: chl ratio (g/g)	Phyto-plankton N fraction (g/g)	Labile POM decay rate (day^{-1})	Max. phyto. growth rate (day^{-1})	½ saturation constant for growth, N (mg/l)	Phyto. settling velocity (m/d)	½ saturation constant for growth, P (mg/l)
	Number of Feasible Parameter Vectors						
1	78	19	66	76	109	75	77
2	68	0	1	79	0	76	70
3	74	201	153	65	111	69	73

5.3 Limitations of the Analysis

While this study has presented valuable new information on the Neuse Estuary's response to nutrient loading reductions, it is important to recognize the study's limitations. This is particularly important given the intended use of the model as an aid to decision-making by environmental regulators. The study's limitations stem primarily from the assumptions and simplifications made in preparing the model's input files, from the choice of the model itself, and from variability assumed to be present in the physical system that is not represented in the model data set. An excellent review of these first two considerations has been presented by Bales and Robbins (1999). As reviewed and discussed in the methods sections, some of their simplifications/assumptions were eliminated or modified by model development, but others

remained. These remaining assumptions/limitations are described here. Several of the assumptions/simplifications were related to the preparation of the data sets, as follows:

- streamflow yields for all basins were assumed to be equal to that of either the Neuse River at Kinston, or the Trent river at Trenton, even though most downstream creeks (e.g. Adams Creek) are a considerable distance from the Neuse or Trent River gauges,

- salinity inflows from the branches and the tributaries were assumed to be negligible,

- water quality in all the tributaries were assumed to be identical to either that of the Neuse River at Streets Ferry or to the Trent River at Trenton,

- the vertical distribution of water quality constituents at the downstream boundary during 1997 and 1998 can be estimated using the vertical distribution of salinity taken at the same time,

- temporal distributions of water quality constituents could be adequately characterized by bi-weekly (1997-1998) or monthly (1991) observations, with linear interpolation used to construct more frequent time records,

- meteorological conditions over the entire model domain were adequately represented by measured values at one location (Cherry Point Naval Air Station),

- wet deposition over the entire model domain was adequately represented by measurements at one location (Morehead City, North Carolina), and

- dry deposition could be accurately estimated by assuming that it was a constant percentage of wet deposition.

Several assumptions/limitations related to the use of a discretized representation of the physical system, and the use of a two-dimensional, laterally-averaged hydrodynamic and eutrophication model. The following assumptions/limitations were relevant to this study as well:

- lateral variations in hydrodynamic and water quality state variables were less important to the fate and transport of heat, mass, and momentum than longitudinal or vertical variations,

- lateral mixing was complete and instantaneous,

- vertical accelerations were small, and

- significant variations over longitudinal scales less than approximately 1 km, or vertical scales less than 0.5 m or temporal scales less than approximately 10 min. were not expected.

Some of the assumptions/limitations were specific to the particular model chosen for the analysis (CE-Qual-W2, Version 3), as follows:

- the phytoplankton population could be represented by three distinct groupings,
- the phytoplankton's carbon:chlorophyll ratio, and nutrient cell quotas were constant,
- all organic matter had the same C:N:P ratio,
- kinetic rate parameters, which could vary with water temperature, were otherwise constant in space and time, and
- benthic nutrient and oxygen fluxes were stoichiometrically related to the rate of sediment organic carbon decomposition, which is assumed to follow first order kinetics.

Finally, some of the assumptions/simplifications were related to the way in which the calibration and uncertainty analyses were performed, as follows:

- since the sampling interval of the monitoring data was a week for the 1997 conditions, and a month for 1991, the calibrated kinetic rate properties were assumed to be appropriate for describing the phytoplankton population response to changing nutrient, temperature, and light levels over these same intervals or longer,
- prediction uncertainty would not have increased markedly had more variable parameters been considered in the analysis of parameter specification uncertainty, and
- reductions in nutrient loading to the estuary would be achieved primarily by reducing the inflow nutrient concentrations rather than the inflow rates themselves.

Together this set of assumptions and simplifications establishes the scope of the questions that can be investigated with the model. Given these assumptions and limitations, it is important to note that there are interesting questions that <u>cannot</u> be investigated with the model as currently developed. For instance, the model cannot be used to investigate the potential for blooms of particular phytoplankton species (e.g. *Pfiesteria*), or to look at the nearshore impact of a particular discharge, or to examine lateral advection of low dissolved oxygen water under particular wind forcings, or to investigate the importance of sediment denitrification to estuarine nutrient cycling. In running the model, it must also be recognized that all model predictions are uncertain to some extent, and that the degree of uncertainty can vary markedly depending upon

the choice of model endpoint. Only by using the model in a manner consistent with its limitations and assumptions can meaningful and defendable conclusions be made regarding the linkage between nutrient loading and water quality conditions in the estuary.

5.4 Need for Additional Research

Based on the results of the study, it can be concluded that the two-dimensional laterally-averaged mechanistic eutrophication model developed as part of this study is capable of simulating the water quality dynamics of the Neuse River Estuary, and that this model can be used to predict the water quality improvement that would result from reduced nutrient loading. One potentially important factor not considered, however, was the extent to which the predictions of water quality improvement are dependent upon the particular year used for simulation. It is expected that different years might produce quantitatively different results if the years differ in the magnitude and timing of nutrient inflow events. Two of three years investigated so far, 1991 and 1997, were considered to be relatively dry years. While 1998 had a period of high flow, neither this year or 1997 had measured chlorophyll concentrations as high as in several of the previous years (Paerl and Pickney 1996). Future research should be conducted to simulate water quality conditions and predict water quality improvement using additional data sets. Inclusion of the 1999 data set is recommended. This year differed significantly from the previous two in the timing and magnitude of inflows (Figure 61). In addition, significant winter and summer algal blooms occurred. Simulating water quality conditions and predicting water quality improvement for this year would therefore provide valuable information on the sensitivity of the results to interannual differences in runoff and nutrient loading.

Prediction capability of the existing model seems to be limited at the present time by the relatively simple sediment diagenesis model employed. The current model uses a single constituent diagenesis model that may not accurately simulate benthic nitrogen fluxes during hypoxic periods. In addition, given the available data set it was not possible to investigate the extent to which nutrient loading might produce long-term changes in sediment conditions. The model results indicate that short-term improvement in dissolved oxygen concentrations as a result of reduced nutrient loading were slight, because of the relatively long response time of the sediments. Future research should therefore focus on improving the sediment prediction capabilities of the eutrophication model. This research should be conducted so as to allow for simulations of sediment changes that result from lower nutrient loading.

Finally, this research demonstrated the utility of an uncertainty analysis, but the effort was limited in its examinations of error sources. In this study, parameter specification error was analyzed, which was assumed to the major contributor to prediction uncertainty. The research utilized a literature review to select variable parameters for analysis. Future research should develop the uncertainty analysis method so that a list of variable parameters can be determined based on model predictions rather than literature review. In addition, future research should be conducted so that a complete error analysis can be conducted that will consider how errors in boundary and initial condition specification produce variability in model prediction. Each of these areas of future research should improve the model's prediction capability or reduce prediction uncertainty

while contributing to our understanding of the links between water quality and nutrient loading, which will in turn allow regulators to better manage our valuable estuarine resources.

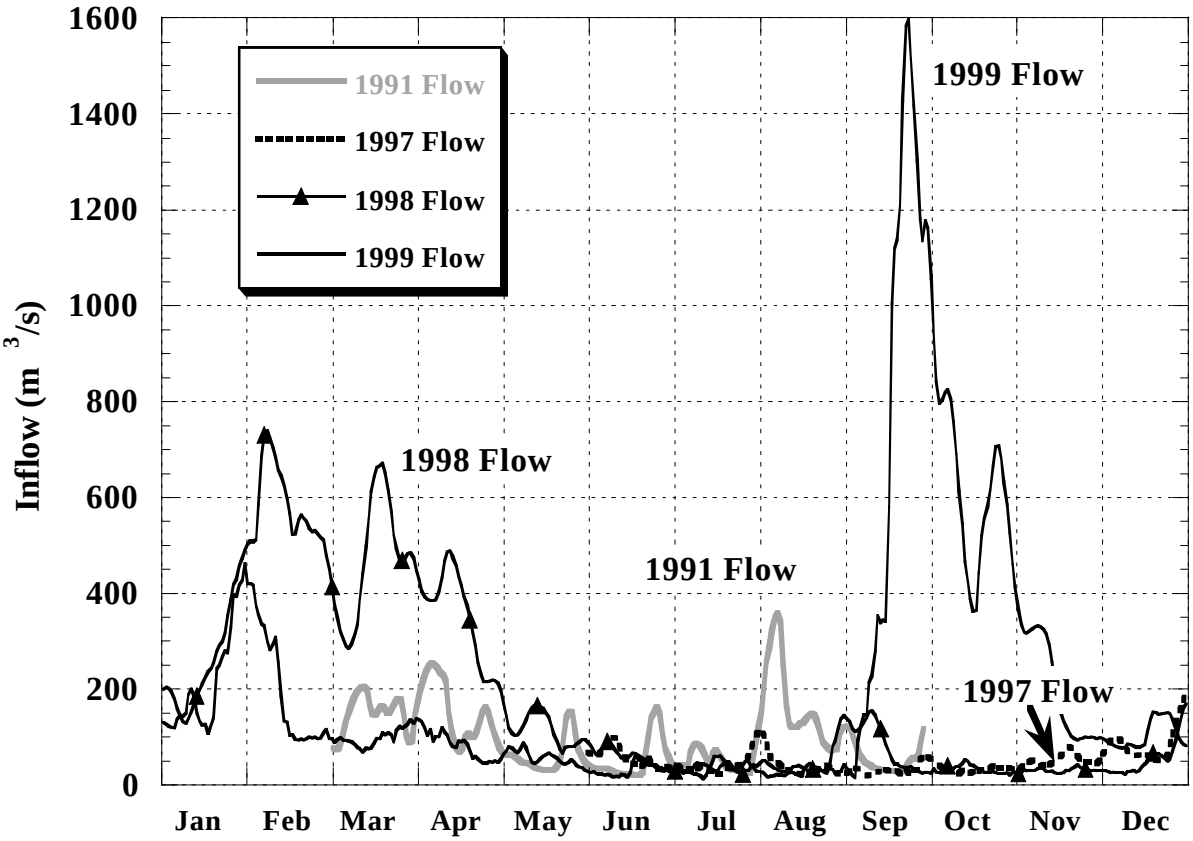

Figure 1. Inflows from the Neuse River to the estuary at Streets Ferry, NC during 1991, 1997, 1998, and 1999.

6. REFERENCES

Adams, B.A. Vanharn. 1998. Parameter distributions for uncertainty propagation in water quality modeling. Ph.D. thesis. Department of Environment, Duke University, Durham, NC.

Ambrose, R. B., Jr., T. A. Wool, and F. Martin. 1993. The water quality analysis simulation Program WASP5 - Part A: Model Documentation. U.S. Environmental Protection Agency, Office of Research and Development, Environmental Research Laboratory, Athens, GA.

Bales, J.D. and J.C. Robbins. 1999. *A Dynamic Water-Quality Modeling Framework for the Neuse River Estuary, North Carolina.* Water-Resources Investigations Report 99-4017. Raleigh: U.S. Geological Survey.

Bowen, J. D. 1997. Evaluating the Uncertainty in Water Quality Predictions - A Case Study. In *Estuarine and Coastal Modeling, Proceedings of the Fifth International Conference*, edited by Malcolm L. Spaulding and Alan F. Blumberg. Reston, Virginia: American Society of Civil Engineers.

Bowen, J.D. 1998. Using eutrophication modeling to predict the effectiveness of river restoration efforts. In *Engineering Approaches to Ecosystem Restoration - Conference Proceedings, 1998 Wetlands Engineering and River Restoration Conference*, edited by Donald F. Hayes. Reston, Virginia: American Society of Civil Engineers.

Bowie, G.L., W.B. Mills, D.B. Porcella, C.L. Campbell, J.R. Pagenkopf, G.L. Rupp, K.M. Johnson, P.W.H. Chan, S.A. Gherini, and C.E. Chamberlin. 1985. *Rates, Constants, and Kinetic Formulations in Surface Water Quality Modeling.* Report EPA/600/3-85/040. Athens, Georgia: U.S. Environmental Protection Agency, ORD, ERL.

Boyer, J.N., R.R. Christian, and D.W. Stanley. 1993. Patterns of phytoplankton primary productivity in the Neuse River estuary, North Carolina, USA. *Mar. Ecol. Prog. Ser.* 97:287-297.

Brown, L.C., and T.O. Barnwell, Jr. 1987. *The Enhanced Stream Water Quality Models QUAL2E and QUAL2E-UNCAS: Documentation and Users Manual.* Report EPA/600/3-87/007. Athens, Georgia: U.S. Environmental Protection Agency.

Burkholder, J.M., C.W. Hobbs, and H.B. Glasgow, Jr. 1995. Distribution and environmental conditions for fish kills linked to a toxic ambush-predator dinoflagellate. *Mar. Ecol. Prog. Ser.* 124:43-61.

Cerco, C., and T.M. Cole. 1993. Three-dimensional eutrophication model of Chesapeake Bay. *Journal of Environmental Engineering*, 119(6):1006-1025.

Christian, R.R., J.N. Boyer, and D.W Stanley. 1991. Multi-year distribution patterns of nutrients within the Neuse River Estuary, North Carolina. *Mar. Ecol. Prog. Ser.* 71:259-274.

Cole, T.M., and E.M. Buchak. 1995. *CE-QUAL-W2: A two-dimensional, laterally averaged hydrodynamic and water quality model, version 2.0, Draft User Manual*. Instruction Report EL-95-1. Vicksburg, MS: Corps of Engineers Waterways Experiment Station.

Giese, G.L, H.B. Wilder, and G.G.Parker, Jr. 1985. *Hydrology of Major Estuaries and Sounds of North Carolina.* Water Supply Paper 2221. Raleigh: U.S. Geological Survey.

Hobbie, J.E., and N.W. Smith. 1975. *Nutrients in the Neuse River Estuary.* Report UNC-SG-75-21. Raleigh: The University of North Carolina Sea Grant Program.

Hydroqual, Inc. and Normandeau Associates. 1995. *A Water Quality Model for Massachusetts and Cape Cod Bays: Calibration of the Bays Eutrophication Model (BEM).* MWRA Enviro. Quality Dept. Tech. Rpt. Series No. 95-8. Boston: Massachusetts Water Resources Authority.

Hydroqual, Inc. 1995. Application of a coupled hydrodynamic/water column/sediment model for the Tar-Pamlico River, North Carolina. Produced for the Tar-Pamlico Basin Association, Greenville, North Carolina.

Luettich, Richard A., Jr., Jesse E. McNinch, James L. Pinckney, Marc Alperin, Christopher S. Martens, Hans W. Paerl, Charles H. Peterson, and John T. Wells. 2000. *Neuse River Estuary Modeling and Monitoring Project Stage 1: Hydrography and Circulation, Water Column Nutrients and Productivity, Sedimentary Processes and Benthic-Pelagic Coupling, and Benthic Ecology.* Report 325-B. Raleigh: The University of North Carolina Water Resources Research Institute.

Lung, W.S. 1988. The role of estuarine modeling in nutrient control. *Water Sci. and Technol*. 20(6/7):243-252.

Mallin, M.A., and H.W. Paerl. 1994. Planktonic trophic transfer in an estuary: Seasonal, diel, and community structure effects. *Ecology*. 75(8):2168-2184.

North Carolina Division of Water Quality (NC DWQ). 1998. Neuse River internal nutrient loading studies, 1996 - 1997. Photocopy. Water Quality Section, Environmental Sciences Branch, Raleigh.

Paerl, H.W. 1987. *Dynamics of Blue-green Algal Blooms in the Lower Neuse River, NC: Causative Factors and Potential Controls.* Report No. 229. Raleigh: The University of North Carolina Water Resources Research Institute.

Paerl, H.W., M.A. Mallin, C.A. Donahue, M. Go, and B.L Peirls. 1995. *Nitrogen Loading Sources and Eutrophication of the Neuse River Estuary, North Carolina: Direct and Indirect Roles of Atmospheric Deposition.* Report No. 229. Raleigh: The University of North Carolina Water Resources Research Institute.

Paerl, H.W., and J.W. Pinckney. 1996. Hypoxia, anoxia and fish kills in relation to nutrient loading in the Neuse River estuary: Why was 1995 a "bad" year? *Water Wise*, 4(2), May 1996. Raleigh: The University of North Carolina Sea Grant Program.

Redfield, A.C., B.H. Ketchum, and F.A. Richards. 1963. The influence of organisms on the composition of seawater, in *The Sea*, edited by M.N. Hill. New York: Wiley-Interscience.

Rizzo, W.M., G.J. Lackey, and R.R. Christian. 1992. Significance of euphotic, subtidal sediments to oxygen and nutrient cycling in a temperate estuary. *Mar. Ecol. Prog. Ser.* 86:51-61.

Rizzo, W.M., and R.R. Christian. 1996. Significance of subtidal sediments to heterotrophically-mediated oxygen and nutrient dynamics in a temperate estuary. *Estuaries.* 19(2B):475-487.

Robbins, J.C., and J.D. Bales. 1995. *Simulation of Hydrodynamics and Solute Transport in the Neuse River Estuary, North Carolina.* Open-File Report 94-511. Raleigh: U.S. Geological Survey.

Rudek, J., H.W. Paerl, M.A. Mallin, and P.W. Bates. 1991. Seasonal and hydrological control of phytoplankton nutrient limitation in the lower Neuse River Estuary. *Mar. Ecol. Prog. Ser.* 75:133-142.

Stanley, D.W., and S.W. Nixon. 1992. Stratification and bottom-water hypoxia in the Pamlico River Estuary. *Estuaries*. 15(3):270-281.

Appendix A. - Model Parameter Specification

```
                                   Neuse River

TITLE C ............................TITLE....................................
        Base case hydro & kinetic parameters, MODMON1_base/9798_025.con
        unsteady run, mannings n=0.025
        Case used to create figures for MODMON 1 WRRI report
        w/ BDOD turned on, Printing only Neuse R. segments
        2 branch, 12 trib system
        printing sal, nuts, OM, phytos, DO, chla, productivity, SOD, seds

TIME CON  TMSTRT   TMEND    YEAR
           151.5   729.5    1997

DLT CON      NDT  DLTMIN   DZMIN     AZC
               2     1.0 0.14e-5     0.5

DLT DATE    DLTD    DLTD    DLTD    DLTD    DLTD    DLTD    DLTD    DLTD    DLTD
             0.0   500.0

DLT MAX   DLTMAX  DLTMAX  DLTMAX  DLTMAX  DLTMAX  DLTMAX  DLTMAX  DLTMAX  DLTMAX
           600.0   600.0

DLT FRN     DLTF    DLTF    DLTF    DLTF    DLTF    DLTF    DLTF    DLTF    DLTF
            0.90    0.90

DLT LIMIT   VISC    CELC
              ON      ON

BRANCH G      US      DS     UHS     DHS      NL
Br 1           2      60       0      -1       1
Br 2          63      65       0      21       1

LOCATION     LAT    LONG   ELBOT      BS      BE   (mean tide level
           35.00   76.92   -8.50       1       2   = middle of layer 4)

INIT CND     T2I
            -2.0

INIT CND    ICEI  WTYPEC
             0.0    SALT

CALCULAT     VBC     EBC     MBC   PQINC     EVC     PRC
             OFF     OFF     OFF      ON     OFF      ON

INTERPOL   QINIC    TRIC   DTRIC    HDIC  QOUTIC    WDIC   METIC
              ON      ON      ON      ON      ON      ON      ON

DEAD SEA   WINDC    QINC   QOUTC   HEATC  AZCALC   DEBUG
              ON      ON      ON      ON     IMP     OFF

HEAT EXCH  SLHTC    SROC     AFW     BFW     CFW   WINDH
              ET     OFF     9.2    0.46     2.0     2.0

ICE COVER   ICEC  SLICEC  ALBEDO   HWICE    BICE    GICE  ICEMIN   ICET2
             OFF  DETAIL    0.25    10.0     0.6    0.07    0.05     3.0

TRANSPORT  SLTRC   THETA
        ULTIMATE    0.50

WSC NUMB    NWSC   WINDH
               1     2.0

WSC DATE    WSCD    WSCD    WSCD    WSCD    WSCD    WSCD    WSCD    WSCD    WSCD
```

```
             0.0

WSC COEF      WSC      WSC      WSC      WSC      WSC      WSC      WSC      WSC      WSC
              0.8

HYD COEF       AX      IDX    CHEZY     CBHE     TSED    AZMAX    DZMAX      CRI    AZMIN
             50.0     50.0     -1.0   7.0E-8      9.6       10      1.0     1.50   1.0e-5

N STRUC      NSTR     NSTR     NSTR     NSTR     NSTR     NSTR     NSTR     NSTR     NSTR
                 0

STR TOP     ESTRT    ESTRT    ESTRT    ESTRT    ESTRT    ESTRT    ESTRT    ESTRT    ESTRT
Br 1
Br 2

STR BOT     ESTRB    ESTRB    ESTRB    ESTRB    ESTRB    ESTRB    ESTRB    ESTRB    ESTRB
Br 1
Br 2

SINK TYPE   SINKC    SINKC    SINKC    SINKC    SINKC    SINKC    SINKC    SINKC    SINKC
Br 1
Br 2

E STRUC      ESTR     ESTR     ESTR     ESTR     ESTR     ESTR     ESTR     ESTR     ESTR
Br 1
Br 2

W STRUC      WSTR     WSTR     WSTR     WSTR     WSTR     WSTR     WSTR     WSTR     WSTR
Br 1
Br 2

N WEIR        NWR
                 0

WEIR SEG      IWR      IWR      IWR      IWR      IWR      IWR      IWR      IWR      IWR


WEIR TOP     EWRT     EWRT     EWRT     EWRT     EWRT     EWRT     EWRT     EWRT     EWRT


WEIR BOT     EWRB     EWRB     EWRB     EWRB     EWRB     EWRB     EWRB     EWRB     EWRB


N WDRWAL      NWD
                 1

W SEGMNT      IWD      IWD      IWD      IWD      IWD      IWD      IWD      IWD      IWD
                 3

W EL          EWD      EWD      EWD      EWD      EWD      EWD      EWD      EWD      EWD
            -1.00

W TOP        EWDT     EWDT     EWDT     EWDT     EWDT     EWDT     EWDT     EWDT     EWDT
                 5

W BOT        EWDB     EWDB     EWDB     EWDB     EWDB     EWDB     EWDB     EWDB     EWDB
                 7

PUMPBACK      JBG      KTG      KBG      JBP      KTP      KBP


N TRIBS       NTR
                12
```

Appendix A. - Model Parameter Specification

TRIB PLACE	TRC	TRC	TRC	TRC	TRC	TRC	TRC	TRC	TRC
	DENSITY	DENSITY	DENSITY	DENSITY	DENSITY	DENSITY	DENSITY	DENSITY	DENSITY
	DENSITY	DENSITY	DENSITY						
TRIB SEG	ITR	ITR	ITR	ITR	ITR	ITR	ITR	ITR	ITR
	3	5	13	15	32	34	41	42	45
	50	55	57						
TRIB TOP	ETRT	ETRT	ETRT	ETRT	ETRT	ETRT	ETRT	ETRT	ETRT
TRIB BOT	ETRB	ETRB	ETRB	ETRB	ETRB	ETRB	ETRB	ETRB	ETRB
DST TRIB	DTRC	DTRC	DTRC	DTRC	DTRC	DTRC	DTRC	DTRC	DTRC
	OFF	OFF							
PRINTER	LJC								
	IV								
HYD PRINT	HPRC	HPRC	HPRC	HPRC	HPRC	HPRC	HPRC	HPRC	HPRC
	OFF	OFF	OFF	OFF	OFF	OFF	OFF	OFF	OFF
	OFF	OFF	OFF	OFF	OFF	OFF	OFF	OFF	OFF
SNP PRINT	SNPC	NSNP	NISNP						
	ON	1	9						
SNP DATE	SNPD	SNPD	SNPD	SNPD	SNPD	SNPD	SNPD	SNPD	SNPD
	0.0								
SNP FREQ	SNPF	SNPF	SNPF	SNPF	SNPF	SNPF	SNPF	SNPF	SNPF
	30.0								
SNP SEG	ISNP	ISNP	ISNP	ISNP	ISNP	ISNP	ISNP	ISNP	ISNP
	2	5	10	15	20	25	30	35	36
SCR PRINT	SCRC	NSCR							
	ON	1							
SCR DATE	SCRD	SCRD	SCRD	SCRD	SCRD	SCRD	SCRD	SCRD	SCRD
	0.0								
SCR FREQ	SCRF	SCRF	SCRF	SCRF	SCRF	SCRF	SCRF	SCRF	SCRF
	1.0								
PRF PLOT	PRFC	NPRF	NIPRF						
	OFF	1	12						
PRF DATE	PRFD	PRFD	PRFD	PRFD	PRFD	PRFD	PRFD	PRFD	PRFD
	0.0								
PRF FREQ	PRFF	PRFF	PRFF	PRFF	PRFF	PRFF	PRFF	PRFF	PRFF
	0.2								
PRF SEG	IPRF	IPRF	IPRF	IPRF	IPRF	IPRF	IPRF	IPRF	IPRF
	2	5	8	11	14	17	20	23	26
	29	32	35						
SPR PLOT	SPRC	NSPR	NISPR						
	OFF	1	12						

Appendix A. - Model Parameter Specification

```
SPR DATE     SPRD     SPRD     SPRD     SPRD     SPRD     SPRD     SPRD     SPRD     SPRD
              0.0

SPR FREQ     SPRF     SPRF     SPRF     SPRF     SPRF     SPRF     SPRF     SPRF     SPRF
              5.0

SPR SEG      ISPR     ISPR     ISPR     ISPR     ISPR     ISPR     ISPR     ISPR     ISPR
                2        5        8       11       14       17       20       23       26
               29       32       35

TSR PLOT     TSRC     NTRS
               ON        1

TSR DATE     TSRD     TSRD     TSRD     TSRD     TSRD     TSRD     TSRD     TSRD     TSRD
              0.0

TSR FREQ     TSRF     TSRF     TSRF     TSRF     TSRF     TSRF     TSRF     TSRF     TSRF
              3.0

XTSR PLOT   XTSRC    NXTSR
               ON       59

XTSR SEG    IXTSR    IXTSR    IXTSR    IXTSR    IXTSR    IXTSR    IXTSR    IXTSR    IXTSR
                2        3        4        5        6        7        8        9       10
               11       12       13       14       15       16       17       18       19
               20       21       22       23       24       25       26       27       28
               29       30       31       32       33       34       35       36       37
               38       39       40       41       42       43       44       45       46
               47       48       49       50       51       52       53       54       55
               56       57       58       59       60       63       64       65

VPL PLOT     VPLC     NVPL
              OFF        1

VPL DATE     VPLD     VPLD     VPLD     VPLD     VPLD     VPLD     VPLD     VPLD     VPLD
              0.0

VPL FREQ     VPLF     VPLF     VPLF     VPLF     VPLF     VPLF     VPLF     VPLF     VPLF
              5.0

CPL PLOT     CPLC     NCPL
              OFF        1

CPL DATE     CPLD     CPLD     CPLD     CPLD     CPLD     CPLD     CPLD     CPLD     CPLD
              0.0

CPL FREQ     CPLF     CPLF     CPLF     CPLF     CPLF     CPLF     CPLF     CPLF     CPLF
              5.0

FLUXES       FLXC     NFLX
              OFF        0

FLX DATE     FLXD     FLXD     FLXD     FLXD     FLXD     FLXD     FLXD     FLXD     FLXD

FLX FREQ     FLXF     FLXF     FLXF     FLXF     FLXF     FLXF     FLXF     FLXF     FLXF

RESTART      RSOC     NRSO     RSIC
              OFF        0      OFF

RSO DATE     RSOD     RSOD     RSOD     RSOD     RSOD     RSOD     RSOD     RSOD     RSOD
```

Appendix A. - Model Parameter Specification

RSO FREQ	RSOF	RSOF	RSOF	RSOF	RSOF	RSOF	RSOF	RSOF	RSOF
CST COMP	CCC	PHC	KF						
	ON	OFF	4						
CST ACTIVE	CAC	CAC	CAC	CAC	CAC	CAC	CAC	CAC	CAC
	ON	OFF	ON	OFF	OFF	ON	ON	ON	ON
	OFF	OFF	ON	ON	ON	ON	ON	ON	ON
	ON	ON	OFF	OFF	ON				
CST DERIVE	CDC	CDC	CDC	CDC	CDC	CDC	CDC	CDC	CDC
	OFF	OFF	OFF	OFF	OFF	OFF	OFF	OFF	OFF
	OFF	OFF	ON	ON	ON				
CST FLUX	CFC	CFC	CFC	CFC	CFC	CFC	CFC	CFC	CFC
	OFF	OFF	OFF	OFF	OFF	OFF	OFF	OFF	OFF
	OFF	OFF	OFF	OFF	OFF	OFF	OFF	OFF	OFF
	OFF	OFF	OFF	OFF	OFF	OFF	OFF	OFF	OFF
	OFF	OFF	OFF	OFF	OFF	OFF	OFF	OFF	OFF
	OFF	OFF	OFF	OFF	OFF	OFF	OFF	OFF	OFF
	OFF	OFF	OFF	OFF	OFF	OFF	OFF	OFF	OFF
	OFF	OFF	OFF	OFF	OFF	OFF	OFF	OFF	OFF
	OFF	OFF	OFF	OFF	ON				
CST ICON	C2I	C2I	C2I	C2I	C2I	C2I	C2I	C2I	C2I
	-2.0	0.0	-2.0	0.0	0.0	-2.0	-2.0	-2.0	-2.0
	-2.0	0.0	-2.0	-2.0	-2.0	-2.0	-2.0	-2.0	-2.0
	-2.0	-2.0	0.0	0.0	0.0				
CST PRINT	CPRC	CPRC	CPRC	CPRC	CPRC	CPRC	CPRC	CPRC	CPRC
	OFF	OFF	ON	OFF	OFF	ON	ON	ON	OFF
	OFF	OFF	ON	ON	ON	ON	ON	ON	ON
	ON	ON	OFF	OFF	ON				
CIN CON	CINAC	CINAC	CINAC	CINAC	CINAC	CINAC	CINAC	CINAC	CINAC
	ON	OFF	ON	OFF	OFF	ON	ON	ON	ON
	OFF	OFF	ON	ON	ON	ON	ON	ON	ON
	ON	ON	OFF	OFF	OFF				
CTR CON	CTRAC	CTRAC	CTRAC	CTRAC	CTRAC	CTRAC	CTRAC	CTRAC	CTRAC
	ON	OFF	ON	OFF	OFF	ON	ON	ON	ON
	OFF	OFF	ON	ON	ON	ON	ON	ON	ON
	ON	ON	OFF	OFF	OFF				
CDT CON	CDTAC	CDTAC	CDTAC	CDTAC	CDTAC	CDTAC	CDTAC	CDTAC	CDTAC
	OFF	OFF	OFF	OFF	OFF	OFF	OFF	OFF	OFF
	OFF	OFF	OFF	OFF	OFF	OFF	OFF	OFF	OFF
	OFF	OFF	OFF	OFF	OFF				
CPR CON	CPRAC	CPRAC	CPRAC	CPRAC	CPRAC	CPRAC	CPRAC	CPRAC	CPRAC
	ON	OFF	ON	OFF	OFF	ON	ON	ON	ON
	OFF	OFF	ON	ON	ON	ON	ON	ON	ON
	ON	ON	OFF	OFF	OFF				
EX COEF	EXH2O	EXSS	EXOM	BETA					
	2.0	0.0	0.0001	0.79					
ALG EX	EXA	EXA	EXA	EXA	EXA	EXA	EXA	EXA	EXA
	0.2	0.2	0.2						
COLIFORM	COLQ10	COLDK							
	1.04	1.4							

Appendix A. - Model Parameter Specification

```
S SOLIDS      SSS
              2.0

ALGAL RATE     AG      AR      AE      AM      AS    AHSP    AHSN   AHSSI    ASAT
Alg 1         3.0   0.050    0.03    0.02   0.080   0.004   0.030  0.0001    20.0
Alg 2         2.4   0.050    0.03    0.02    0.10   0.004   0.020  0.0001    60.0
Alg 3         3.8   0.050    0.03    0.02    0.20   0.020   0.300  0.0001   100.0

ALGAL TEMP    AT1     AT2     AT3     AT4     AK1     AK2     AK3     AK4
Alg 1         0.1     5.0    22.0    35.0    0.05    0.80    0.70    0.01
Alg 2         5.0    23.0    25.0    35.0    0.01    0.99    0.99    0.01
Alg 3         5.0    25.0    35.0    40.0    0.01    0.60    0.99    0.30

DOM        LDOMDK  RDOMDK   LRDDK
             0.12   0.001   0.001

POM        LPOMDK  RPOMDK   LRPDK    POMS    APOM
             0.06   0.001   0.001    0.35    0.75

OM RATE      OMT1    OMT2    OMK1    OMK2
              4.0    20.0     0.1    0.99

CBOD         KBOD    TBOD    RBOD
             0.25   1.047    1.85

PHOSPHOR     PO4R   PARTP
            0.015     1.2

AMMONIUM     NH4R   NH4DK
             0.20    0.25

NH4 RATE    NH4T1   NH4T2   NH4K1   NH4K2
              5.0    20.0     0.1    0.99

NITRATE     NO3DK    NO3S   O2NO3
             0.05    0.10    0.65

NO3 RATE    NO3T1   NO3T2   NO3K1   NO3K2
              5.0    20.0     0.1    0.99

SILICA       DSIR    PSIS   PSIDK  PARTSI
              0.1    0.25    0.05     0.2

IRON          FER     FES
              0.5     2.0

SED CO2      CO2R
              0.1

STOICHMT    O2NH4    O2OM    O2AR    O2AG    BIOP    BION   BIOSI    BIOC   ACHLA
             4.57     1.4     1.4     1.4   0.008   0.070   0.011    0.45    74.6

O2 LIMIT    O2LIM
             0.20

SEDIMENT     SEDC   PRNSC  SEDRIC   SEDCI  RSEDCI
               ON      ON      ON     1.0     1.0

SED RATE    SODT1   SODT2   SODK1   SODK2
              4.0    30.0     0.1    0.99

SED DECAY     SDK    FSOD     SDC    SEDB    SOMS  BDODDK    RSDK   LRSDK
              .04     1.0     OFF   0.001   0.001     2.0    0.01    0.01
```

```
S DEMAND     SOD     SOD     SOD     SOD     SOD     SOD     SOD     SOD     SOD
             0.0     0.0     0.0     0.0     0.0     0.0     0.0     0.0     0.0
             0.0     0.0     0.0     0.0     0.0     0.0     0.0     0.0     0.0
             0.0     0.0     0.0     0.0     0.0     0.0     0.0     0.0     0.0
             0.0     0.0     0.0     0.0     0.0     0.0     0.0     0.0     0.0
             0.0     0.0     0.0     0.0     0.0     0.0     0.0     0.0     0.0
             0.0     0.0     0.0     0.0     0.0     0.0     0.0     0.0     0.0
             0.0     0.0     0.0     0.0     0.0     0.0     0.0     0.0     0.0
             0.0     0.0     0.0

RSI FILE...............................RSIFN...................................
        rsi.npt - not used

QWD FILE...............................QWDFN...................................
        ../qwd.npt

BTH FILE...............................BTHFN...................................
        ../bth_n4b_man_025.npt

MET FILE...............................METFN...................................
        ../met_9798.npt

VPR FILE...............................VPRFN...................................
        vpr.npt - not used

LPR FILE...............................LPRFN...................................
        ../lpr_9798_025.npt

QIN FILE...............................QINFN...................................
Br 1    ../qin_br1_9798.npt
Br 2    ../qin_br2_9798.npt

TIN FILE...............................TINFN...................................
Br 1    ../tin_br1_9798.npt
Br 2    ../tin_br2_9798.npt

CIN FILE...............................CINFN...................................
Br 1    ../cin_br1_9798.npt
Br 2    ../cin_br2_9798.npt

QOT FILE...............................QOTFN...................................
Br 1    qot_br1.npt - not used
Br 2    qot_br2.npt - not used

QTR FILE...............................QTRFN...................................
Tr 1    ../qtr_tr1_9798.npt
Tr 2    ../qtr_tr2_9798.npt
Tr 3    ../qtr_tr3_9798.npt
Tr 4    ../qtr_tr4_9798.npt
Tr 5    ../qtr_tr5_9798.npt
Tr 6    ../qtr_tr6_9798.npt
Tr 7    ../qtr_tr7_9798.npt
Tr 8    ../qtr_tr8_9798.npt
Tr 9    ../qtr_tr9_9798.npt
Tr 10   ../qtr_tr10_9798.npt
Tr 11   ../qtr_tr11_9798.npt
Tr 12   ../qtr_tr12_9798.npt

TTR FILE...............................TTRFN...................................
Tr 1    ../ttr_tr1_9798.npt
Tr 2    ../ttr_tr2_9798.npt
Tr 3    ../ttr_tr3_9798.npt
```

```
Tr 4    ../ttr_tr4_9798.npt
Tr 5    ../ttr_tr5_9798.npt
Tr 6    ../ttr_tr6_9798.npt
Tr 7    ../ttr_tr7_9798.npt
Tr 8    ../ttr_tr8_9798.npt
Tr 9    ../ttr_tr9_9798.npt
Tr 10   ../ttr_tr10_9798.npt
Tr 11   ../ttr_tr11_9798.npt
Tr 12   ../ttr_tr12_9798.npt

CTR FILE...............................CTRFN....................................
Tr 1    ../ctr_tr1_9798.npt
Tr 2    ../ctr_tr2_9798.npt
Tr 3    ../ctr_tr3_9798.npt
Tr 4    ../ctr_tr4_9798.npt
Tr 5    ../ctr_tr5_9798.npt
Tr 6    ../ctr_tr6_9798.npt
Tr 7    ../ctr_tr7_9798.npt
Tr 8    ../ctr_tr8_9798.npt
Tr 9    ../ctr_tr9_9798.npt
Tr 10   ../ctr_tr10_9798.npt
Tr 11   ../ctr_tr11_9798.npt
Tr 12   ../ctr_tr12_9798.npt

QDT FILE...............................QDTFN....................................
Br 1    qdt_br1.npt - not used
Br 2    qdt_br2.npt - not used

TDT FILE...............................TDTFN....................................
Br 1    tdt_br1.npt - not used
Br 1    tdt_br2.npt - not used

CDT FILE...............................CDTFN....................................
Br 1    cdt_br1.npt - not used
Br 2    cdt_br2.npt - not used

PRE FILE...............................PREFN....................................
Br 1    ../pre_br1_9798.npt
Br 2    ../pre_br2_9798.npt

TPR FILE...............................TPRFN....................................
Br 1    ../tpr_br1_9798.npt
Br 2    ../tpr_br2_9798.npt

CPR FILE...............................CPRFN....................................
Br 1    ../cpr_br1_9798.npt
Br 2    ../cpr_br2_9798.npt

EUH FILE...............................EUHFN....................................
Br 1    euh_br1.npt - not used
Br 2    euh_br2.npt - not used

TUH FILE...............................TUHFN....................................
Br 1    tuh_br1.npt - not used
Br 2    tuh_br2.npt - not used

CUH FILE...............................CUHFN....................................
Br 1    cuh_br1.npt - not used
Br 2    cuh_br2.npt - not used

EDH FILE...............................EDHFN....................................
Br 1    ../edh_br1_9798.npt
Br 2    edh_br2.npt - not used
```

Appendix A. - Model Parameter Specification

```
TDH FILE...............................TDHFN...................................
Br 1    ../tdh_br1_9798.npt
Br 2    tdh_br2.npt - not used

CDH FILE...............................CDHFN...................................
Br 1    ../cdh_15c_9798.npt
Br 2    cdh_br2.npt - not used

SNP FILE...............................SNPFN...................................
        9798_025.snp

TSR FILE...............................TSRFN...................................
        9798_025.tsr

PRF FILE...............................PRFFN...................................
        9798_025.prf

VPL FILE...............................VPLFN...................................
        9798_025.vpl

CPL FILE...............................CPLFN...................................
        9798_025.cpl

SPR FILE...............................SPRFN...................................
        9798_025.spr

FLX FILE...............................KFLFN...................................
        kfl.opt

WSF FILE...............................WSFFN...................................
        wsf.opt

XTSR FILE..............................XTSRFN..................................
        9798_025.xtsr
```